DISSERTATION APPROVAL FOR THE DOCTORAL DISSERTATION IN THE EMERGING
INFECTIOUS DISEASES GRADUATE PROGRAM

Title of Dissertation: "A20 Functional Domains Regulate Subcellular Localization and NF-Kappa B
activation"

Name of Candidate: Michael Washington
Doctor of Philosophy Degree
August 15, 2013

DISSERTATION AND ABSTRACT APPROVED:

DATE:

_____   11/1/13

Dr. Edward Mitre
DEPARTMENT OF EMERGING INFECTIOUS DISEASES
Committee Chairperson
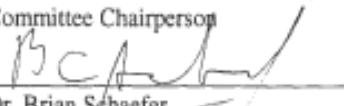
_____   11/3/13

Dr. Brian Schaefer
DEPARTMENT OF EMERGING INFECTIOUS DISEASES
Dissertation Advisor
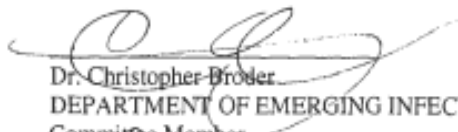
_____   11-1-13

Dr. Christopher Broder
DEPARTMENT OF EMERGING INFECTIOUS DISEASES
Committee Member

_____   11/12/13

Dr. Rajat Varma
National Institute of Allergy and Infectious Disease
Committee Member

Report Documentation Page		*Form Approved* *OMB No. 0704-0188*

1. REPORT DATE **14 AUG 2013**	2. REPORT TYPE **Final**	3. DATES COVERED **-**

4. TITLE AND SUBTITLE	5a. CONTRACT NUMBER
A20 Functional Domains Regulate Subcellular Localization and NF-kB Activation	5b. GRANT NUMBER
	5c. PROGRAM ELEMENT NUMBER

6. AUTHOR(S)	5d. PROJECT NUMBER
Michael A. Washington	5e. TASK NUMBER
	5f. WORK UNIT NUMBER

7. PERFORMING ORGANIZATION NAME(S) AND ADDRESS(ES) **Uniformed Services University of the Health Sciences 4301 Jones Bridge Road Bethesda, Maryland 20814**	8. PERFORMING ORGANIZATION REPORT NUMBER

9. SPONSORING/MONITORING AGENCY NAME(S) AND ADDRESS(ES)	10. SPONSOR/MONITOR'S ACRONYM(S)
	11. SPONSOR/MONITOR'S REPORT NUMBER(S)

12. DISTRIBUTION/AVAILABILITY STATEMENT
Approved for public release, distribution unlimited

13. SUPPLEMENTARY NOTES
Ph.D. Dissertation of MAJ Michael A. Washington completed at USUHS in August 2013., The original document contains color images.

14. ABSTRACT
A20 is a structurally and functionally complex molecule that represents a central node in the immune response activation network. It is a dual ubiquitin editing molecule that is capable of altering the stability and protein-protein interactions of substrate molecules. A20 tends to remain sequestered into punctate structures in the cytoplasms of both lymphoid and non-lymphoid cells. It is a negative regulator of NF-kB activation and has been shown to modify the activity of several members of the NF-kBÛ²nsignal transduction pathway. The B-cell lymphoma-10 protein or Bcl10 is a central member of this pathway. Here we show that A20 colocalizes with overexpressed Bcl10 in HEK-293 cells and that it colocalizes with Bcl10 filaments in a stimulation dependent manner in T-lymphocytes. We also demonstrate that the last three zinc fingers of A20 are able regulate the stability of Bcl10 and that conversely, a Bcl10 interacting protein (BinCard) regulates the stability of A20. Understanding the subcellular localization and biochemical activity of A20 is an essential prerequisite for the development of therapeutic A20 modulation strategies and the identification of small-molecule compounds capable of altering A20 function. The experimental data and resulting model of the regulatory activities of A20 presented in this dissertation will serve as a starting point for further investigations into the physiological role and therapeutic potential of this important and complex molecule.

15. SUBJECT TERMS
Immunology A20 TNFAIP3 Biodefense Emerging Infectious Disese

16. SECURITY CLASSIFICATION OF:			17. LIMITATION OF ABSTRACT	18. NUMBER OF PAGES	19a. NAME OF RESPONSIBLE PERSON
a. REPORT **unclassified**	b. ABSTRACT **unclassified**	c. THIS PAGE **unclassified**	**UU**	**185**	

Abstract

Title of Dissertation: A20 Functional Domains Regulate Subcellular Localization and NF-κB Activation

Michael A. Washington, Doctor of Philosophy, 2013

Dissertation directed by:

Brian C. Schaefer, Ph.D.
Associate Professor, Department of Emerging Infectious Disease
Uniformed Services University of the Health Science (USUHS)

A20 is a structurally and functionally complex molecule that represents a central node in the immune response activation network. It is a dual ubiquitin editing molecule that is capable of altering the stability and protein-protein interactions of substrate molecules. A20 tends to remain sequestered into punctate structures in the cytoplasms of both lymphoid and non-lymphoid cells. It is a negative regulator of NF-κB activation and has been shown to modify the activity of several members of the NF-κB signal transduction pathway. The B-cell lymphoma-10 protein or Bcl10 is a central member of this pathway. Here we show that A20 colocalizes with overexpressed Bcl10 in HEK-293 cells and that it colocalizes with Bcl10

filaments in a stimulation dependent manner in T-lymphocytes. We also demonstrate that the last three zinc fingers of A20 are able regulate the stability of Bcl10 and that conversely, a Bcl10 interacting protein (BinCard) regulates the stability of A20. Understanding the subcellular localization and biochemical activity of A20 is an essential prerequisite for the development of therapeutic A20 modulation strategies and the identification of small-molecule compounds capable of altering A20 function. The experimental data and resulting model of the regulatory activities of A20 presented in this dissertation will serve as a starting point for further investigations into the physiological role and therapeutic potential of this important and complex molecule.

A20 FUNCTIONAL DOMAINS REGULATE SUBCELLULAR

LOCALIZATION AND NF-κB ACTIVATION

By

Michael A. Washington

Dissertation submitted to the Faculty of the Program in Emerging Infectious

Disease of the Uniformed Services University of the Health Sciences in

partial fulfillment of the requirements for the degree of Doctor of Philosophy

2013.

DEDICATION

This work is dedicated to Ariana, Ishmael, Ruthie and Syrena Rose. It

is also dedicated to all of my family and friends who have been

supportive of my military and scientific careers.

Acknowledgments

TABLE OF CONTENTS

List of Figures

Chapter 1

General Introduction

The Ubiquitin-Editing Molecule A20

Tumor necrosis factor alpha (TNF-α) induced protein 3 or TNFAIP3 has recently emerged as a potent regulator of both innate and adaptive immunity (117, 118). This unique molecule, also known as A20, is critical for controlling the duration and intensity of the various cytoplasmic signals involved in lymphocyte activation and for modulating the response of non-lymphoid cells to pro-inflammatory stimuli. A20 is expressed in almost all vertebrate tissues (113). However, the highest levels of expression have been found in lymphoid tissue, underscoring the important role of this molecule in lymphocyte activation.

Early research into the distribution of A20 has shown that both unstimulated and naïve lymphocytes tend to display relatively high baseline levels (113). Surprisingly, these levels rapidly decrease upon stimulation of the T-cell receptor (TCR). Disruptions in A20 expression have been implicated in the development of several distinct hematological malignancies and numerous immune system mediated pathologies (108, 117). In particular, polymorphisms in the A20 locus are associated with the development of Sezary syndrome, cutaneous T-cell lymphoma, MALT lymphoma, Hodgkin's lymphoma and specific types of diffuse large B-cell

lymphoma (6, 13, 47, 60, 99, 116). Previously published data also suggests that polymorphisms in A20 are associated with the development and prognosis of specific autoimmune diseases such as lupus, rheumatoid arthritis, and psoriasis (12, 62).

It is of interest to note that A20 appears to be essential for the immunological control of infection (68, 109). Indeed, several viral pathogens have targeted A20 as a means of modulating the host immune response to promote their proliferation and survival. Both the human T-cell lymphotropic virus (HTLV) and the measles virus express proteins that modulate A20 activity in host cells (27, 56, 57, 118). In addition, knock-out mice lacking functional A20 in myeloid cells are protected against lethal influenza virus infection (68, 81), underscoring the role of A20 in modulating infectious disease outcome.

A20 is an ubiquitin-editing molecule (22, 23, 43). Ubiquitin is a small peptide that can be covalently attached to substrate proteins as a monomer or as a multimer. Interestingly, multimeric ubiquitin is capable of assuming one of several of spatial conformations. Depending on the conformation of the ubiquitin tag, substrate proteins are targeted for either degradation or

functional modification (123). In this manner, the ubiquitin modification system can have a profound impact on a broad array of cellular functions.

A20 displays a high degree of functional and structural complexity, suggesting that this molecule confers a significant survival advantage to vertebrate species. The functional complexity derives from the fact that A20 has the ability to modulate the ubiquitin status of substrate molecules in one of two ways: it can either remove ubiquitin from the substrate by a specific cysteine protease activity localized to the amino terminus (N-terminus) or it can add ubiquitin molecules by a ubiquitin ligase activity which has been mapped to the carboxyl (C) terminus (124).

The structural complexity of A20 derives from the fact that the full-length molecule is composed of 790 amino acids that are arranged into an intricate 3-dimensional structure (53, 117, 118). This is approximately double the number of amino acids comprising the average eukaryotic protein (approximately 360 amino acids). In addition, A20 has a modular structure. It is composed of eight spatially and structurally distinct domains, each with a unique function. An ovarian tumor (OTU) domain has been identified at the N-terminus. This domain is believed to confer the ability to remove ubiquitin chains from substrate molecules. The C-terminal region is

composed of a series of seven similar, but distinct domains with homology to the zinc (Zn) finger structural motif (see Figure 1). These domains confer the ability to add ubiquitin attachments to substrate molecules (124). These domains also serve as protein-protein interaction interfaces that allow the dimerization and multimerization of A20 thus conferring a molecular scaffolding capability (44, 51, 82).

The Discovery and Cloning of A20

A20 was first described by Vishva Dixit and co-workers at the University of Michigan in 1990 (18). The Dixit group was investigating the molecular nature of the mechanisms resulting in the inflammatory response, and was interested in determining the effects of tumor necrosis factor alpha (TNF-α) on endothelial cells. They utilized human umbilical vein endothelial cells (HUVEC) as an *in vitro* model for endothelial tissue and utilized the technique of differential plaque hybridization as a means of determining the number and identity of the genes that are up-regulated in the presence of TNF-α. In order to restrict their analysis to genes that can be classified as "rapid response" genes, they performed the TNF-α stimulation of their HUVEC cells in the presence of protein synthesis inhibitors. This restricted

Figure 1. The domain structure of A20. A20 is composed of 790 amino acids. It has a modular structure consisting of eight separate domains. The N-terminal domain has homology to the Drosophila ovarian tumor protein and has ubiquitin protease activity. The C-terminal region is composed of seven zinc finger motifs. These domains are involved in protein-protein interactions and A20 dimerization. Zinc finger 4 has been shown to have ubiquitin ligase activity (118).
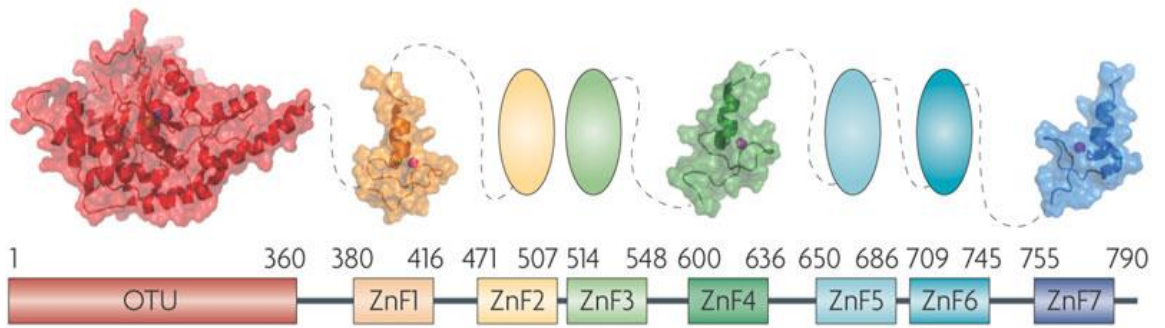
their analysis to those genes which can be up-regulated without intermediary protein synthesis. Initially, forty-nine specific cDNAs were found to be up-regulated. Further studies revealed that these arose from six unique genes (18). Three of these six genes were found to represent novel cDNAs, one of which was labeled A20 in reference to the grid coordinates on which it was located on one of the differential display hybridization filters that were initially analyzed by the group (Vishva Dixit, Department of Protein Engineering, Genentech, personal communication). A20 was found to fit all of the criteria for a primary response gene. The definition of a primary response gene used by the group was a gene that is rapidly induced upon stimulus and capable of being up-regulated in the presence of a protein synthesis inhibitor. The novel cDNA (A20) met these criteria by being rapidly inducible within one hour after stimulation and maintaining that capability in the presence of the protein synthesis inhibitor cyclohexamide.

The particular differential plaque hybridization technique used in the initial detection of A20 allowed the sequencing of 1.5 kilobases (kb) of A20 mRNA. The results of a series of northern analyses, predicted that the full length A20 mRNA should be at least 4kb in length. Anthony Opipari of the Dixit laboratory led the effort to further characterize the A20 protein and to sequence the complete mRNA. This was accomplished by utilizing the

initial 1.5kb sequence as a probe with which to screen a group of TNF-induced cDNA libraries (82). The end result of this process was that four overlapping clones were identified from which the complete mRNA sequence could be derived. Bioinformatics analysis of this sequence revealed that the complete A20 cDNA has a 66 nucleotide untranslated region (UTR) at the 5' end and a 2001 nucleotide untranslated region at the 3' end. Furthermore, a consensus polyadenlyation signal was identified, as well as an ATTTA motif which is known to regulate the stability of primary response mRNAs displaying relatively short half-lives (82).

The complete A20 cDNA is composed of 4400 nucleotides which generate a 790 amino acid protein upon translation. A comparison matrix analysis revealed the presence of multiple internal repeats within the carboxyl-terminal portion of the predicted protein. An alignment of these repetitive regions revealed the presence of a series of conserved cysteine residues with a pattern similar to the relatively common and well characterized cysteine-cysteine zinc finger motif (82).

Zinc finger domains were first described by Jonathon Miller and others at Cambridge University (52). The first crystal structure of the zinc finger domain was published by Carl Pabo and co-workers at Johns Hopkins

University (86). The traditional description of the zinc finger motif involves one zinc atom bound by two cysteine and two histidine residues separated by a linker region of about 12 amino acid residues. The separating linker residues typically form either an alpha-helix or a beta pleated sheet, which is usually able to interact with DNA, RNA or protein (90). The A20 zinc finger motif is unique in that the zinc atom is stabilized by four equally spaced cysteines forming a motif that has been described in the literature as a cysteine-cysteine zinc finger motif (82).

Zinc fingers are typically involved facilitating the regulation of cellular processes by mediating protein-protein interactions. They are also involved in the modification of DNA transcription by interacting directly with the double helix. However, zinc fingers may also have catalytic activity. There are currently over 300 enzymes known to coordinate with a zinc atom in the catalytic core. Indeed, the presence of the zinc atom is a perquisite for the catalytic activity of certain classes of metalloenzymes (73, 75, 90). Zinc is hypothesized to increase the nucleophilicity of the residues within the enzyme catalytic core. Therefore, the presence of zinc finger motifs in A20 may indicate either DNA binding capability, protein binding capability, or catalytic activity.

More recent studies have revealed that certain zinc fingers have the ability to bind ubiquitin, which is (as previously mentioned) a substrate for A20 (110). Ubiquitin binding zinc finger domains have been described in a wide variety of eukaryotic taxa ranging from yeast to mammals indicating an early evolution and distribution of these structures (90). Interestingly, the ubiquitin binding properties of A20 zinc fingers seem to be restricted to zinc fingers 4 and 7 (7, 114). A crystal structure of zinc finger 7 in a complex with ubiquitin was published in 2012 by Tokunaga and colleagues (Figure 2). It demonstrated the interaction of the linker regions of the zinc finger domain with the ubiquitin molecule and underscored the role of the zinc finger domains in the process of ubiquitin modification (114).

A20 Promoter Structure

As previously stated, A20 is a functionally, as well as, a structurally complex molecule. In addition to the modular nature of A20 and the structural complexity of the eight domains, the functional complexity of this molecule is evident the structure of the A20 promoter and the resulting mechanisms of transcriptional activation. The human A20 gene is located on the long arm chromosome 6 at position 23 (6q23). The mouse homolog

Figure 2. Crystal structure of A20 zinc finger 7 bound to ubiquitin.
A20 zinc fingers participate in protein-protein interactions and scaffolding
activity. Zinc fingers 4 and 7 have the ability to bind to both ubiquitin
monomers and ubiquitin chains.   The crystal structure of zinc finger 7
bound to ubiquitin has been determined at 1.7 angstrom resolution.
Ubiquitin is depicted in grey. Zinc finger 7 is depicted in orange. The zinc
atom is depicted as a grey sphere and coordinating residues are depicted in
green. The pink sphere represents a potassium ion associated with zinc
finger 7. The pink and magenta boxes show the two binding sites between
the zinc finger and ubiquitin while the inset shows a close up of the linkage
between ubiquitin monomers (114).
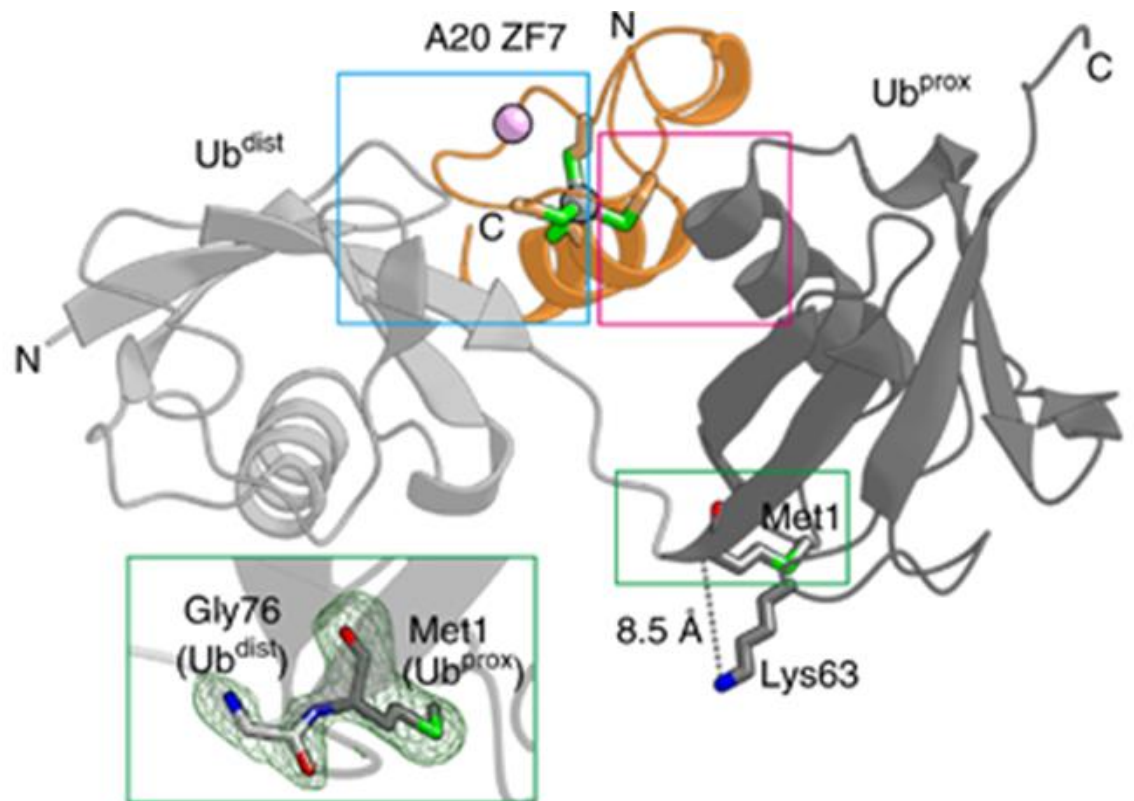
of A20 is located on chromosome 10 at position 13 (118). The observation

that A20 is a rapid response gene which can be quickly induced upon cell

stimulation in the presence of protein inhibitors immediately led to much

speculation and inquiry into the mechanisms regulating the activation of

A20 transcription. One of the first studies to investigate this issue was

performed in the laboratory of Rivka Dikstein at the Weizman Institute in

Israel (1). The Dikstein group was interested in the general activation

mechanisms of NF-κB inducible genes and used A20 as a model system.

Currently, three discrete processes are recognized as essential for gene

transcription. These are initiation, elongation and termination. The Dikstein

group chose to investigate the initiation step of A20 transcription (2).

Generally, initiation begins with the binding of a of a specific transcription

factor (usually a transcription factor known as transcription factor II-D or

TFIID) to the promoter region of the gene in question. The binding of

TFIID promotes the assembly of a protein complex consisting a series of

TATA binding proteins (TBP), RNA polymerase II, and associated factors.

The completed complex is then able to catalyze the remaining steps of

transcription. Interestingly, the Dikstein group found that the stimulation of

endothelial cells with TNF-α does not increase the rate of TFIID binding to

the A20 promoter as would be expected if TNF-α stimulation directly

initiated the transcription of A20 (2). This result led to the hypothesis that

TFIID and the general transcription apparatus are constitutively associated

with the promoter and that TNF- stimulation somehow functions to enhance

the rate of transcription, rather than initiate transcription *de novo*. This

hypothesis was later confirmed (1). Further studies by the Dikstein group

identified six binding sites for the SP-1 transcription factor in the A20

promoter (2). This is a constitutively active transcription factor which was

subsequently demonstrated to increase the rate of the interaction of TFIID

with the promoter region. Sequence analysis also revealed the presence of a

unique sequence feature known as an E-box and an elongation inhibitory

element or ELIE motif downstream from the SP1 binding site. These motifs

are transcription factor binding sites which have been found to be associated

with rapidly inducible proteins. The ELIE motif has been shown to bind a

factor known as USF1 which allows it to control the activity of a

transcriptional repressor known as DRB sensitivity inducing factor or DSIF.

The identification of the elements which bind to the A20 promoter has led to

the formulation of the current paradigm of A20 transcriptional activation

(Figure 3). This paradigm involves the constitutively active transcription

factor SP-1 permanently inhabiting SP-1 binding sites on the A20 promoter.

Figure 3. Structure of the A20 promoter and mechanism of activation.

The structure of the A20 promoter demonstrates the complexity of A20 regulation. The promoter consists of six SP-1 transcription factor binding sites followed by an E-box overlapping an ELIE motif. This is then followed by two κB binding sites and the core promoter region. SP-1 is constitutively bound to the SP-1 binding site mediating the recruitment of the basal transcription apparatus to the core promoter. However, transcription is initially under the control of the transcription factor USF1 which is sufficient for only one round of transcription due to inhibition by DSIF. NF- κB binding to the κB sites tends to displace USF1 from the E-box placing DSIF under the control of NF- κB which allows multiple rounds of transcription to occur (113).

A. Structure of A20 promoter

E-box ELIE κB κB core

transcription start site

B. Basal activity

TAFs CBP p300
TFIID RNA pol II
TBP
USF1 E-box ELIE κB κB core RNA pol II DSIF

single round of transcription initiation
elongation under control of USF1
pausing of elongation
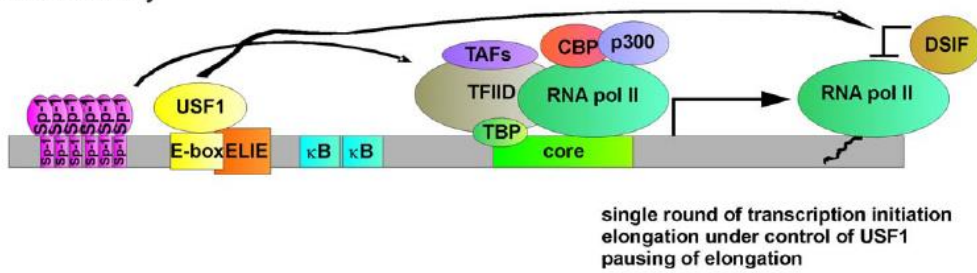
C. Activation upon stimulation

TAFs CBP p300
TFIID RNA pol II
TBP
E-box ELIE p65 p50 κB κB core RNA pol II DSIF

multiple rounds of transcription initiation
elongation under control of NF-κB

17
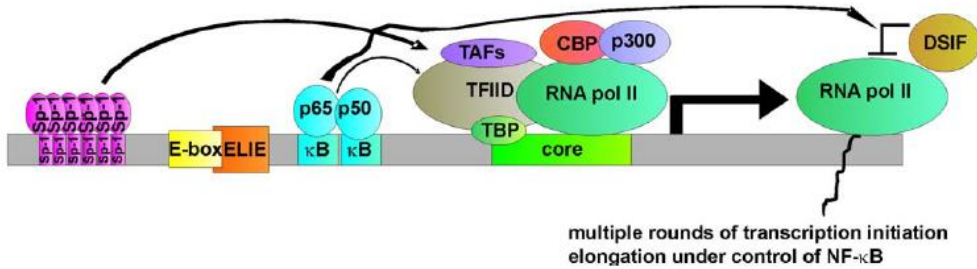
This situation allows TFIID, RNA polymerase II and associated factors to bind to the core promoter and initiate a single round of transcription. Continuous transcription activity is blocked by DSIF which is under the control of USF1 which occupies the E-box/ELIE motifs. NF-κB binding displaces USF1 releasing negative control of DSIF, and allowing the process of continuous transcription to occur (1, 2, 118). It should be noted that this paradigm was derived mainly from data acquired using non-lymphoid cell types. Lymphoid cells may express alternate transcription factors or similar factors with altered stoichiometry which may account for the constitutive activation of A20 in lymphoid cells (113). A20 transcripts are also regulated by micro-RNA, which functions to increase the complexity and diversity of the expression patterns of this unique molecule (49).

The Function of A20

The Dixit group performed the initial characterization of A20 function (117, 118). It is of interest to note that the first function to be described for A20 was that of an anti-apoptotic protein (55). They based their choice of experiments and preliminary models on a group of previous studies that had shown that resistance to the cytotoxic effects of TNF-α could be conferred

by primary TNF-α inducible gene products. Since A20 was a primary response product of TNF-α stimulation, they began the characterization of this protein by seeking to determine whether it was somehow involved in resistance to TNF-α mediated apoptosis (55).

The Dixit group initiated studies analyzing the effects of TNF-α stimulation on a specific cell line known as MCF-7. The MCF-7 cell line is a breast cancer mammary cell line that was originally isolated from a 69-year-old patient at by the Michigan Cancer Foundation (106). This cell line was of interest to the Dixit group in exploring the role of TNF-α on apoptosis due to the fact that growth and proliferation can be inhibited in a TNF-α dependent manner in one particular group of subclones but not in others. It was subsequently found by the experimental treatment of sensitive versus resistant MCF-7 cell lines with a combination of TNF-α and cyclohexamide, that the apoptosis-resistant phenotype could be positively correlated with an increased induction of A20 (55). The group verified the role of A20 in protection from TNF- mediated apoptosis by cloning the complete coding sequence of A20 into the mammalian expression vector psFFV-neo, followed by transfection into the NIH-3T3 cell line which is a

standard fibroblastic cell line that is normally susceptible to TNF-α

mediated apoptosis (55). After positive selection of the resulting clones with

neomycin and verification of A20 expression, they compared the survival of

A20 expressing NIH-3T3 cells following stimulation with TNF-α with cells

that had been transfected with empty vector. Again, a positive correlation

was observed between the expression of A20 and protection from TNF-α

mediated cell death.

The elucidation of the molecular and structural requirements

necessary for A20 to block or inhibit TNF-α mediated apoptosis originated

in the studies of Alexandra Krikos and others, also of the Dixit lab (54).

Their initial goal was to identify to the transcription start site of the A20

gene. They began this work with the isolation of an A20 cDNA containing

the complete 5' end of the molecule from a cDNA library. Subsequently,

they mapped the transcription start site by a combination of S1 nuclease and

primer extension analyses. This study was the first to suggest a role for NF-

κB in A20 regulation. Upon sequencing the 5' untranslated region of the

A20 cDNA, Krikos and co-workers identified two tandem κB elements

extending from -45 to -54 and from -57 to -66 (54). These elements had

been previously shown to have sequence homology to protein binding sites

in the κ light chain enhancer and by the time of this study, had been characterized as the binding sites for the ubiquitous transcription factor NF-κB.

This group of investigators next proceeded to demonstrate that mutation or elimination of the κB elements leads to a loss of induction by TNF-α in a Jurkat T-lymphocyte model. In addition, they performed a series of gel shift experiments which demonstrated that the incubation of a labeled double stranded A20 probe encompassing the κB elements with nuclear extract from TNF-α treated or untreated Jurkat T-cells leads to the formation of a specific TNF-α-inducible DNA-protein complex. These results suggested that NF- κB binds to the κB elements in the A20 promoter. This hypothesis was strengthened by the fact that HIV-1 κB elements were able to compete with A20 κB elements for binding with the nuclear extracts derived from TNF-α treated Jurkat T-cells. These studies gave the first direct evidence that A20 is activated by the binding of NF-κB to κB elements in the A20 promoter (54).

The fact that the A20 promoter contains κB binding sites coupled with the observation that NF-κB is able to physically bind to these sites suggested that A20 may be part of a negative feedback loop and that it may be

involved in the negative regulation of NF-κB activation in endothelial cells (54). This hypothesis was confirmed by an elegant series of experiments performed by Jeffrey Cooper and others in the laboratory of Christiane Ferran at Harvard (14). Since they were aware that earlier studies had shown that A20 is able to prevent TNF-α mediated apoptosis and that A20 was most likely under the control of the NF- κB transcription factor, the Ferran group decided to determine whether A20 is capable of modulating other TNF-α mediated responses in endothelial cells or if the effects of A20 are limited strictly to the process of apoptosis.

The Ferran group began by taking bovine aortic endothelial cells (BAEC) and transfecting them with a mammalian expression vector containing the complete A20 coding sequence. Thereafter, they verified that A20 could indeed be expressed by the transfected cells and performed an experiment in which they demonstrated that A20 can down regulate the TNF-α mediated expression of an endothelial adhesion promoting molecule known as E-selectin (14). E-selectin is typically expressed on the surface of TNF-α activated endothelium and had previously been used as a marker of activation. The fact that A20 could down regulate the expression of E-selectin indicated that A20 not only modulates the apoptotic response to

TNF-α but that A20 is able to modulate endothelial cell activation (14). The Ferran group then went on to show that A20 expression can negatively regulate the expression of interleukin 8 (IL-8) and IκBα (an inhibitor of NF-κB), which are also indicators of endothelial cell activation.

In order to determine whether the observed activities of A20 were limited to TNF-α stimulation and to exclude the possibility of a local and specific effect, the Ferran group showed that A20 was able to block the activation of endothelial cells in response to lipopolysaccharide (LPS), hydrogen peroxide and phorbol myristate acetate (PMA) stimulation. These data demonstrated that the effects of A20 are both broad and global (14, 26). Since the expression of endothelial cell markers could be under the control of multiple transcription factors besides NF-κB, an experiment was designed to determine whether A20 could be demonstrated to have a direct and specific effect on NF-κB. They co-transfected BAECs with an NF-κB luciferase reporter construct that depends singularly upon NF-κB binding to specific promoter elements for activation and an expression vector containing the A20 coding sequence in non-active control vector. This model system was then used to demonstrate that the expression of A20 directly from the mammalian expression vector was able to block the activation of the NF-κB reporter following stimulation of the cells with

either TNF- or LPS. In addition, control experiments showed that A20 was

not able to block the activation NF-κB independent reporter plasmids.

These results demonstrated the inherent specificity of A20 as a negative

regulator of NF-κB (14, 26).

A20 Mechanisms of Action

The first hints alluding to the nature of the mechanism by which A20

down regulates the expression of NF-κB came from the work of a group of

investigators at the Bastholm laboratory of the Danish Cancer Society

Research Center (44). A 1996 publication by this group demonstrated that

over-expression of A20 in a model cell culture system does not affect the

binding of TNF-α to the TNF-α receptor located at the cell surface (44).

This implied that the action of A20 must occur in within the cell cytoplasm

and that A20 must act upon the signal transduction machinery involved in

the formation of TNF-α responses.

By 1999, knowledge of the TNF-α pathway was rather robust. It had

been shown that the engagement of the TNF-α receptor by TNF-α leads to

the recruitment several proteins to the cytoplasmic domain of this receptor

(102, 124). One of the first proteins to interact with these receptor elements

was designated TRADD (TNF- α receptor-associated death domain) this

protein interacts with other death domain containing proteins, one of which

is known as FADD (Fas-associated death domain). FADD has been found

to initiate the pro-apoptotic signaling cascade. TRADD was also found to

interact with the receptor interacting protein or RIP and the TNF-α receptor

associated factor-2 (TRAF-2), which were both found to be involved in the

TNF-α mediated induction of NF-κB (35, 36, 104, 107). It had also been

determined by Song and co-workers that A20 is capable of physically

interacting with TRAF2 as well as with a complex between TRAF2 and an

associated TRAF molecule known as TRAF1 (107). It is of interest to note

that Song and co-workers determined that the interaction between A20 and

the TRAF molecules appeared to be mediated by the N-terminal domain.

However, it was also shown that overexpression of the zinc finger domains

without the N-terminus is sufficient to enable the down regulation of NF-κB

(107). These results suggested an attractive mechanism of A20 function in

which the N-terminal portion of A20 was responsible for directing it to

substrate molecules and that the zinc finger domains were responsible for the

catalytic activity resulting in the down-regulation of NF-κB.

Armed with the knowledge stated above, and a tentative model of A20 action in mind, a group of researchers in Belgium led by Rudi Beyaert set out to determine the precise mechanism of A20 dependent inhibition of NF-κB (35, 36). These investigators initially conducted a series of experiments which confirmed that A20 was able to down-regulate the expression of NF-κB dependent genes and that the effect was not specific to a given marker, indicating that the effects on NF-κB were broad rather than local. They next sought to determine whether A20 affected the ability of NF-κB to translocate into the nucleus and bind to DNA.

As a means of addressing this issue, the Beyaert group utilized the technique of the gel shift assay. They took a murine fibrosarcoma cell line and transfected it with either an empty expression vector, a vector containing the coding sequence for green fluorescent protein, or a vector containing the coding sequence for A20. The group, also transfected each these cell types with an NF-κB specific luciferase reporter. The cells were then stimulated with TNF- α and evaluated by gel shift assay to determine whether the binding of NF-κB to target sequences led to the slower migration of the resulting complex. Surprisingly, what they found was that A20 was able to down-regulate the expression of the NF-κB dependent luciferase reporter

without blocking the translocation of NF-κB into the nucleus and binding to DNA (35).

This group then went on to show by the confocal microscopy of cells transfected with A20-GFP fusion proteins, that A20 is localized to the cytoplasm and does not appear to enter the nucleus which indicates that, despite the fact that A20 contains several zinc finger domains it most likely does not function by binding directly to DNA and the modulation of gene transcription (35). This result reinforced the concept that the effects of A20 are due to its activities in the cell cytoplasm. As a means of defining the precise step at which A20 influences the TNF-α pathway, the Beyeart group next utilized another cell culture model in which they determined whether A20 was capable of blocking or interfering with NF-κB activation induced by the over-expression of TNF-α, TRADD, RIP, TRAF2 or the NF-κB inducing kinase (NIK). Interestingly, this experiment showed that A20 is able to block the activation by NF-κB by TNF-α, TRADD, RIP and TRAF2 (35, 36). However, A20 was not able to block the activation of NF-κB by NIK which is operates downstream from TRADD, RIP and TRAF2. This result demonstrates that the NF-κB activation inhibiting function of A20

appears to function at the level of TRADD, TRAF2 and RIP in the TNF-α

pathway (35, 36).

In 2001, a team led by Peter Kilshaw at Barbraham Institute in

Cambridge analyzed human expressed sequence tags using the basic local

alignment search tool or BLAST. They identified two A20 homologues

(25). One was named Cezanne and the other TRABID. The amino acid

sequences of these two proteins revealed that they displayed a striking level

of homology to the A20 amino-terminus. The group performed several

reporter experiments in human embryonic kidney cells (HEKs) which

demonstrated that Cezanne is also a negative regulator NF-κB (25). Studies

involving the yeast-two hybrid system revealed that Cezanne is able to bind

to polyubiquitin. Further bioinformatic analyses revealed that the N-

terminal domain of Cezanne has homology to the Drosophila ovarian tumor

domain or OTU domain.

The Drosophila OTU domain is the prototype for a family of proteins

first described by Kira Makarova at the Uniformed Services University (71).

This family of proteins was predicted to have proteolytic activity due to the

presence of conserved histidine and cysteine residues which may interact to

form the basis of an enzyme catalytic core. However, no catalytic activity

had been demonstrated for any member of the OTU family at the time the

Kilshaw group was investigating Cezanne. In order to determine whether

the OTU domain of Cezanne has catalytic activity, the Kilshaw group

utilized the yeast two hybrid system. They mutated the predicted catalytic

cysteine residue of Cezanne (cysteine 209) by replacement with serine.

They then proceeded to determine the interaction of the mutated Cezanne

with polyubiquitin and compare those results with wildtype Cezanne.

Interestingly, it was observed that when the catalytic domain of Cezanne is

mutated there is an increase in polyubiquitin binding (25). This indicates

that the mutated protein is able to bind to polyubiquitin but lacks that ability

to cleave it. They next demonstrated that wildtype Cezanne is indeed able to

cleave ubiquitin chains within the cell cytoplasm by the co-transfection of

HeLa cells with tagged wildtype Cezanne or catalytically inactive Cezanne

and differentially tagged ubiquitin. After a brief incubation period the cells

were treated with MG132 which is a proteosomal inhibitor. The result was

that the full length wildtype Cezanne was able to reverse the buildup of

ubiquitinated cellular proteins produced by MG132 treatment. However, the

catalytically inactive Cezanne had no effect (25). This was the first direct

evidence that the OTU domain had catalytic activity and that this activity

occurred in the cytoplasm. Since the N-terminus of A20 has homology to

the OTU domain of Cezanne, this was also the first evidence that A20

contains an OTU domain and that this OTU domain may have ubiquitin

editing catalytic activity (24, 25).

Final proof that the A20 OTU domain did in fact have catalytic

activity and that this activity was necessary for the down regulation of NF-

κB by A20 came from the work of Ingrid Wertz and others of the Division

of Oncology at Genentech (124). In a landmark 2004 Nature publication,

Wertz and co-workers demonstrated that A20 can catalyze the *in vitro*

ubiquitination of substrate proteins via a unique ligase activity (124). They

also showed that this ubiquitin ligase activity depends solely on zinc finger

4. In addition, they showed that A20 ubiquitinates the target molecule with

a specific form of the ubiquitin chain known as K48-linked ubiquitin. This

is the form of the ubiquitin chain in which the individual ubiquitin

monomers are linked via lysine 48. This linkage produces a distinct chain

geometry which accelerates the degradation of substrate molecules by

specifically targeting them to the proteosome (124). To determine whether

this activity is involved directly in the down-regulation of NF-κB, the group

went on to show that recombinant A20 purified from E. coli is able to

directly ubiquitinate the NF-κB pathway member RIP *in vitro*. This was the

first demonstration that A20 has ubiquitin ligase activity and that this

activity was specific for a member of the NF-κB activation cascade. However, these results were perplexing to the investigators given the fact that A20 contains an OTU domain which was previously shown to be an ubiquitin protease and not a ligase. Hence A20 appeared to display paradoxical properties.

This paradox was resolved when it was shown that A20 specifically removes K63-linked ubiquitin from substrate molecules (124). The geometry of K63-linked ubiquitin chains is distinct from that of K48-linked chains. K63-linked ubiquitin is not recognized by the proteosome and therefore tends to increase the stability of the substrate and may confer scaffolding capability. In this way, the Dixit group was able both to derive and experimentally demonstrate a model by which A20 controls NF-κB activation by removing stabilizing ubiquitin chains from substrate molecules followed by the addition of decay accelerating ubiquitin chains (124). Thus, A20 was found to function as a dual-ubiquitin editing molecule which functions by accelerating the decay and blocking the scaffolding activity of signal transduction mediators (Figure 4).

The fact that A20 is a large and structurally complex molecule has hampered attempts to generate a crystal structure of the complete protein.

Figure 4. A20 mechanism of Action. A20 can be defined as a dual ubiquitin editing molecule. The OTU domain catalyzes the removal of K63 linked ubiquitin from substrate molecules by a cysteine protease-like mechanism. This removes scaffolding capabilities and destabilizes the substrate. Zinc finger 4 has ubiquitin ligase activity and adds K48 linked ubiqutin to the substrate molecule. K48 linked ubiquitin targets the substrate to the proteosome for degradation (43).
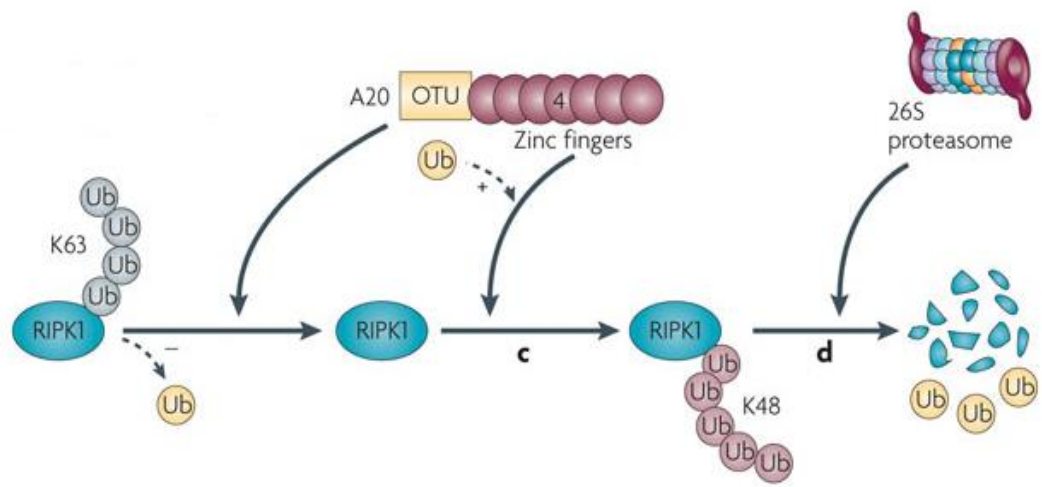
However, a crystal structure for the OTU domain has been obtained by Barford and there are crystal structures available of individual zinc finger domains (53). The resolution of the A20 OTU structure has revealed that this domain is composed of a wedge shaped molecule consisting of ten alpha helices and 10 beta strands (Figure 5). The current hypothesis regarding the relationship of the structure of the OTU domain to the function of A20 is that the expansive wedge shape of the molecule has evolved to enable the binding of large ubiquitin substrate chains. The catalytic core is similar to previously described cysteine proteases in that it consists of a catalytic cysteine residue (cysteine 103), a histidine residue which functions to activate the nucleophilicity of cysteine 103 by proton abstraction (histidine 256), and an asparagine residue (asparagine 70) which functions to stabilize histidine 256 (53).

Knowledge of the structure of the OTU domain and the architecture of the catalytic core enabled researchers to speculate upon the mechanism of action of the OTU domain based upon earlier studies with the more common and well characterized cysteine proteases. It is currently believed that the reaction begins with the removal of a proton from the thiol group of cysteine

Figure 5. Crystal structure of the A20 OTU domain. The OTU domain consists of ten alpha helices and ten beta sheets which form a flat-expansive surface to facilitate the binding of ubiquitin monomers and chains. The catalytic core is situated directly in the center of the domain and consists of a nucleophilic cysteine, a histidine, and stabilizing threonine and asparagine residues (53).
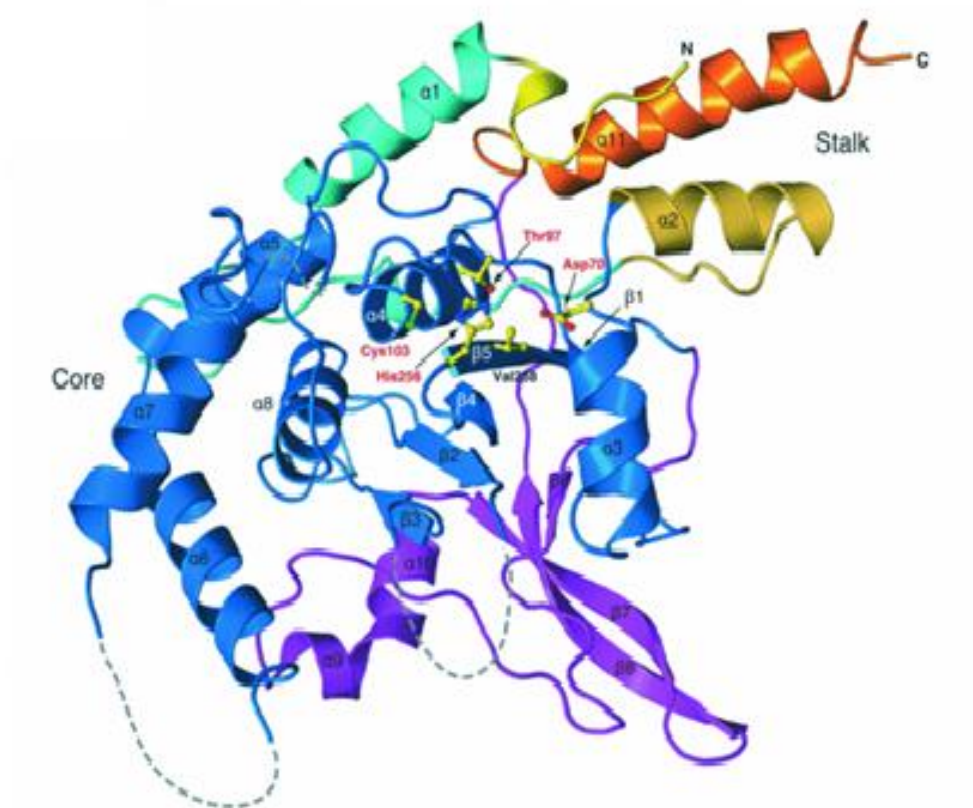
103 by histidine 256. Next, a nucleophilic attack on the carbonyl carbon of the substrate occurs. This releases an amino group containing substrate fragment. This is followed by the removal of a proton from histidine 256 returning it to the original state and the formation of a thioester bound between cysteine 103 and the remaining carboxy-terminal substrate fragment. This thioester bound is then hydrolyzed releasing the substrate and returning the enzyme to the original state (53).

The Role of A20 in the Immune Response

The initial characterization of the A20 molecule by the Dixit group revealed that A20 is highly expressed in lymphoid tissue (113). It was also revealed that A20 is constitutively expressed in immature T-lymphocytes as well as in naïve lymphocytes. The activation of T-cells has been shown to lead to the rapid down-regulation of A20 (113). This is in contrast to the kinetics observed in fibroblasts and endothelial cells in which cell activation by the TNF-α or LPS stimulation leads to an increase in A20 expression.

The first conclusive demonstration of the role of A20 in the regulation of the immune response and the inflammatory cascade in an intact animal, as opposed to cultured cells, came from the laboratory of Dr. Averil Ma at the

37

University of California, San Francisco (4, 59, 115). The Ma laboratory

utilized a gene targeting technique which enabled them to replace the ATG

initiation codon of A20 along with the first 250 residues of the protein with a

neomycin expression cassette in a group of experimental mice.   Western

blotting of the resulting knock-out mice revealed that expression of A20 was

lost. A20 knock-out pups tended to be runted as early as 1 week of age and

did not live as long as wildtype mice. A histological analysis of several of

the tissues recovered from these mice revealed a high degree of

inflammation in all tissues that were examined (59). Notable was the gross

appearance of the liver which showed pale acelluar regions in the A20

knock-out, the gross appearance of the kidney, which was atrophied in the

knock-out and the extensive inflammatory response visible on hematoxlyin

and eosin stained tissue sections (59). An interesting observation made

during this study was that flow cytometric analysis of A20 knock-out spleen

and liver tissue showed an increase in the numbers of activated lymphocytes,

granulocytes and macrophages providing evidence that A20 was involved in

the negative regulation of these cell types. Also of note was the fact that

knock-out mice were extremely sensitive to LPS administration in

comparison with wildtype strains and the fact that thymocytes from A20

knock-out mice displayed an increased sensitivity to TNF-α mediated

apoptosis (59). Further work showed that the severe inflammation that characterizes these knock-outs can be alleviated by the administration of antibiotics which clear endogenous flora. These results clearly demonstrated that A20 plays a role in the activation and duration of the innate immune response by regulating the initiation inflammatory cascade as well as in the adaptive immune response by regulating the activity of lymphocytes (4, 59,115).

A20 as a Negative Regulator of T-lymphocyte Activation

T-cells are central to the initiation and maintenance of the adaptive immune response. They are involved in the development of both the cell mediated and humoral arms of host defense. There are numerous subtypes of T-cells and with few exceptions; they all express a similar form of T-cell receptor (TCR). The TCR is a transmembrane heterodimer which is obligatorily associated with a group of signal transducing transmembrane molecules known as CD3. The CD3 molecules extend further into the cytoplasm than the TCR heterodimer and contains immunoreceptor tyrosine based activation motifs (ITAMs) on their cytosolic domains (48, 58, 105).

These motifs are important in the initiation of the signaling cascade that results in T-cell activation.

T-cell activation typically commences when the TCR engages an antigenic peptide which is associated with a major histocompatibility complex (MHC) molecule on the surface of an antigen presenting cell (dendritic cell, B-cell or macrophage). This association provides the first signal necessary for T-cell activation (47, 105). The second signal is provided by a constimulatory molecule. The best characterized costimulatory molecule is B7, which is present on all antigen presenting cells. B7 interacts with a molecule known as CD28 on the surface of the certain T-cells. Once signal 1 and signal 2 are engaged, the T-cell will up regulate expression of the IL-2 receptor, the cytokine IL-2 and activation-associated cytokine expression. The net result is that the T-cell will undergo a process of proliferation and differentiation into an effector state (Figure 6).

In the cytosol, T-cell receptor engagement leads to the phosophorylation of the ITAMs at specific tyrosine residues. This activates a tyrosine kinase cascade which ultimately leads to calcium release from intracellular stores and the activation of a protein kinase known as PKC-Ө (47, 105). This kinase phosphorylates a protein known as the CARD-

containing MAGUK 1 protein (CARMA1), which subsequently undergoes a

conformational change allowing it to interact with the B-cell lymphoma 10

(Bcl10) protein (93). The Bcl10 protein is constitutively bound to the

mucosa associated lymphoid tissue 1 protein (MALT1). The resulting

complex between BCL10, MALT1, and CARMA1 is called the CBM

complex (93). The formation of the CBM complex results in the recruitment

of a TRAF molecule known as TRAF6. TRAF6 is believed to have

ubiquitin ligase activity and mediates the ubiquitination of BCL10 and

MALT1. This allows the recruitment of a specific complex known as the

IKK complex to the CBM complex leading to the ubiquitination and

phosphorylation of the IKK complex, allowing it to catalyze the

phosphorylation the inhibitor of κB (IκBα). This triggers the degradation of

this molecule by the proteosome and allows NF-κB to translocate into the

nucleus (93, 133). NF-κB then activates the transcription of genes involved

in the proliferation and differentiation of the T-cell (Figure 7).

A 2008 Nature Immunology report by Rudi Beyaert's group in

Belgium demonstrated that T-cell activation results in the enzymatic

activation of MALT1 leading to the development previously

uncharacterized proteolytic activity and the recruitment of A20 into a

Figure 6. Two signal model for T-cell activation. T-cells require at least two signals for activation. Signal 1 is acquired by the interaction of the dimeric T-cell receptor with antigenic peptide in association with an MHC molecule. Signal 2 is acquired when a costimulatory molecule on the surface of the APC interacts with a constimulatory receptor on the surface of the T-cell. In this case the costimulatory molecule is B7 and the receptor is CD28. Once both signals are acquired the T-cell upregulates expression of the IL-2 receptor, begins to express IL-2 and stimulatory cytokines and undergoes a process of proliferation and differentiation which leads to a transition to an effector state. Copyright 2008 from Janeway's Immunobiology, Seventh Edition by Murphy. Reproduced by permission of Garland Science/Taylor & Francis LLC (50).

Stimulation of naive T cell

APC

MHC class I
T-cell receptor
B7
CD28

1 2

T cell

RECOGNITION

Proliferating T cell

IL-2
IL-2 receptor

1

PROLIFERATION

DIFFERENTIATION

Active effector T cells kill virus-infected target cells

1

kill

1

EFFECTOR FUNCTION
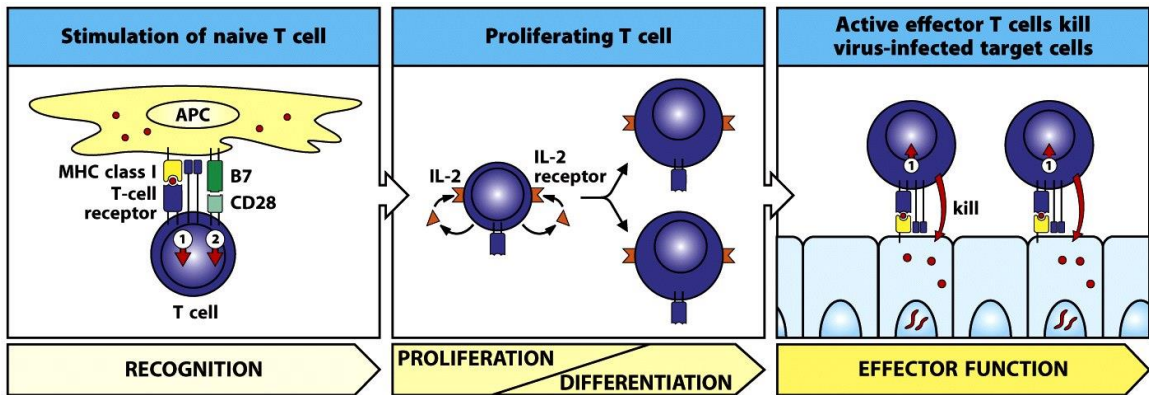
Figure 8-25 Immunobiology, 7ed. (© Garland Science 2008)

43

Figure 7. Intracellular events following T-cell receptor stimulation.
Stimulation of the T-cell receptor initiates a kinase cascade resulting in the
activation of PKC-theta. PKC-theta phosphorylates the scaffolding
molecule CARMA1 resulting in a conformational change in CAMA1 which
allows the recruitment BCL10 and MALT1. The complex formed by
CARMA1, BCL10, and MALT1 is known as the CBM complex. The CBM
complex recruits the ubiquitin ligase TRAF6 which participates in recruiting
and ubiquitinating the IKK complex allowing this complex to interact with
the inhibitory IkB proteins associated with NF-κB. The end result is that
IkB is phosphorylated and then ubiquitinated with K48 linked ubiquitin
resulting in the proteosomal degradation of IkB and the translocation of NF-
κB to the nucleus (121).
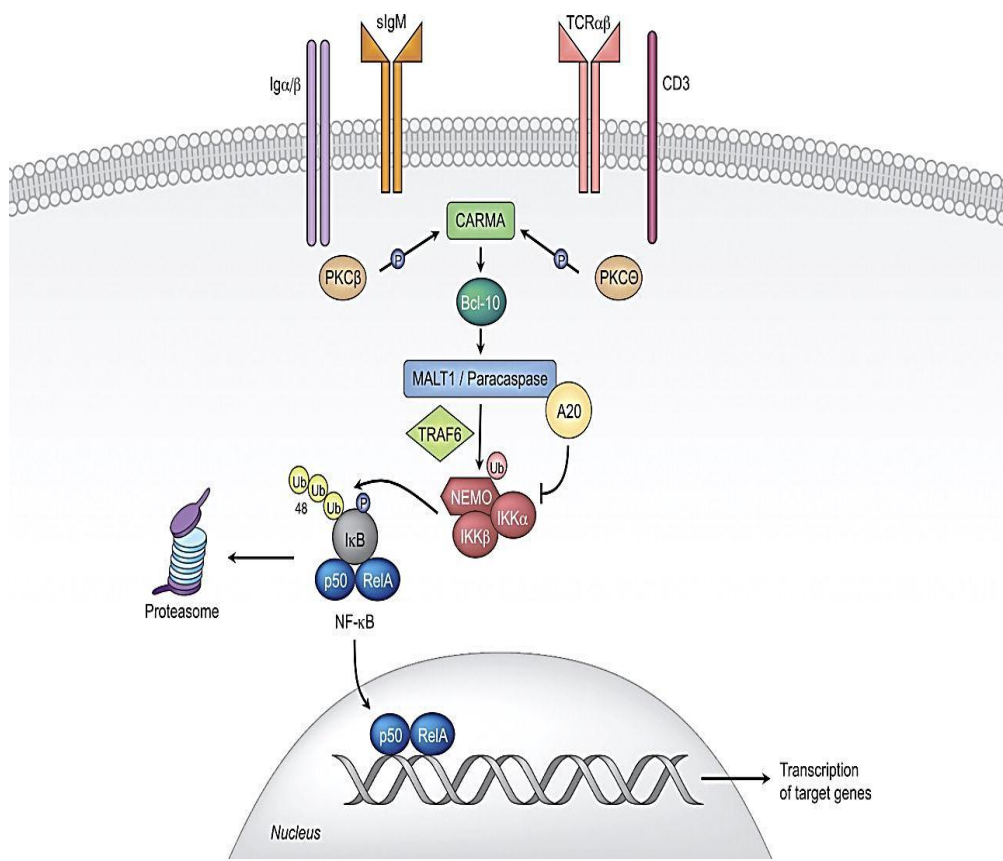
complex with MALT1 and BCL10 (15). This results in the cleavage of A20

at a specific arginine residue, which suggested to the Beyaert group that

TCR stimulation leads to the degradation of inhibitory A20 allowing T-cell

activation to proceed (15). This data compliments earlier observations that

T-cell activation results in a down-regulation of A20 levels in the cytoplasm.

Approximately 1 year after the Beyaert publication, Daniel Krappmann's

group in Germany described the exact biochemical mechanism by which

A20 may actually down-regulate T-cell activation (22). They were able to

demonstrate that A20 can interact with MALT1 upon T-cell activation and

catalytically remove K63-linked ubiquitin chains from this molecule. They

hypothesized that the removal of these chains prevents the formation of a

stable complex between MALT1 and the IKK complex thereby inhibiting

the activation of NF-κB (22). This was the first demonstration of A20

acting on a specific target in T-lymphocytes.

A20 and the host response to viral infection

Since A20 is a potent regulator of the inflammatory pathway and has

been shown to play a role in the negative regulation of T-lymphocytes, it

seems reasonable to suspect that A20 might also play a role in regulating the

pathogenesis of viral infection, and in fact numerous studies have shown this to be the case (117). The first study to demonstrate that A20 expression can be regulated by viral infection was performed by the Dixit group in 1992 (56). They demonstrated that the LMP1 protein of the Epstein Barr virus induces A20 expression in fibroblast cells. In a later publication, this group was able to show that the Tax protein of the human T-cell leukemia virus (HTLV-1) was capable of inducing the up-regulation of A20 expression (57). These data suggested a role for A20 in either the initiation or maintenance of viral infection. Since those initial studies, it has been shown that A20 expression can be regulated by the human cytomegalovirus, the influenza virus, Sendai virus, the measles virus P protein and the hepatitis C virus core protein (64, 67, 81, 118, 122). Interestingly, A20 is also involved in the regulation of intracellular parasite infection (109, 123). Given the role of A20 as a negative regulator of the immune response it seems likely that sometime during the co-evolution of these pathogens with their vertebrate hosts, the ability to modulate A20 expression was acquired. It is likely that this ability enabled persistence of the virus in the host tissue environment conferring a survival advantage. Indeed, it has been shown that the up-regulation of A20 by the measles virus P protein and by the Sendai

virus results in clear suppression of the signaling apparatus of the innate immune response (118, 122).

The role of A20 in modulating the pathogenesis of influenza virus infection has been studied in great detail. This is due to the fact that influenza-A virus infection had been previously shown to induce NF-κB expression in airway epithelial cells (68, 81). A recent publication by Onose and others has shown that influenza A virus infection activates the expression of A20 in bronchial epithelial cells and lung tissues from mice, and that overexpression of A20 results in the depression NF-κB activity (see Figure 8) (81). These results suggest that A20 should have a protective effect on the respiratory epithelium during influenza-A virus infections. This is a reasonable hypothesis, given that fact that it depresses the inflammatory response. However, a study involving the deletion of A20 in murine myeloid cells by Maelfait and others gave a contradictory result (68). In this study, knockout mice were generated with a deletion in the A20 gene occurring only in the myeloid cell type. It was then shown that bone marrow derived macrophages or alveolar derived macrophages from these mice express increased quantities of cytokines, chemokines, and other mediators in response to stimulation when compared to wild-type mice (68). This study conclusively demonstrated that knockout mice for A20 in myeloid

cells tended to be protected against the immunopathology resulting from sub-lethal doses of influenza intranasal administration. In addition, they were also protected against lethal influenza virus infections. These results indicate that A20 may represent a central regulator of the immune response to viral infection since the deletion of this single protein in a single cell type can have dramatic effects on disease outcome (68).   +

A20 is also involved in mediating the mechanism of viral induced oncogenic transformation. A20 has been shown to regulate the activity of a protein known as K13 which is involved in Karposi sarcoma herpesvirus (KSHV) mediated cell transformation (72). K13 can directly activate NF-κB by interacting with the IKK complex and is also capable of up-regulating the genes responsible for transformation. Overexpression of A20 blocks K13 induced activity. This is most likely due to ubiquitin modulation, although ubiquitin modifying activity has not been conclusively demonstrated.

Molecular complex formation in the activation of T-lymphocytes

The signal transduction pathway associated with T-cell activation occurs in the three dimensional space of the cytoplasm. The rate at which T-cell activation can occur is limited by the time required for each of the

Figure 8. Demonstration of increased expression of A20 following influenza A virus infection in murine lung tissue. Mice were inoculated by the intranasal route with either influenza A virus or a PBS control. Mice were sacrificed on day 4 post-inoculation and lung tissue was harvested. The tissue was stained with either an anti-A20 antibody or a PBS control (81).

Influenza virus-infected mice   Uninfected mice

Anti-A20 antibody

Rabbit IgG

A   100 μm

B   100 μm

C   100 μm

D   100 μm
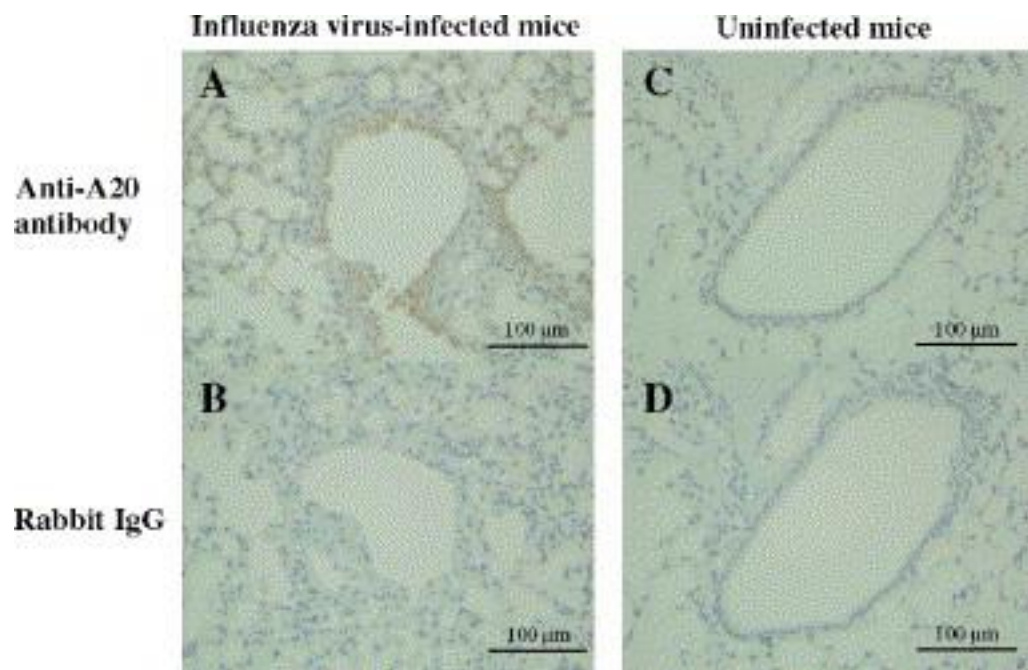
interacting proteins to encounter and interact with one another. If T-cell

activation was based solely on diffusion it would be a slow and inefficient

process and most likely would not occur fast enough to enable the organism

to combat infectious threats in real time. Therefore, it is reasonable to

suspect that the proteins involved in a critical signal transduction process

would be membrane bound or sequestered to specific locations within the

cytoplasm (5). This would limit the distance that each would have to travel

in order to interact with one another and in essence transform the signal

transduction process from diffusion limited process to a solid state process in

which there is direct communication between each protein or in which each

protein is confined to a small space facilitating efficient physical interaction

(5). Indeed, confocal microscopy has revealed that the adapter protein

Bcl10, when overexpressed in HEK-293T cells, tends to sequester into

discrete locales within the cytoplasm forming a filamentous structure. It has

also revealed that this sequestered protein is able to recruit members of the

TRADD family and other signaling intermediates (34).

Recent research by the our laboratory at the Uniformed Services

University of the Health Sciences has revealed the existence of molecular

complexes consisting of BCL10, MALT1, and CARMA1, which form in

response to T-cell activation (92). Indeed, with the application of confocal microscopy and fluorescently labeled BCL10 and MALT1, our group was able to show that BCL10 and MALT1 begin to form discrete structures in the cytoplasm of T-cells about 20 minutes post-stimulation with plate bound anti-CD3 (Figure 9). These structures coalesce into filamentous molecular complexes which persist until about 90 minutes post-stimulation at which point they begin to degrade. Our group has also uncovered evidence to support the hypothesis that the formations of these structures are necessary for NF-κB activation. Our group has coined the term POLKADOTS or punctate and oligomeric killing or activating domains transducing signals to describe these structures (92).

Interestingly, A20 also tends to form punctate structures in the cytoplasm of various cell types (119). These structures have been found in human embryonic kidney cells, L929 cells which are derived from mouse connective tissue, rheumatoid arthritis fibroblast like synoviocytes (RA-FLS) and African green monkey kidney (COS-7) cells (Figure 10) (25). It is interesting to note that A20 has also been shown to localize with lysosomal vesicles in COS-7 cells (63). This data may indicate that these punctate

Figure 9. T-cell receptor activation is associated with the formation of molecular complexes consisting of MALT1 and BCL10. BCL10 and MALT1 have been observed to form discrete punctuate structures in the cytoplasm of D10 T-cells 20 minutes following stimulation with anti-CD3. By 1hr post-stimulation these structures coalesce into filamentous aggregations. By 2hrs post-stimulation BCL10 tends to degrade while filamentous structures formed by MALT1 persist (90).

B Nomarski Bcl10-CFP MALT1-YFP

0 min

20 min

60 min

90 min

120 min

55
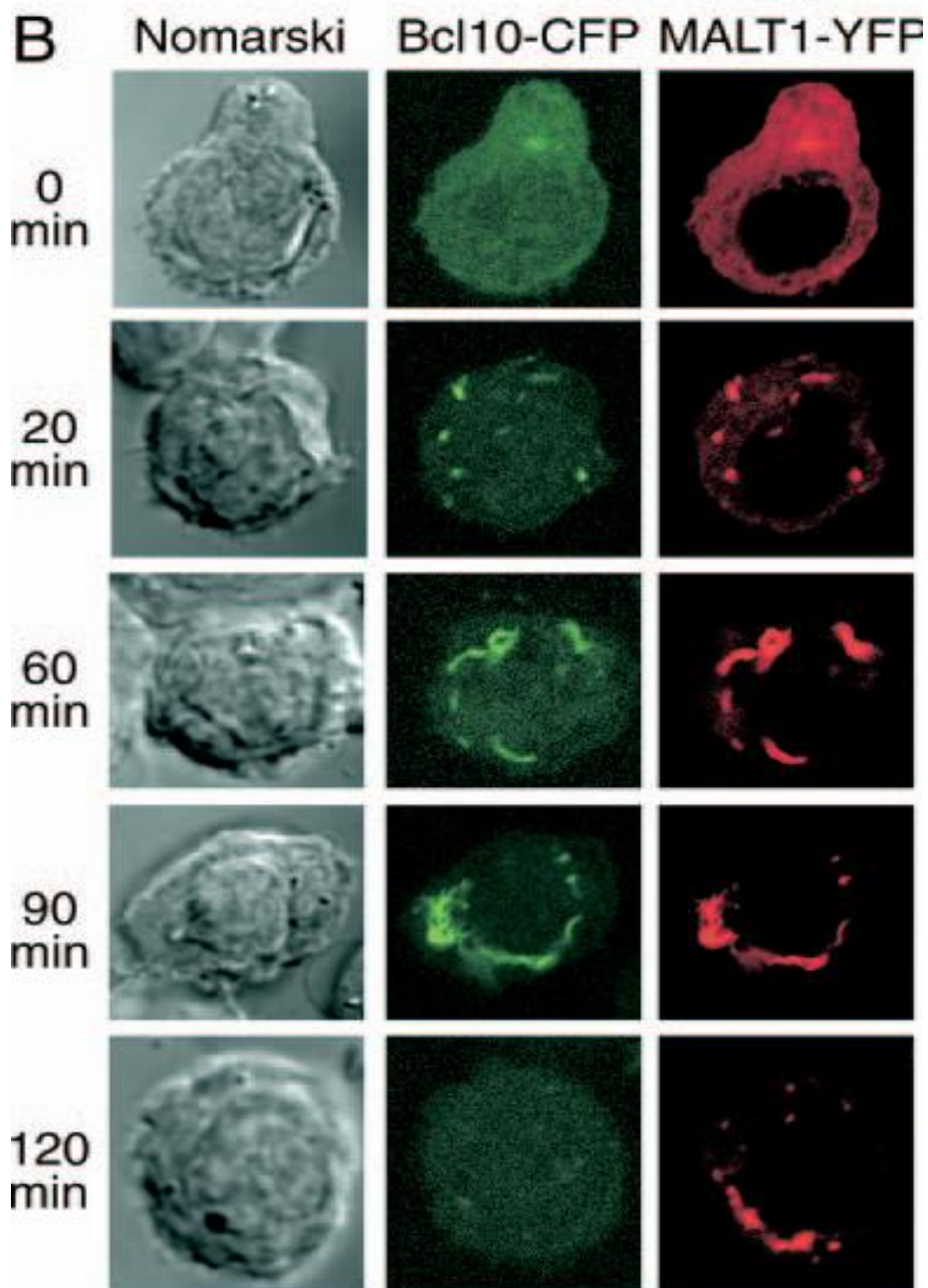
Figure 10. A20 forms punctate structures in the cytoplasm of several cell lines. A20 overexpression in the cytoplasm of HEK-293 cells leads to the formation of punctate structures. HEK-293 cells transfected with an expression vector encoding an A20-green fluorescent protein (GFP) fusion (119).

FLAG-A20
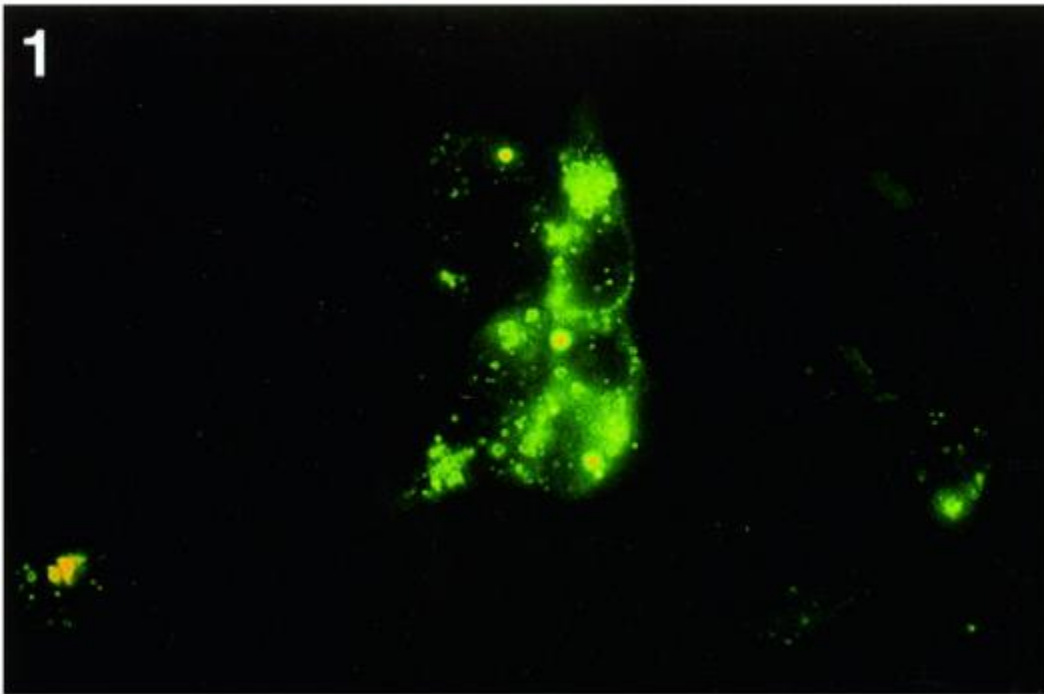
structures represent a membrane-bound cytoplasmic pool of A20 or alternatively, that A20 is involved in the process of lysosomal as well as proteosomal degradation of substrate molecules. One intriguing observation is that these structures morphologically resemble the POLKADOTS formed during T-cell activation and therefore (if morphology is related to function) may be similarly involved in the regulation of intracellular signaling (92).

Surprisingly, despite fact that A20 is recruited to MALT1 during T-cell activation, that A20 and MALT1 appear to have a reciprocal interaction and that the punctate structures formed by A20 resemble POLKADOTS, there are currently no publications describing whether A20 is either recruited to POLKADOTS or if it plays a role in their formation and stability. Indeed, a literature review has revealed that the majority of published articles dealing with the subject of A20 localization describe research performed in non-lymphoid cell types (PubMed search term: A20, accessed May 2013). Furthermore, there are very few publications regarding the physical interactions, colocalization, or reciprocal interactions that occur between A20 and the members of the CBM complex in either lymphoid or non-lymphoid cell types.

A Brief History of Biological Warfare

The history of biological warfare refers to the use of biological agents or the products of biological agents as a means of gaining a strategic or tactical advantage over an enemy and can be traced back to the classical period. However, the most descriptive account of early biological warfare involved the siege of Caffa in the 14th century (126). Caffa is located in what is now Feodosija, Ukraine. From the early to the mid-14th century it was a prosperous merchant city and was a main port for Genoese merchant vessels. Overtime, a rivalry developed between the Genoese merchants and the Mongol rulers of the region. As a form of defense and to protect their financial assets, the Genoese fortified the city of Caffa by surrounding it with two concentric walls. Eventually, the city was attacked by a Mongol army under the leader Janibeg. The siege of Caffa lasted from 1343 until 1344. The Mongol force was defeated by an Italian relief force. A second siege was attempted on the city. However, this time the Mongol forces found themselves besieged, not by an army but by an epidemic of plague. The disease decimated the Mongol troops and as a final effort to force the capitulation of the Genoese, they began to hurl the bodies of the dead over the city walls. An epidemic was soon established within the city walls. However, the Mongols were eventually forced to negotiate and end the siege

due to the blockade of essential supply routes by the Genoese navy. It is hypothesized, that the siege of Caffa led to the establishment of plague in the Mediterranean basin and was the source of the initial infection that eventually spread across Europe and became known as the "Black Death" (126). If this account is true, then the events which occurred during the siege of Caffa demonstrate the inherent destructive power of biological weapons and the potential consequences of their use during battle.

It is significant to note, that the germ theory of disease was not established until the latter half of the 19th century. Therefore, the Mongols were operating with little to no knowledge concerning the nature of the organisms with which they were dealing. Without this knowledge, the effectiveness of their technique could not be predicted which is most likely why the hurling of corpses was applied as a final effort toward securing victory and not as an initial means of achieving strategic and tactical momentum. Thus, at the latter half of the 14th century, biological weapons were most likely considered to be unreliable and unpredictable and were not commonly employed as a primary weapon system.

Once the germ theory of disease was established, individual organisms could be correlated with specific disease states and the outcome resulting from infection could, to some extent, be predicted. This

advancement made the application of biological weapons more reliable. However, the strategic advantage of these agents was still unpredictable due to a lack of knowledge concerning the mechanisms of pathogenesis, the biochemical characteristics of the organisms in question, and the nature of host immune responses.

During the early to late 20th century advances in biochemistry led to an increased ability to define the characteristics of an individual biological agent and to both predict and manipulate its characteristics. As a consequence, the idea of employing biological weapons to gain a strategic or tactical advantage became feasible. Advances in industrial processes and chemical engineering enabled both the United States and the Soviet Union to stabilize, standardize and stockpile numerous biological agents for use in war (91). Despite these advances, biological weapons were never employed on a large scale due to the remaining issues of instability of the organisms in the environment and the inability to control the magnitude infection and ensure the safety of friendly forces.

Modulation of Host Immunity as a Biological Threat

The period of time encompassing the late 20th century to the early 21st century was a period of unparalleled advances in the biological sciences. The pathogenesis of many diseases had been defined at the molecular level and the gradual rise in computing power coupled with the diffusion of knowledge through the internet led to an increase in the ability to manipulate biological agents. Such manipulations were usually performed with the goal of advancing general knowledge and to improve public health. However, they often had unintended consequences. For example, researchers working at the Australian Commonwealth Scientific and Industrial Research Organization (CSIRO) and the Australian National University collaborated on a project designed to determine whether it was possible to generate sterile mice by administering the eggshell protein Zona pellucida 3 (ZP3) into female mice by infection with a recombinant ectromelia virus (ECTV) expressing this protein (77). As a means of increasing anti-ZP3 antibody production in experimental animals, the investigators coinfected the cells with a recombinant mousepox virus expressing interleukin-4 (IL-4). IL-4 is a cytokine which is involved in perturbing the immune response toward an antibody mediated response. The investigators reasoned that co-infection with this virus would boost antibody production and have no adverse effect

on the animals. To their surprise, the expression of IL-4 led to a complete

suppression of the immune response against mousepox virus and all 10 of

the initial experimental animals died from mouse pox infection, including

those which had already been vaccinated against mousepox (77). This study

illustrates how manipulating the immune response can artificially increase

the lethality of a virus and circumvent currently available countermeasures

such as vaccine administration.

A20 Modulation as a means of Altering Host Immunity

A20 is a central regulator of the immune system (117, 118). This has

been demonstrated in the studies of Averil Ma and co-workers who showed

that A20 deletion in a mouse model leads to inflammation and death

resulting from normal flora (4). This has also been demonstrated in the

work of Maelfait and co-workers who demonstrated that the deletion of A20

in myeloid lineage cells can protect mice against a lethal challenge with

influenza-A virus (68, 77). It is a significant observation that such a

profound effect on the immune response can be regulated by a single

protein. The fact that A20 appears to have a non-redundant function in the

immune response indicates that A20 is a critical vulnerability and represents

an influential node in the network regulating the immune response that is amenable to intentional manipulation (68).

It is conceivable that current or future biological weapons designers will target A20 as a means of increasing the lethality of currently existing biological weapons or that they will design new genetically modified organisms with the ability to modulate A20 activity. A major obstacle toward the large scale employment of biological weapons is decay of the organism in the environment (112, 126). An aerosol distributed organism modified to modulate A20 in such a way as to down regulate the host immune response could be effective at a far lower concentration, than a wildtype organism, thereby circumventing environmental decay.

It has recently been discovered that cholera toxin is able to bind to A20, forming insoluble complexes that are not able to interact with substrate molecules (61). This interaction results in the inhibition of endosome-lysosome fusion and the degradation of epithelial barriers. It is conceivable that a binary weapon consisting of cholera toxin and a bacterial agent such as anthrax could be developed. The action of cholera toxin on the host cells would facilitate the spread of the anthrax toxins thereby increasing virulence (28, 41). Understanding the normal subcellular distribution and interactions

of A20 is necessary for the recognition of A20-modulating pathogens and the development of reliable countermeasures.

Specific Aims and Hypotheses

The subcellular localization of proteins is directly related to their function and proteins tend to operate within an environmental context. Macromolecular crowding, pH, and the chemical properties of local protein species all play a role in determining the behavior of proteins in a given region of the cytosol (5). It has been estimated that at least one-half of all proteins in the cell need to be transported from the site of synthesis, across one or more cellular membranes to reach a final functional destination (5). In addition, several proteins have been found to require proteolytic cleavage once reaching their functional location for complete activity. Protein cleavage and localization may serve as a means of increasing the diversity of protein function while maintaining economy in terms of protein synthesis (42, 76, 88, 94). In addition, aberrant protein cleavage and mislocalization have been implicated in the development of various disease states and malignancies.

Given the central role of A20 in the process of inflammation and the

regulation of both the innate and the adaptive immune responses,

understanding the subcellular localization of this protein and the

consequences of cleavage by the paracaspase MALT1 may allow insight

into the development of hematological malignancies and the mechanisms by

which infectious agents modulate the host immune response (88). In

addition, this knowledge is essential for the recognition and intentional

modulation of A20 activity by engineered biological agents. Therefore, the

focus of this dissertation is the characterization of the subcellular

localization of A20 and the consequences of proteolytic cleavage of A20 by

MALT1. These topics were addressed by the following specific aims:

Specific Aims

Specific Aim #1: Define the assembly and dynamics of the A20 punctate

structures formed in HEK-293 cells.

Hypotheses

- *Localization of A20 into punctate structures requires an intact*

    molecule. Truncated A20 will display a diffuse localization

    pattern.

•*A20 punctate structures are non-membrane bound and in dynamic*

association with the cytoplasm.

Specific Aim #2: Determine whether A20 is involved in the regulation of Bcl10 stability in HEK-293 cells.

Hypotheses

- *A20 is a negative regulator of Bcl10 in HEK-293 cells.*
- *A20 is itself under the regulation of other Bcl10-interacting molecules.*

Specific Aim #3 Evaluate the localization of A20 in T-lymphocytes.

Hypotheses

- *A20 forms punctate structures in the cytoplasm of T-cells.*
- *Localization of A20 in T-cells is regulated by TCR signaling.*

Chapter 2

Materials and Methods

Tissue culture

Human embryonic kidney cells (HEK-293T) were utilized as a model

non-lymphoid cell line (31). They were maintained at 37ºC in an

atmosphere of constant humidity and 5% CO_2 in Dulbecco's modified

Eagles Medium. This medium was supplemented with a combination of

heat inactivated 10% fetal bovine serum and 1% penicillin G/streptomycin

sulfate/gentamycin sulfate/glutamine (PSGG) supplement. D10 T-cells were

utilized as a model lymphocyte cell line (48). They were also maintained in

an atmosphere of constant humidity and 5% CO2 at 37ºC. D10 cells were

propagated in Clicks (EHAA) medium supplemented with PSGG and the

cytokine IL-2.

Antibodies

A20 was detected with the Imgenex murine IgG_1, kappa anti-A20

antibody (catalog number IMG-161A). This antibody was raised against full

length human A20. The epitope has been mapped to the A20 carboxy

terminal domain (amino acids 440-790). It recognizes both human and

mouse A20. A20 was also detected with two experimental rabbit antibodies

from Aviva Systems Biology. One of these antibodies, ARP61327_50

recognizes the N-terminal domain of A20 (amino acids 350-400) and the other one, ARP61326_P050 which recognizes the carboxy terminus of A20 (amino acids 695 to 745). Bcl10 was detected with mouse anti-Bcl10 from Santa Cruz Biotechnology, catalog # sc-5273 which recognizes amino acids 168-233. It was also detected with rabbit anti-Bcl10 from Santa Cruz Biotechology (catalog # sc-5611) which recognizes the N-terminal amino acids 1-197. P62 was detected with the Sigma polyclonal rabbit anti-p62/SQSTM1, catalog # P0067. LC3 was detected with rabbit anti-LC3 from Novus Biologicals, catalog #NB100-2220.

Confocal Microscopy

Confocal microscopy was performed using the Zeiss LSM 710 laser scanning confocal microscope (76). Images files were stored on an external hard drive and transferred to an appropriate desktop computer for processing. The resulting image files were processed using both the Zen and Zen-light versions the Zeiss imaging software package. Processing included adjusting the image control settings to achieve optimum contrast and color balance and saving the images in a tagged image file (TIF) format. Further processing was performed in Adobe Photoshop, and the final images were

again saved as TIF files. Fluorescence recovery after photobleaching (FRAP) was also performed with the use of the Zeiss 710 and the Zen software suite (45).

Plasmid and vector construction

The cDNA encoding A20 was initially obtained from IMAGE consortium expressed sequence tag (EST) clones. The polymerase chain reaction (PCR) was utilized to amplify full length A20 (amino acids 1-790), the OTU domain (amino acids 1-360), zinc fingers (ZNF-) 4-7 (amino acids 600-790), and ZNF- 1-7 (amino acids 380-790) using either full length or domain specific primers. The resulting products were then utilized to generate an HA-A20-YCit fusion, and HA-OTU-YCit fusion, and a HA-ZNF-1-7-YCit fusion. YCit refers to an engineered variant of the originally described yellow fluorescent protein and HA refers to an epitope tag derived from the influenza hemagglutinin surface glycoprotein (33). The resulting fusion proteins were then cloned into the pcDNA3 vector (Invitrogen) and used for HEK-293 transfections. This vector has been optimized for the expression of heterologous proteins in mammalian systems. An HA-Bcl10-GFP fusion had been previously developed in the Schaefer laboratory and

cloned into pCDNA3, and this construct was used for the studies reported here. For the stable transfection of T-cells, Flag-A20-TagRFP-T, Flag-ZNF-1-7-TagRFP-T, and Flag-ZNF-47-TagRFP-T fusions were generated and cloned into the pEhyg retroviral vector (96). Resulting virus was then used to infect D10 T-cells previously stably transduced with pEneo-Bcl10-GFP or wildtype D10 T-cells (98). After transduction, cell lines were selected with the appropriate antibiotics. We were able to generate cell lines co-expressing A20-tagRFPT or an A20-tagRFPT truncated mutant plus Bcl10-GFP, as well as cell lines expressing A20-tagRFPT or an A20-TagRFPT mutant alone. FLAG, refers to a synthetic epitope tag that has been added to the N-terminus of the proteins in question to facilitate tracking with anti-FLAG antibodies. TagRFPT refers to a monomeric version of the TagRFP red fluorescent protein with a serine to threonine mutation at position 158 to improve photostability (97).

T-cell stimulation

When T-cell stimulation was performed for analysis by confocal microscopy, glass coverslips were acid-etched and coated with poly-D-lysine. They were then incubated overnight at 4ºC immersed in a solution of

anti-CD3. The next day the coverslips were washed six times with a

solution of phosphate buffered saline (PBS) and sodium azide. After the

final wash, approximately 2×10^5 T-cells were placed on top of the coverslip

and incubated for the appropriate amount of time (58). After incubation, the

cells were fixed with a solution of 2% paraformaldehyde. After 10 min, the

cells were then washed again with PBS azide and mounted on a glass slide

with a glycerol-based mounting solution for imaging. For experiments in

which cells were stained with primary and secondary antibodies, following

fixation, cells were permeabilized with a 0.2% solution of trition X-100

followed by blocking with DMEM, followed by removal of the block and

addition of the primary antibody. After an incubation period of 1 hr to

overnight, the cells were then washed several times in PBS/azide and

incubated with the secondary antibody. Following secondary antibody

incubation, cells were washed with PBS/azide and mounted on a glass slide,

as described above.

Preparation of HEK-293 Cells for Analysis by Confocal Microscopy

HEK-293 cells were prepared for confocal microscopy by an analogous procedure to that used for T-cell analysis. Briefly, after transfection, the cells were allowed to grow overnight in six well tissue culture plates in which poly-d lysine coated glass coverslips had been placed. About 1×10^5 cells were used per treatment. Following appropriate media changes, the cells were fixed with a solution of 2% paraformaldehyde and either attached to a glass slide for analysis or permeabilized and treated with the appropriate antibodies.

Preparation of HEK-293 Cells for Analysis by Immunoblotting

When HEK-293 cells were to be analyzed by immunoblotting. About 6×10^5 cells were plated in each well of a 6 well tissue culture plates and the appropriate treatment was performed. Following a media change, the cells were harvested by scraping and pipetting and transferred to a 15 ml conical tube, where they were washed once with PBS followed by lysis by boiling in 2X SDS-PAGE loading buffer. Genomic DNA was disrupted by sonication and the lysates were stored at 4ºC.

SDS PAGE Immunoblotting Procedure

SDS-PAGE refers to sodium dodecyl sulfate polyacrylamide gel electrophoresis (8). The procedure used in this study is based on the Laemmli method. This method employs a two-tiered gel system in which the bottom tier is referred to as the resolving gel and the upper tier is referred to as the stacking gel. Resolving gels were prepared by combining a 30% acrylamide mix, 1.0M Tris (pH 8.8), 10% SDS, 30% ammonium persulfate, tetramethylethylenediamine (TEMED), and H_2O. The resulting solution was then poured into a Hoefer vertical gel apparatus, covered with a thin layer of H_2O and allowed to incubate at room temperature for at least 30 min to allow the polymerization process to occur. The next day, a 5% tris-glycine stacking gel was made by combining a 30% acrylamide mix with 1.0M Tris (pH 6.8), 10% SDS, ammonium persulfate, TEMED ,and H_2O. This solution was then placed directly on top of the resolving gel once the thin layer of H_2O was removed. A 15 well comb was placed in the stacking gel as a means of creating wells for sample addition. The solution was then allowed to polymerize for one hour. Samples to be analyzed on the SDS-PAGE gel were boiled for 5 min at 100 ºC. They were next loaded into the wells of the SDS-PAGE gel at a volume of 15-20 μl. A standardized molecular weight marker was added to one of the wells and any empty wells

were also loaded with a molecular weight marker to prevent sample

diffusion. The gel was then run at 100V until the sample entered the

resolving gel. The voltage was then increased at 50V increments every 15

minutes until a final voltage of 250 was obtained. The gel was allowed to

run until the markers were clearly separated. Subsequently, the gel

apparatus was disassembled and the gel was trimmed to an appropriate size.

A semi-dry transfer apparatus was utilized to transfer proteins directly from

the gel to a nitrocellulose membrane. This was accomplished by adding a

small amount of transfer buffer to the surface of the apparatus and evenly

distributing it. Next, three sheets of absorbent paper were cut to the

dimensions of the gel and placed on the transfer apparatus, a sheet of

nitrocellulose was also cut to the dimensions of the gel and placed on top of

the absorbent paper. This was followed by the gel and three more sheets of

absorbent paper. In order to ensure proper electrical conductance, the both

the absorbent paper and the nitrocellulose membrane were soaked in transfer

buffer prior to their placement on the transfer apparatus. The transfer buffer

consisted of 0.04% SDS, 20% methanol, 48mM Tris, 39mM glycine and

H_2O. Once the transfer apparatus was assembled, transfer was performed by

connecting the apparatus to a power supply and applying an electrical

current to the apparatus at a rate equivalent to gel surface area. For example,

a 200 square centimeter gel would receive a current of 200 milliamps. The transfer was allowed to progress for 2 hours. After the completion of the transfer step, the apparatus was disassembled and the nitrocellulose membrane was removed. The membrane was then blocked in a blotto solution. Blotto was first described by Johnson and Elder in 1984, it consists of a 5% w/v solution of dehydrated milk, Tris (pH 7.5) and H_2O. Blocking was allowed to proceed for approximately 1 hour, the membrane was then incubated with the appropriate primary and secondary antibodies. Generally, the membrane was incubated with primary antibodies (diluted in blotto) overnight with constant agitation in the cold room at 4ºC. After washing with PBS three times for 15 minutes each time, the membrane was then incubated with secondary antibody (also diluted in blotto) for three hours at room temperature with agitation. The dilutions of the antibodies were performed according to manufacturer specifications. Following the incubation with the secondary antibody, the membrane was again washed with PBS and developed with the West Dura super signal substrate by Pierce and imaged with the Fuji LAS-3000 CCD camera system. The images were saved on an external hard drive and post-collection analysis and modification was performed using Photoshop.

Transfections

Transfections were performed using the chemical based transfection method described by Graham and van der Eb in 1973 (31). This method utilizes the formation of insoluble calcium phosphate precipitates which incorporate plasmid DNA. These complexes are added to the cells, which are able to ingest them by an undescribed mechanism resulting in the plasmid DNA being transported to the nucleus and associated with the general transcription machinery. All transfections in this study were performed using the HEK-293 cell line. A transfection procedure began with the plating of 600,000 cells in a well of a six well plate. These cells were initially maintained in DMEM media until the day of transfection, 24 hours later. On this day, the DMEM was aspirated out of the well and replaced with Iscove's modified Dulbecco's medium or IMDM. Calcium phosphate precipitates of plasmid DNA were prepared by mixing an appropriate amount of plasmid DNA with 7.5ul of 2.5M $CaCl_2$ and sterile H_2O to a final volume of 75 ul. This solution was then mixed with 75 ul of 2✕ Hepes (140mM NaCl, 1.5mM $NaPO_4$, 50mM Hepes, pH 7.05). After a 1 minute incubation the resulting mixture was added drop-wise to the cells in IMDM media. The plate was then rocked gently by hand to facilitate equal distribution of the calcium phosphate-DNA precipitates and incubated at

37ºC and 5% CO_2 overnight. The following day, the media was replaced

with DMEM and the cells were incubated for another 24 hour period. On

the final day, the cells were recovered from the six well plate by scraping

and pipetting, washed one time with PBS and lysed in 2× SDS-PAGE lysis

buffer as described above. Cell lysates were stored at 4ºC until an analysis

by SDS-PAGE was performed.

Luciferase Assays

The NF-κB luciferase assay was performed as a means of assessing

the physiological functionality of A20 and A20 truncated mutants. This

assay was performed by taking approximately 100,000 HEK 203 cells, and

plating them in a six well plate. One well was assigned for each treatment.

The cells were then transfected with a mixture of the following plasmids:

HA-Bcl10-GFP as an NF-κB activator, pBVI-NF-κB-Luc as a luciferase

reporter plasmid which expresses luciferase under the control of an NF-κB

inducible promoter, pEF1-Bos-β-gal, a β-galactosidase reporter plasmid

used as a transfection control, pcDNA-p35 a plasmid which expresses the

baculovirus anti-apoptotic protein p35 to promote cell survival. pBluescript

was added to maintain total DNA concentration to a constant level (600 ng).

pcDNA3 constructs containing the coding sequence of full length A20 or zinc fingers 4-7 were used as potential NF-κB inhibitors. After a 48 hour incubation and appropriate media change, cells were washed with PBS and incubated with the Promega reporter lysis buffer. They were then lysed on ice by pipetting. Lysates were next vortexed and centrifuged and supernatants were transferred into either a 96 well luciferase plate or a 96 well plate for performing a β-galactosidase assay. Detection of luciferase activity was measured by the ability to cleave luciferin to yield a fluorescent product. Light generation was detected by a luminometer. The expression of β-galactosidase was detected by measuring 420 nm absorbance in a spectrophotometer equipped with a 96-well plate holder.

Chapter 3

Results

Full length A20 is required for the formation of static punctate cytoplasmic structures in HEK-293 cells

The formation of punctate cytoplasmic structures by A20 has been previously observed in fixed HEK-293 cells, live HEK-293 cells, and live NIH 3T3 cells (25, 119). Biochemical experiments have indicated that A20 segregates into insoluble structures in the cytoplasm and tends to associate with lysosomes (63). At the present time, there is no data regarding the minimum domains of A20 necessary for the formation punctate cytoplasmic structures or if the formation of these structures is required for the ubiquitin editing function of this molecule.

We addressed this issue by taking HEK-293 cells, transfecting them a mammalian expression vector (pCDNA3) expressing either an HA-A20-YCit fusion protein, an HA-OTU-YCit fusion protein, an HA-ZNF-1-7-YCit fusion, or a combination of HA-OTU-YCit and HA-ZNF-1-7-YCit. Transfected cells were then evaluated by confocal microscopy. The goal of this experiment was to determine whether full length A20 is required for the formation of punctate structures in HEK-293 cells or if it is possible for a truncated mutant to form these structures. The results are presented in Figure 11.

Figure 11. Full length A20 is required for the formation of punctate cytoplasmic structures in HEK-293 cells. HEK-293 cells were transfected with pCDNA3 expressing HA-A20-YCit, HA-OTU-YCit, HA-zNF-1-7-YCit, or a combination of HA-OTU-YCit and HA-zNF-1-7-YCit. Transfected cells were then evaluated by confocal microscopy using the Zeiss LSM 710.
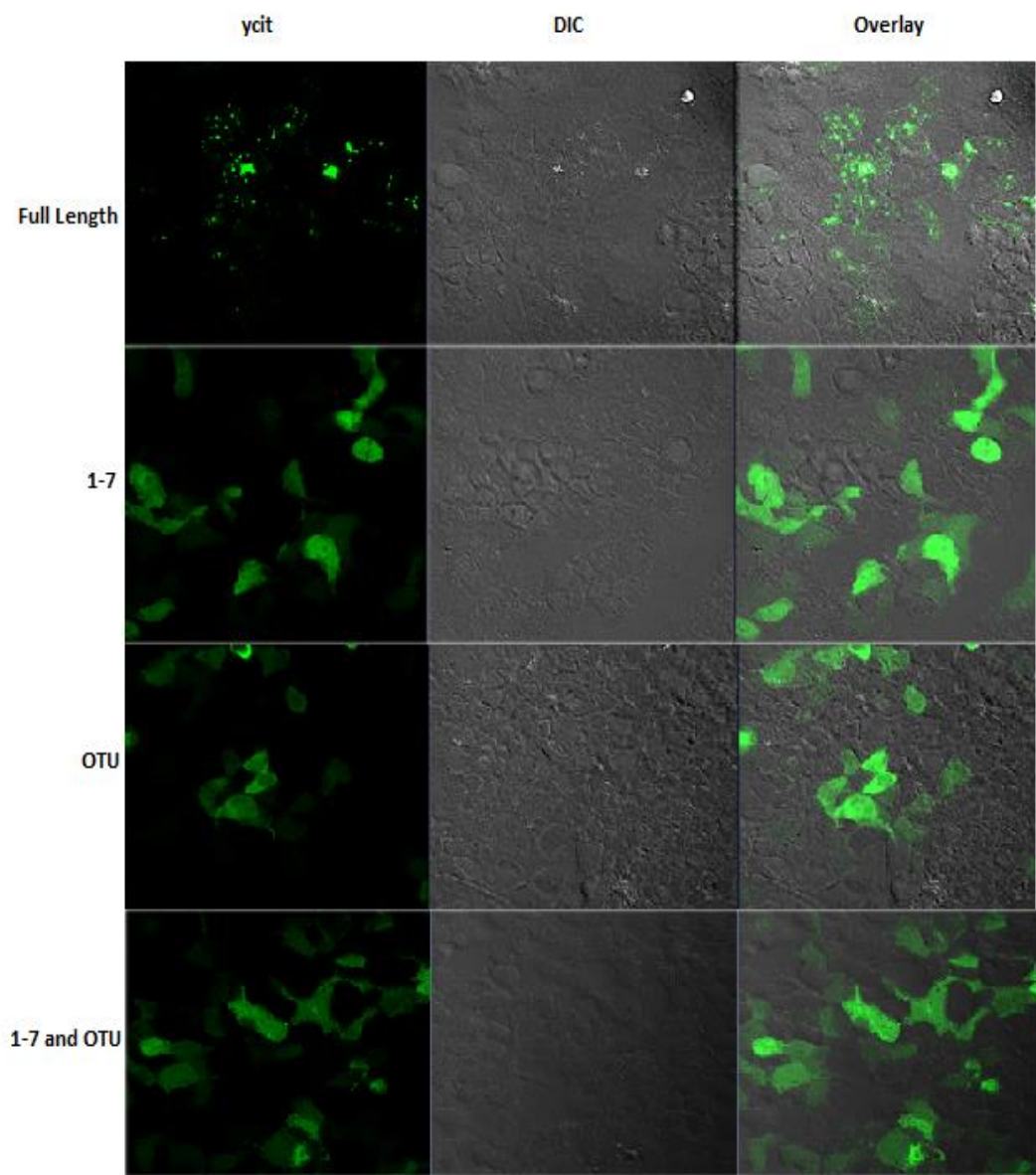
In this study, full length A20 was found to form punctate structures in the cytoplasm of the HEK-293 cells, as expected. However, zinc fingers 1-7 tended to be diffuse in the cytoplasm and did not localize into discrete cytoplasmic structures. It is interesting to note that the zinc finger 1-7 fragment seems to be evenly distributed between both the cytoplasm and the nucleus, as there is no central clearing indicating exclusion from the nucleus. The OTU domain was also evenly distributed in the cytoplasm. However, nuclear exclusion is visible in some of the cells, indicating that the OTU domain is preferentially localized to the cytoplasm. This may indicate the presence of a nuclear export signal, indicate that the OTU domain preferentially binds to cytoplasmic proteins, or indicate that the OTU domain is unable to efficiently pass through the nuclear pore complex. We also performed a co-transfection of the OTU domain and zinc fingers 1-7. The goal of this experiment was to determine whether or not the presence of the OTU domain and the zinc finger domain in the cytosol is sufficient for the formation of punctate structures. The resulting data are also presented in Figure 11. As can be deduced from the images, co-expression of the OTU domain and the zinc finger domain is not sufficient to allow the formation of A20 punctate structures.

In order to determine whether the A20 punctate structures are static

membrane bound structures or whether they are dynamic structures which

are at equilibrium with the cytosolic A20 pool, we performed a series of

FRAP (fluorescence recovery after photobleaching) experiments using the

Zeiss LSM 710 confocal microscope (45). In these experiments, live HEK-

293 cells expressing A20-YCit, zinc fingers 1-7-YCit, or OTU-YCit were

visualized using standard low laser power to visualize the protein fusions.

Next, the laser was focused at high power on a specific region of interest

(ROI), causing the fluorescent dye to bleach. The ROI was continually

monitored for the return of fluorescence after photobleaching, indicating

diffusion of protein from the unbleached area into the bleached area. As

Figures 12 and13 demonstrate, when full length A20-YCit is photobleached

with a high power laser, the punctate structure residing in the region of

interest loses fluorescence immediately. Moreover, fluorescence and does

not recover during the 5 minutes post-photobleaching visualization period.

This indicates that the A20-YCit localized within the punctate structures are

not in a dynamic association with the cytosol. Such a situation could reflect

that full-length A20 is membrane bound, or within a vesicle. Interestingly,

the OTU-ycit fusion appears more granular in live cells than it did in the

fixed cells (compare with Figure 11). When this domain is photobleached at

a given region of interest it recovers after 20 seconds and when the zinc finger 1-7-ycit fusion is photobleached it recovers after only 5 seconds. The difference in recovery time may be due to the OTU domain interacting with ubiquitinated proteins in the cytosol, thereby restricting it to specific locales within the cytoplasm. Alternatively, this difference in recovery times may reflect a mobility-inhibiting conformation the case of the OTU domain or a tightly packed mobility enhancing conformation in the case of the zinc finger motifs.

There are several ways that these data can be interpreted. The lack of punctate structure formation from truncated A20 may indicate that a specific protein conformation is required for A20 to aggregate. In other words, punctate structure formation may be a conformational phenomenon. Another possibility is that truncation of A20 results in the destruction of a particular linear epitope or domain that is required for punctate structure formation. It may also be that the synergistic action of the cysteine protease and ubiquitin ligase domains are required for this specific form of subcellular localization. It is conceivable that A20 cytosolic punctate structures represent intracellular stores of A20 which are maintained in an inactive state by sequestration in cytoplasmic vesicles and activated by cleavage and release from these vesicles.

Figure 12: Full length A20 cytosolic punctate structures are not in dynamic equilibrium with the cytosol but truncated mutants are freely diffusible. Live HEK-293 cells were imaged at 60✕ during the FRAP experiment. The results show that photobleached full length A20 punctate structures do not recover up to five minutes post-bleaching. Images A-C represent 0 seconds, 4 seconds, and 5 minutes post-bleaching respectively. Zinc fingers 1-7 are freely diffusible in the cytoplasm and recover at 5 seconds post-bleaching, D-F represent 0 seconds, 5 seconds and 30 seconds respectively. The OTU domain is also freely diffusible but recovers at a slower rate than zinc fingers 1-7, G-I represent 0 seconds, 4 seconds, and 20 seconds respectively.

**Fluorescence Recovery
After Photobleaching**

Full Length
A20

Zinc fingers
1-7
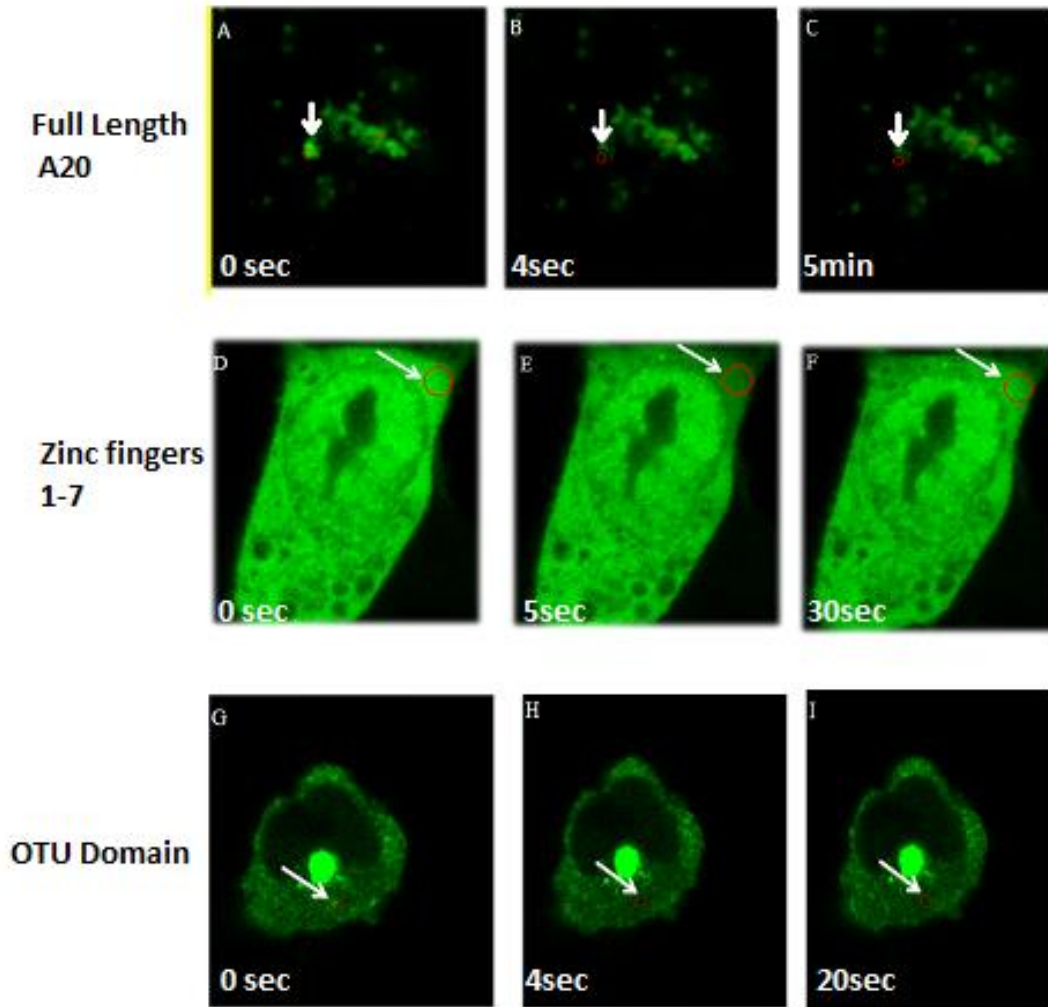
OTU Domain

Figure 13. Fluorescence intensity vs. time curves of the FRAP experiments demonstrating that full length A20 is static in the cytosol while zinc fingers 1-7 and the OTU domain are freely diffusible. Image A shows a representative fluorescence recovery curve for the full length A20-ycit fusion. The green line represents fluorescence intensity and the white line represents an unbleached control region. Fluorescence intensity is plotted on the y-axis and time is plotted on the x-axis. The point at which the green line drops represents the point of photobleaching at which the intensity dropped to 0. No recovery was seen for A20 punctate structures. Image B is a representative FRAP experiment for the zinc fingers 1-7-ycit fusion. In this case, the white line represents the fluorescence intensity and no control point was used. The quick recovery of zinc fingers 1-7 is evident by the V-shaped plot. Image C represents the results for the OTU domain. In this case, the green line represents the intensity of the fusion protein. OTU did not bleach as well as the zinc fingers but it did recover indicating free diffusion.

A. Full Length A20 (Green line=FL-A20 intensity White line=control region)

Time (Min)
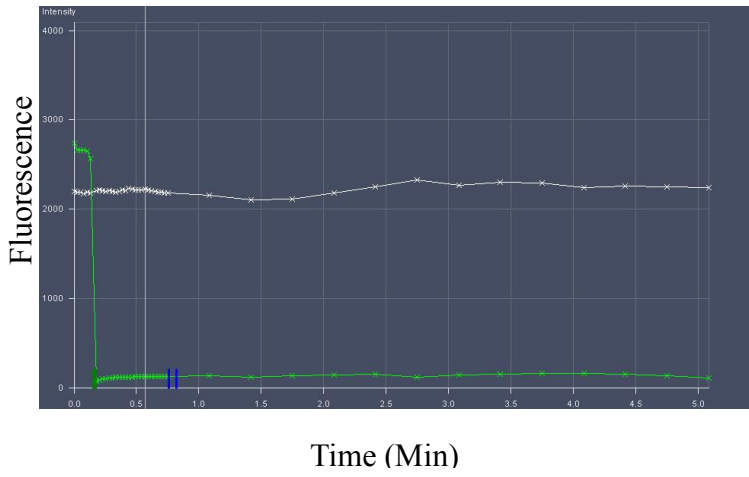
B. Zinc Fingers 1-7 (White line=ZNF- 1-7 intensity)

Time (Min)
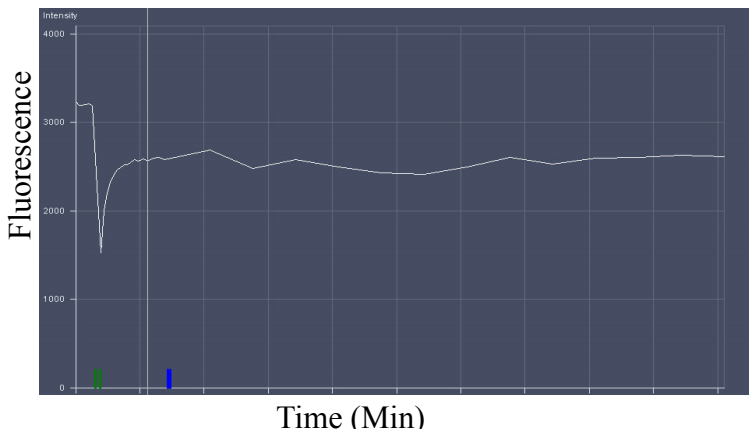
C. OTU Domain (Green line=OTU intensity White line=control region)

Time (Min)
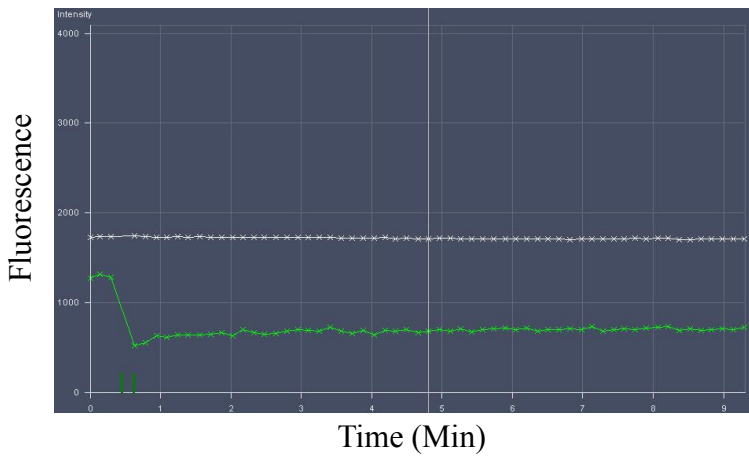
Endogenous A20 is recruited to Bcl10 filaments in HEK-293 Cells

Previous research has shown that overexpression of Bcl10 is sufficient to cause NF-κB activation (34, 124). It has also been shown that overexpressed Bcl10 tends to form elongated filamentous structures within the cytoplasm, and that these structures are able to recruit various members of the NF-κB-associated signaling cascade (34). Given that A20 has been shown to regulate NF-κB activation by Bcl10 and that Bcl10 has been shown to regulate the activity of A20, we sought to determine whether Bcl10 filaments are capable of recruiting A20 in the cytoplasm of HEK-293 cells. This was accomplished by transfecting HEK-293 cells with a high concentration of pcDNA3 expressing HA-Bcl10-GFP followed by evaluation by confocal microscopy. A total of 1500 ug of plasmid was found to reliably lead to the formation of intracellular filaments, so this was chosen as the amount of plasmid for this study. Following transfection, the cells were permeabilized with Triton X-100 and stained with an anti-A20 antibody which recognizes the C-terminal domain. The secondary antibody was labeled with Alexa Fluor 647 to facilitate the visualization of A20. The results are presented in Figure 14. It is interesting to note that the transfection of 1500 ug of pcDNA3 expressing HA-Bcl10-GFP did in fact result in the formation filamentous structures composed of aggregated Bcl10

Figure 14: A20 is recruited to Bcl10 filaments in the cytoplasm of HEK-293 cells. HEK-293 cells were transfected with 1500ug of pcDNA3 expressing HA-Bcl10-GFP. The cells were then permeabilized and stained with anti-A20 followed by a secondary antibody labeled with the Alexa-Fluor 647 dye. Image A is a 60X DIC image of an individual HEK-293 cell. Image B is a fluorescent image of the same cell showing the location of the GFP signal, indicating the presence of Bcl10-GFP. Image C is a fluorescence image specific for Alexa Fluor 647 which shows the localization of A20 and image D is an overlay.
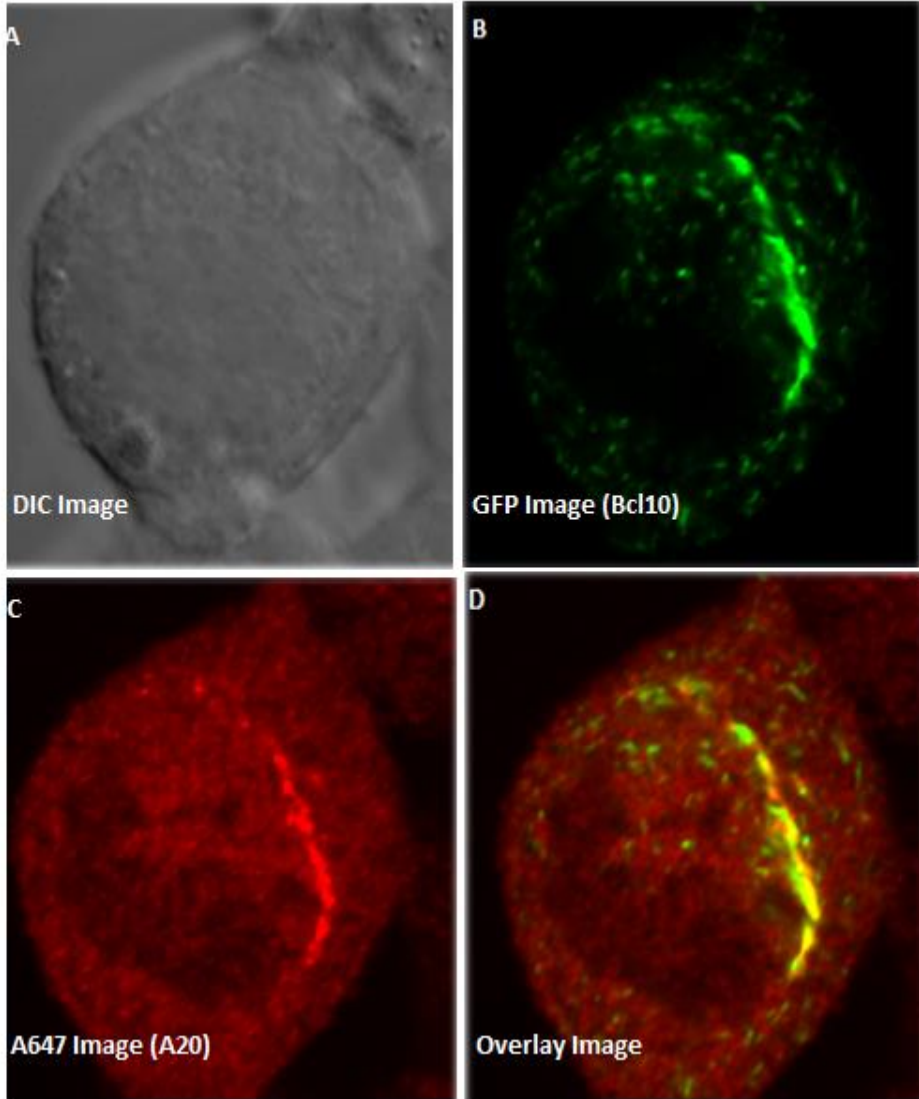
in the cytoplasm (Image B). In this particular experiment, the Bcl10

filaments are dispersed throughout the cytosol. However, there is a

concentrated localization on the right side of the cell and little to no Bcl10 is

present in the nucleus. The Alexa-Fluor 647 or A20 signal is evenly

dispersed throughout the cell, however there is a clear co-localization on the

right side of the cell where the A20 signal overlaps with the Bcl10 signal in

a one to one fashion indicating recruitment of A20 to the Bcl10 filaments.

Typically A20 expression is down-regulated in non-lymphoid cells and

highly induced upon the activation of the NF-κB cascade. Therefore, the

A20 present in the cytosol in the HEK-293 cells used in this experiment

most likely represent protein that was produced during Bcl10 mediated NF-

κB activation. These data suggest that the A20 protein produced under

Bcl10 mediated NF-κB activation remains stable in the cytoplasm and is

recruited to Bcl10 filaments. The mechanism of Bcl10 mediated recruitment

of A20 was not explored in this study. However, Bcl10 is known to contain

a caspase recruitment domain (CARD), which is a known protein-protein

interaction interface (34). Also, Bcl10 is ubiquitinated during signaling to

NF-κB, and A20 is binds to some ubiquitinated molecules (128). To

exclude the possibility that A20 was recruited to a particular spatial

geometry of the Bcl10 filament, we evaluated several filament types.

Representative data for this study are presented in Figure 15 which shows that A20 can be recruited to short globular filaments as well as to the long extended conformation seen in Figure 14.

The recruitment of A20 into Bcl10 filaments may occur for several reasons. A20 is known to be a potent negative regulator of NF-κB activation, and A20 may be recruited to Bcl10 mediated complexes as a means of rapidly inactivating the NF-κB enhancing effects of Bcl10. Alternatively, A20 may localize to ubiquitinated complexes as a prepositioning step and it may remain associated with these complexes until an as yet undiscovered signal activates A20 and causes the inactivation of the NF-κB signaling cascade. It is also a distinct possibility that A20 plays an unknown role in propagating the NF-κB activating signal mediated by Bcl10. The zinc finger domains of A20 are known to have the ability to act as protein-protein interfaces and in this instance A20 may be functioning as a scaffolding molecule. Further research is required to clarify the role of A20 in the Bcl10 induced signaling complex.

A20 Prevents the Assembly of Bcl10 filaments in HEK-293 Cells

As stated previously, A20 has been shown to have a negative impact upon NF-κB activation mediated via Bcl10 and Malt1 (110). However,

Figure 15: The geometry of Bcl10 filaments does not alter their ability to recruit A20. This Figure shows a representative 60X image of a short globular Bcl10 filament. A. DIC image. B. GFP image showing the localization of Bcl10. C. Alexa Fluor 647 image showing the localization of A20. D. Overlay.

A — DIC Image

B — GFP Image (Bcl10)

C — A647 Image (A20)

D — Overlay Image
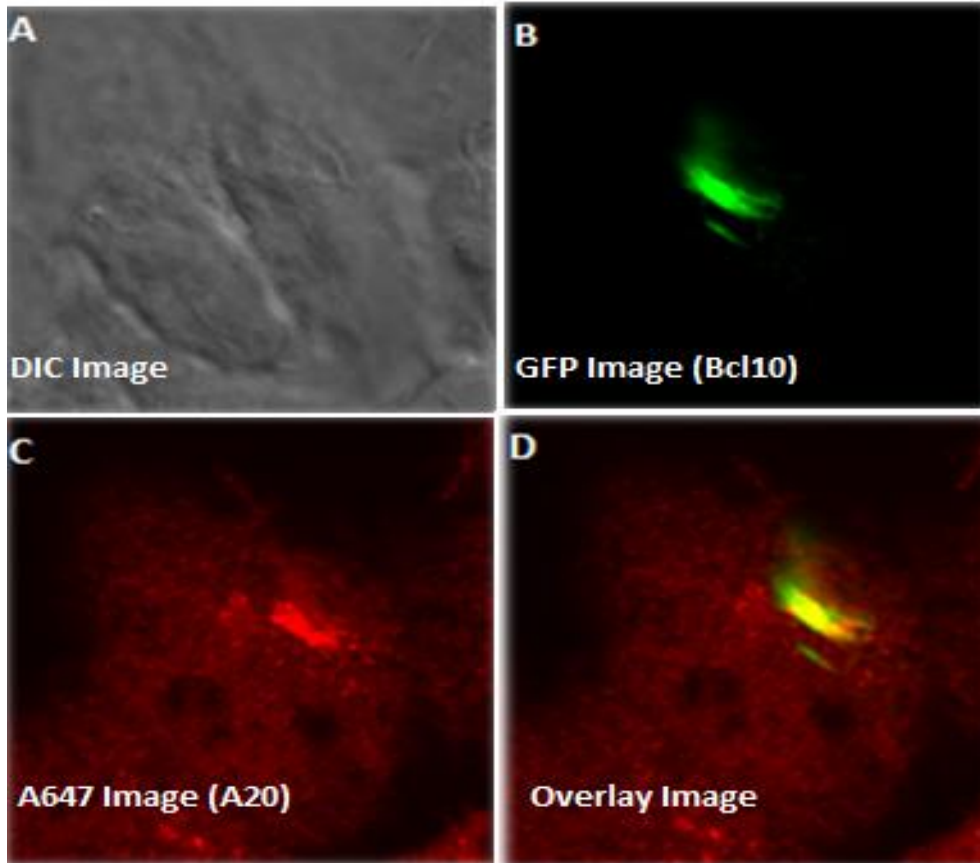
there is currently no published literature indicating whether or not A20 is involved in regulating the formation or stability of Bcl10 filaments. To address this issue, we performed a series of experiments in which we co-transfected a constant amount ofpcDNA3 expressing HA-Bcl10-GFP with an increasing quantity of pcDNA3 expressing HA-A20 with no fluorescent protein. We then evaluated the transfected cells by confocal microscopy. Interestingly, we found that the signal from filaments typically formed by HA-Bcl10-GFP decreased in a linear fashion with the increase in HA-A20 (Figure 16). Most striking was the fact that a comparison of cells transfected with HA-Bcl10-GFP only vs. cells co-transfected with HA-Bcl10-GFP and 500 ng HA-A20. This comparison revealed that the Bcl10-GFP signal in the A20-co-transfected cells was more elongated and diffuse. This may indicate destabilization of the Bcl10 filaments. Indeed, when 1500 ng of A20 was used, the Bcl10 filaments were completely absent. These data indicate that A20 is involved in regulating the formation and stability of Bcl10 filaments and suggests that the recruitment of A20 to Bcl10 filaments may represent a negative regulatory process.

A20 zinc fingers 4-7 but not full length A20 negatively regulate the stability of Bcl10

Since our imaging data revealed that A20 colocalizes with Bcl10 in the cytoplasm of HEK-293 cells and tends to negatively regulate the formation and stability of Bcl10 filaments in the cytoplasm, we sought to determine whether A20has a negative impact upon the stability of the Bcl10 protein itself. To do this, we again utilized the technique of DNA transfection and the titration of plasmid concentration. However, rather than evaluating the transfected cells by confocal microscopy, we assessed Bcl10 protein levels by SDS-PAGE followed by immunoblotting for the proteins of interest with the appropriate antibodies. We began by transfecting HEK-293 cells with 1500 ng of a pcDNA3 HA-Bcl10-GFP expression vector. The cells were then transfected with 0 to 800 ng of pcDNA3-HA-A20-YCit. After the appropriate incubation time and media changes, the cells were harvested and whole cell lysates were prepared. The lysates were then denatured by boiling in 1✗ Laemmli buffer, run on an SDS-PAGE gel, transferred to nitrocellulose and probed with a rabbit anti-HA antibody. Representative results are presented in Figure 17. Interestingly, there was little to no effect on HA-Bcl10-GFP stability with increasing concentrations of full-length A20. These data suggest that full-length A20 does not promote Bcl10 proteolysis. A recent publication by the laboratory of Rudi

Beyaert in Belgium reported that A20 in T-lymphocytes is cleaved upon T-cell receptor stimulation The cleavage site in human A20 has been mapped to arginine 439 and results in the release of a 37kd N-terminal A20 fragment (15). Their data also suggest that the N-terminal cleavage product is unstable in the cytoplasm and degrades after a short period of time. The Beyaert group hypothesized that this cleavage process evolved as a means of dampening the NF-κB inhibitory effect of A20 to promote T-cell activation. Interestingly, the cleavage site in human A20 is located between zinc fingers 1 and 2, while the cleavage site in mouse A20 is located between zinc fingers 4 and 7. Our imaging studies of HA-zinc finger 4-7-GFP fusions suggest that this A20 fragment is not unstable in the cytosol and tends to have diffuse localization. We therefore asked whether the A20 zinc fingers 4-7 fragment has an effect on Bcl10. in HEK-293 cells. We transfected HEK-293 cells with a constant quantity of pCDNA3- HA-Bcl10-GFP, and an increasing quantity of vector expressing HA HA-Zinc finger 4-7-ycit. After transfection and incubation, the cells were lysed in 2✕ SDS PAGE buffer and the lysates were evaluated by Western Blot using an anti-Bcl10 antibody as a probe. This experiment revealed that the levels of Bcl10 protein decrease with increasing quantities HA-Zinc finger 4-7-ycit (Figure 18). These results suggest that zinc fingers 4-7 display an activity distinct

Figure 16: A20 negatively regulates the formation and stability of Bcl10 filaments in HEK-293 cells. HEK-293 cells were transfected with either 2000 ng of pcDNA3-HA-Bcl10-GFP or co-transfected with pcDNA3- HA-Bcl10-GFP and 500ng-1500ng of pcDNA3- HA-A20.   A-C, no A20. D-F, 500 ng of A20. G-I, 1500 ng of A20. Note that the Bcl10-GFP fluorescence signal becomes diffuse with a reduction in intense Bcl10 filaments as A20 concentrations are increased.

GFP Image (Bcl10)	DIC Image	Overlay

0ng A20

500ng A20

1500ng A20
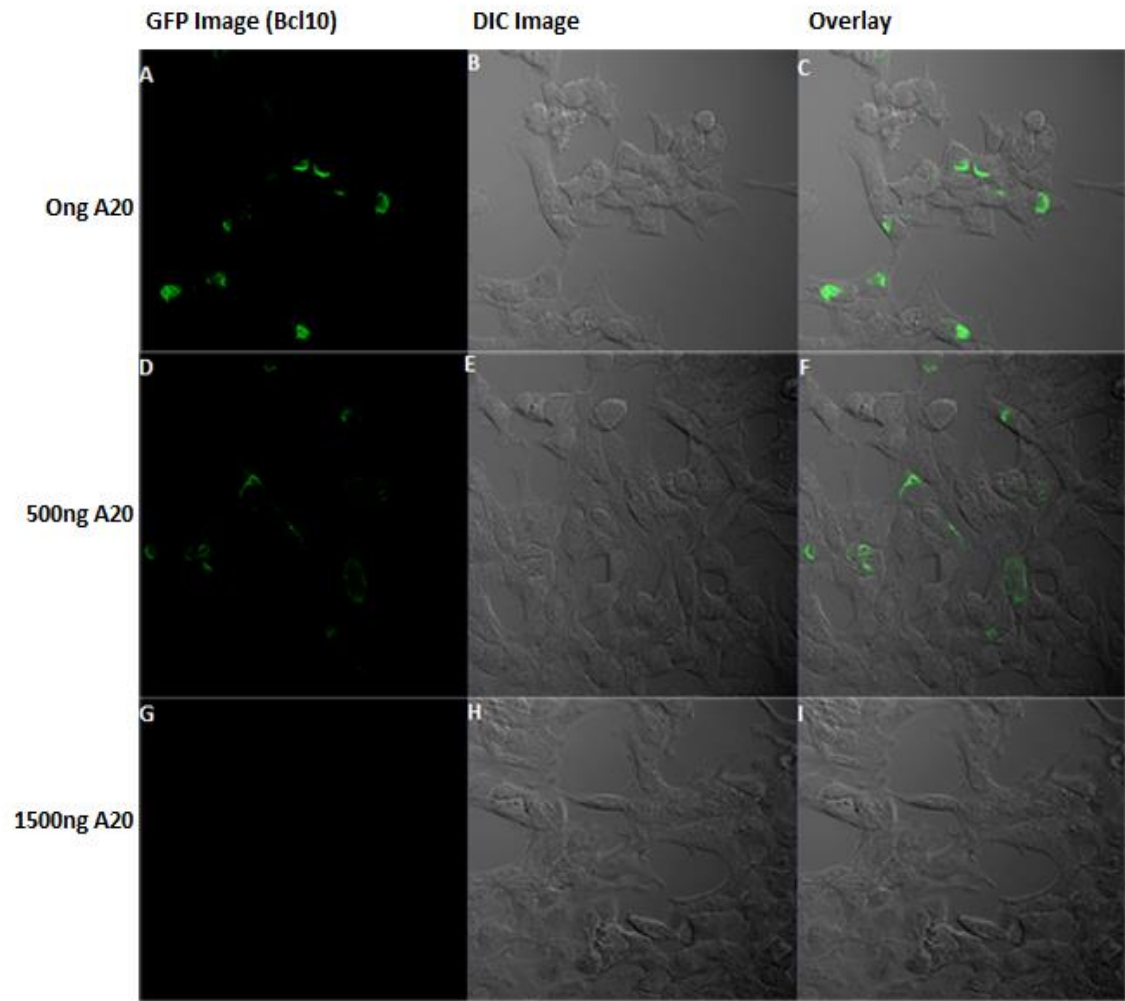
Figure 17: Increasing concentrations of full length A20 has a negligible effect on Bcl10 stability in HEK-293 cells. HEK-293 cells were transfected with 800ng of pcDNA3- HA-Bcl10-GFP and increasing concentrations of pcDNA3-HA-A20-ycit. Cells were lysed in 1X SDS-PAGE sample buffer and lysates were separated on a 15% acrylamide gel followed by Western transfer to nitrocellulose and probing with rabbit anti-HA. The membrane was then stripped and reprobed with anti-GAPDH as a loading control.
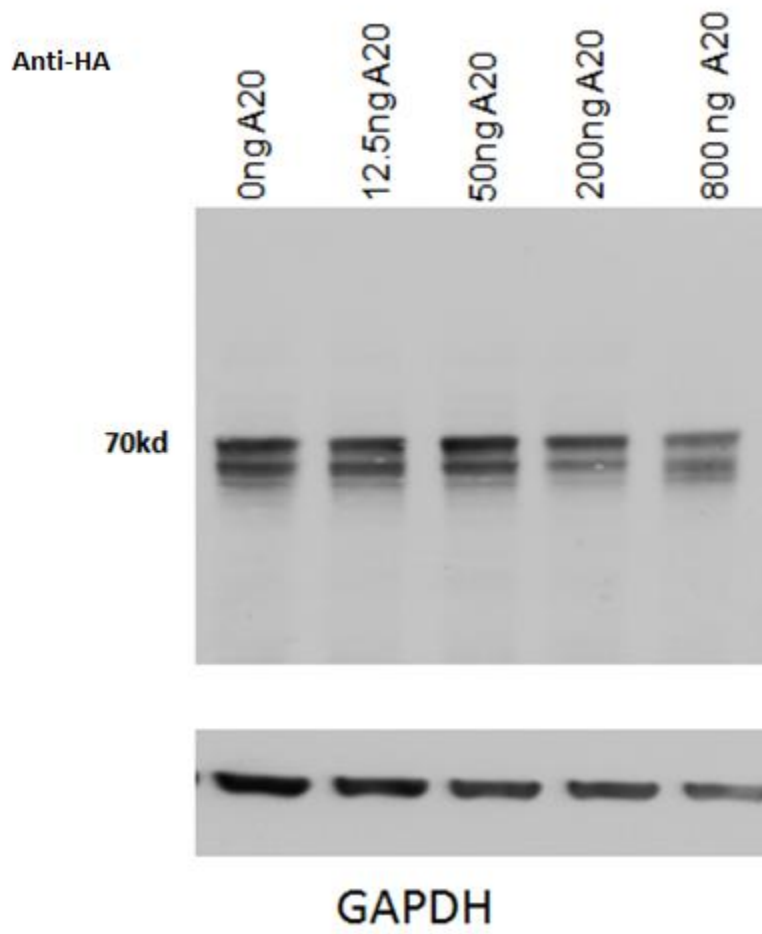
Figure 18: Zinc fingers 4-7 cause the degradation of HA-Bcl10-GFP in a dose dependent manner in HEK-293 cells. HEK-293 cells were transfected with a constant quantity of vector expressing HA-Bcl10 –GFP (800ng). Increasing quantities of vector expressing HA-ZNF- 4-7-YCit were co-transfected. Cell lysates were evaluated on a 10% acrylamide gel followed by Western transfer and detection with a rabbit anti-Bcl10 primary antibody followed by an HRP conjugated secondary. The membrane was then stripped and reprobed with anti-GAPDH as a loading control.

Anti-Bcl10

0ng A20 4-7   50ng A20 4-7   500ng A20 4-7   1500ng A20 4-7

70kd
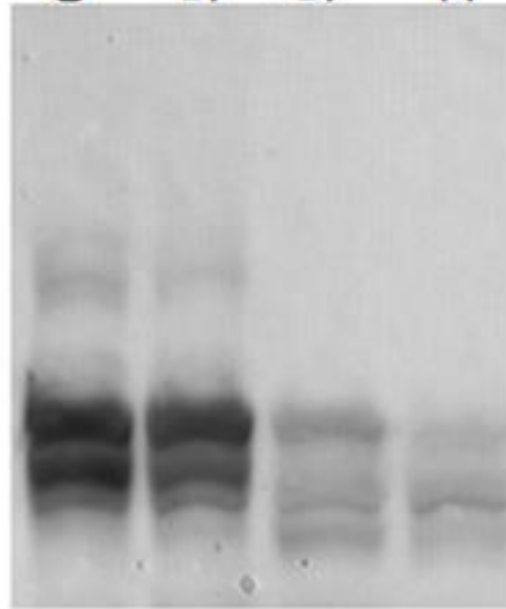
GAPDH
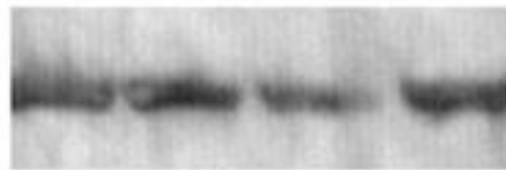
from full-length A20, and that expression of this fragment accelerates the proteolysis of Bcl10.

Intriguingly, there appeared to be Bcl10 cleavage products visible on the blot in the lanes with high levels of HA-ZNF-4-7-YCit. To confirm the formation of a Bcl10 cleavage product, we repeated the experiment and evaluated the results on a higher concentration acrylamide gel. Indeed, a lower molecular weight Bcl10cleavage product was visible (see Figure 19). This indicates either that A20 zinc fingers 4-7 may have an intrinsic enzymatic ability and is able to directly cleave Bcl10, or that this fragment is capable of recruiting the necessary enzymatic machinery to effect Bcl10 proteolysis. To determine whether this activity is specific to Bcl10 or whether zinc fingers 4-7 accelerate the degradation of proteins in a non-specific manner, we co-transfected HEK-293 cells with 500ng of a vector expressing GFP and increasing quantities of A20 zinc fingers 4-7. No GFP degradation was observed (see Figure 20). This indicates that zinc fingers 4-7 have a specific activity against Bcl10. A dose response was also performed in which endogenous MALT1 was evaluated with increasing concentrations of zinc fingers 4-7. We observed no degradation of MALT1, again confirming specificity (data not shown). As stated above, ubiquitination of Bcl10 is a crucial regulator of signaling to NF-κB. In

Figure 19: Dose response of HA-Bcl10 to increasing quantities of A20-Zinc fingers 4-7 in HEK-293 Cells. Cells were transfected with 800ng of a vector expressing HA-Bcl10-GFP and increasing quantities of a vector expressing HA-A20-zinc finger 4-7-ycit. A 15% acrylamide gel was used to evaluate the lysates. Rabbit anti-Bcl10 was used for detection. The arrow indicates a possible Bcl10 cleavage product.
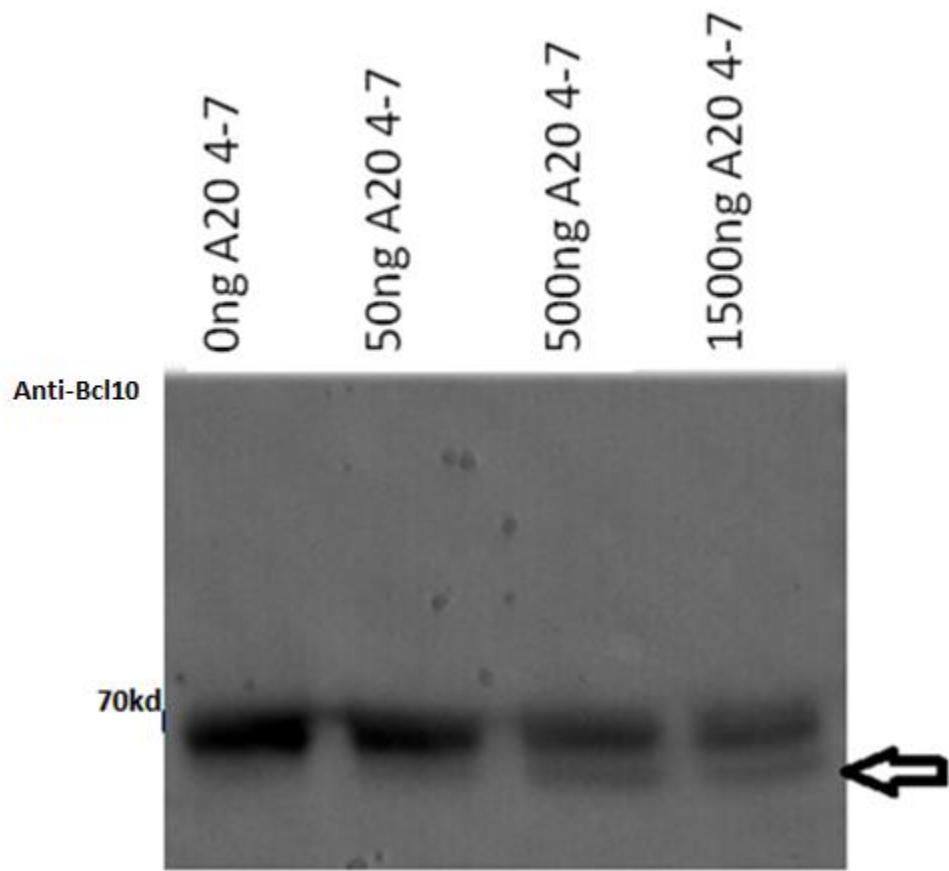
Figure 20: A20 zinc fingers 4-7 have no effect on pcDNA3-GFP expression levels. HEK-293 cells were transfected with 500ng of a vector expressing GFP and increasing quantities of a vector expressing HA-zinc fingers 4-7-ycit. Lysates were evaluated on an 8% acrylamide gel and the resulting blot was probed with anti-GFP.

0ng A20 4-7

100ng A20 4-7

1500ng A20 4-7

Anti-GFP

30kd

GAPDH
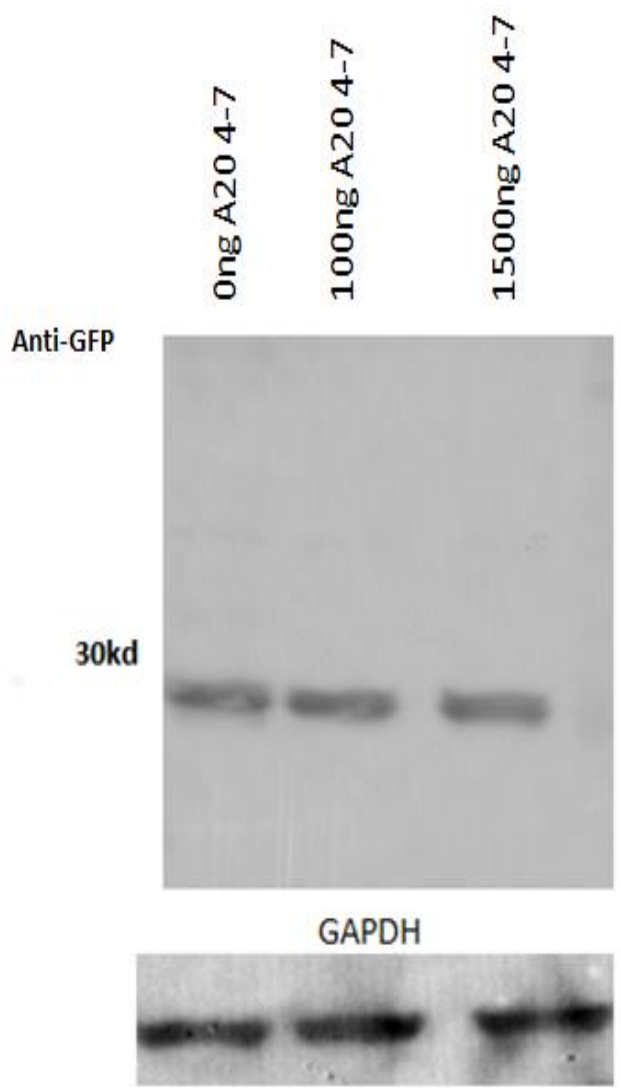
particular, it has been shown that the ubiquitination of Bcl10 at lysines 31

and 63 are essential for the recognition of this molecule by the NF-κB

essential modulator (NEMO), which is the non-catalytic component of the

IκB kinase (IKK) complex that directs terminal activation of NF-κB (127).

The recognition of Bcl10 by NEMO is necessary for NF-κB activation.

Since A20 is known to down-regulate Bcl10 mediated NF-κB activation, we

sought to determine whether ubiquitination of lysines 31 and 63 are required

for the degradation of Bcl10 by zinc fingers 4-7. This was done by

transfecting HEK-293 cells with a vector expressing a Bcl10 fusion protein

in which lysines 31 and 63 are replaced with arginine. The cells were co-

transfected with increasing concentrations of a vector expressing HA-zNF-4-

7-ycit and evaluated by a Western blot probed with anti-Bcl10. A linear

decrease in anti-Bcl10 signal was observed indicating that ubiquitination at

lysine 31 and 63 are not required for A20 zinc fingers 4-7 to mediate the

degradation of Bcl10 (see Figure 21). It should be noted that a complete

map of Bcl10 ubiquitination sites has not yet been compiled and therefore,

zinc fingers 4-7 may bind to alternative Bcl10 ubiquitination sites. In

addition, the ubiquitination status of Bcl10 may change during cell

activation. This may facilitate the interaction of A20 with Bcl10 at specific

times and in specific subcellular locations. As a

Figure 21: A20 zinc fingers 4-7 do not require the ubiquitination of Bcl10 at positions 31 and 63 to accelerate the degradation of Bcl10. HEK-293 cells were transfected with 800ng of a vector expressing HA-Bcl10-kkrr-YCit and increasing concentrations of a vector expressing HA-Zn-finger 4-7 YCit. Lysates were analyzed on an 8% acrylamide gel and the resulting blot was probed with rabbit anti-Bcl10. The membrane was then stripped and reprobed with anti-GAPDH as a loading control.
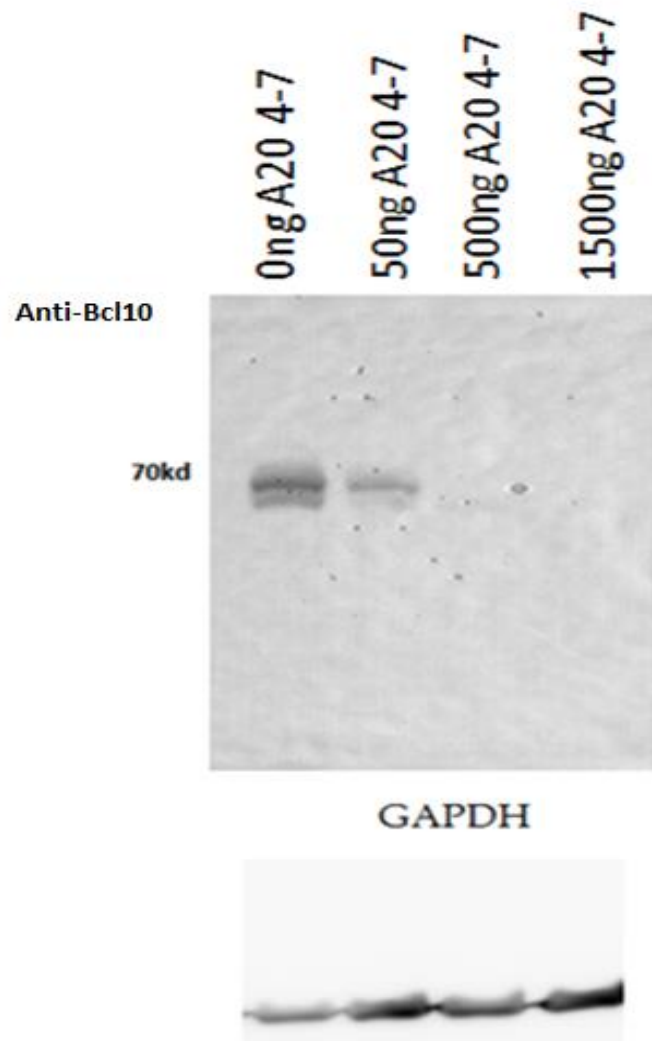
means of evaluating the physiological relevance of zinc finger 4-7 activity,

we performed an NF-κB luciferase assay. HEK-293 cells were transfected

with a series of plasmids including an NF-κB reporter in which luciferase

expression is under the control of a minimal promoter plus five NF-κB

binding sites. HA-Bcl10- GFP was used as an NF-κB activator and HA-

A20-YCit and HA-zNF-4-7-YCit were co-transfected. Interestingly,

although both full length A20 and zinc fingers 4-7 were able to down-

regulate NF-κB activation, full length A20 more effective (see Figure 22).

This result may suggest that while full-length A20 does not cleave Bcl10, it

has other activities that potently inhibit Bcl10-mediated NF-κB activation.

The intact A20 molecule may thus act on the NF-κB signaling pathway, in a

manner that is mechanistically distinct from the activity of the c-terminal

ZNF-4-7 domains. More functional studies are required to resolve this issue.

Zinc finger domains 1-7 and 4-7 can be independently recruited to Bcl10
filaments in HEK-293 cells

The majority of the data accumulated during this study indicate that

zinc fingers 4-7 are capable of catalyzing the degradation of Bcl10.

However, there are currently no published studies indicating whether the

Figure 22: NF-κB luciferase assay demonstrating that zinc fingers 4-7 have physiological activity. An NF-κb luciferase assay was performed in HEK-293 cells with cotransfection of Bcl10 and either full-length A20 or A20 zinc fingers4-7.

Comparison of NFkB inhibition (Full Length A20 vs Zinc fingers 4-7)
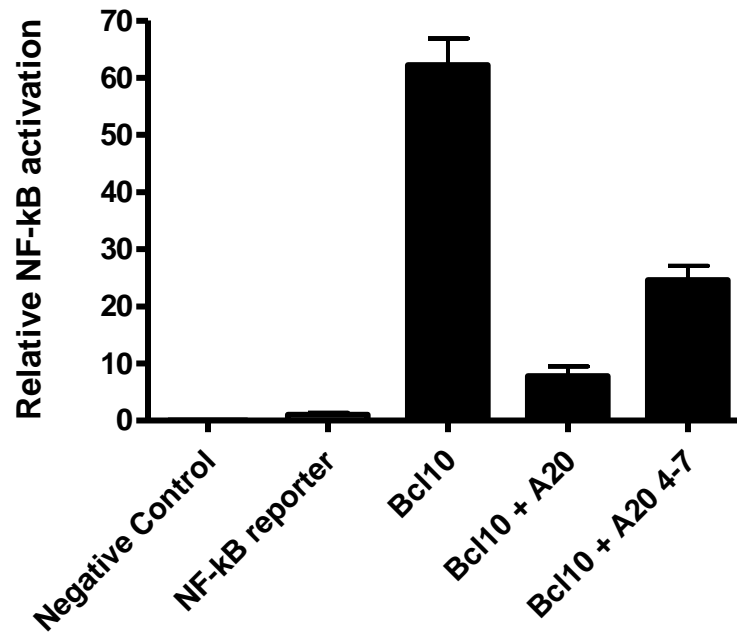
zinc finger domains are capable of interacting with Bcl10 or whether the

zinc fingers are capable of independently co-localizing with Bcl10 filaments.

Therefore, we decided to determine the localization patterns of the A20 zinc

finger domains with respect to Bcl10 in HEK-293 cells. Cells were co-

transfected with 800 ng of a pcDNA3 vector expressing HA-Bcl10-GFP and

800 ng of pEhyg expressing either Flag-zNF-1-7-TagRFP-T or Flag-zNF-4-

7-TagRFP-T. The transfected cells were then evaluated by confocal

microscopy. Bcl10 formed globular filamentous structures as expected, and

both A20 zinc fingers 1-7 and A20 zinc fingers 4-7 were recruited (see

Figure 23).   These data represent the first report of the association of A20

zinc finger domains with Bcl10 filaments. These data also represent the first

report suggesting an independent function for the zinc finger domains and

illustrate the fact that an intact A20 protein is not required for the interaction

between A20 and Bcl10.

A20 colocalizes with Bcl10 during T-cell activation

There are very few publications which explore the role of A20 in T-

lymphocytes and at the current time there are no data concerning the

localization of A20 during T-cell stimulation. Since we have been

Figure 23: A20 zinc finger domains are independently recruited to Bcl10 filaments. HEK-293 cells were transfected with a vector expressing HA-Bcl10-GFP and a vector expressing either Flag-ZNF-1-7-TagRFPT or Flag-ZNF-4-7-TagRFPT. Transfected cells were evaluated by confocal microscopy. Images A-D show cells co-transfected with Bcl10 (green) and Zinc fingers 1-7 (red) expression plasmids. Images E-H shows cells co-transfected with Bcl10 (green) and zinc fingers 4-7 (red).

	DIC	GFP (Bcl10)	TagRFP-T (A20)	Overlay
Zinc Finger 1-7	A	B	C	D
Zinc Finger 4-7	E	F	G	H
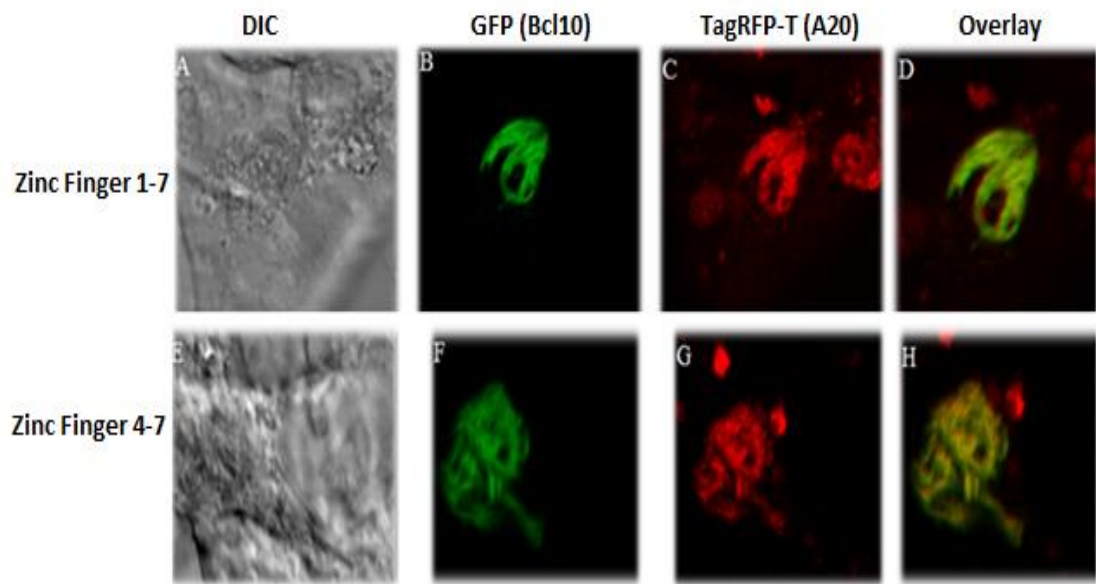
accumulating data suggesting that A20 is involved in the regulation of Bcl10 stability, we sought to determine whether A20 colocalizes with Bcl10 in the cytoplasm of T-cells. D10 T-cells stably expressing HA-Bcl10-GFP were stimulated with plate bound anti-CD3 for 0 - 60 minutes. We fixed and permeabilized the cells and stained with anti-A20 and an Alexa-fluor 647 secondary antibody. The cells were then evaluated by confocal microscopy (see Figure 24). At 0 minutes post stimulation, Bcl10 was diffuse in the cytoplasm and A20 tended to form punctate structures as previously described. By 20 minutes post-stimulation Bcl10 began to form long filamentous structures which also colocalized with A20. However, by 1 hour post-stimulation, the filamentous structures were no longer apparent, and only punctate structures of both Bcl10 and A20 remained. There was sporadic co-localization between the A20 punctate structures and the Bcl10 punctate structures. These data provide proof that A20 is recruited to Bcl10 in T-lymphocytes and that this event is stimulation dependent.

Since zinc fingers 4-7 have been previously shown to bind ubiquitin and since our studies have shown that zinc fingers 4-7 may have a novel Bcl10 degrading catalytic activity, we wanted to determine whether zinc fingers 4-7 can be independently recruited to Bcl10 in D10 T-cells. D10 T-

Figure 24: Endogenous A20 colocalizes with exogenous Bcl10 during T-cell stimulation. D10 T-cells stably expressing HA-Bcl10-GFP were stimulated for 0 minutes to 1 hour with plate bound anti-CD3. The cells were then stained with Imgenex anti-A20 to detect endogenous A20 and evaluated by confocal microscopy.

| DIC | GFP | Alexa-Fluor 647 | Overlay |

0 min

20 min

1hr
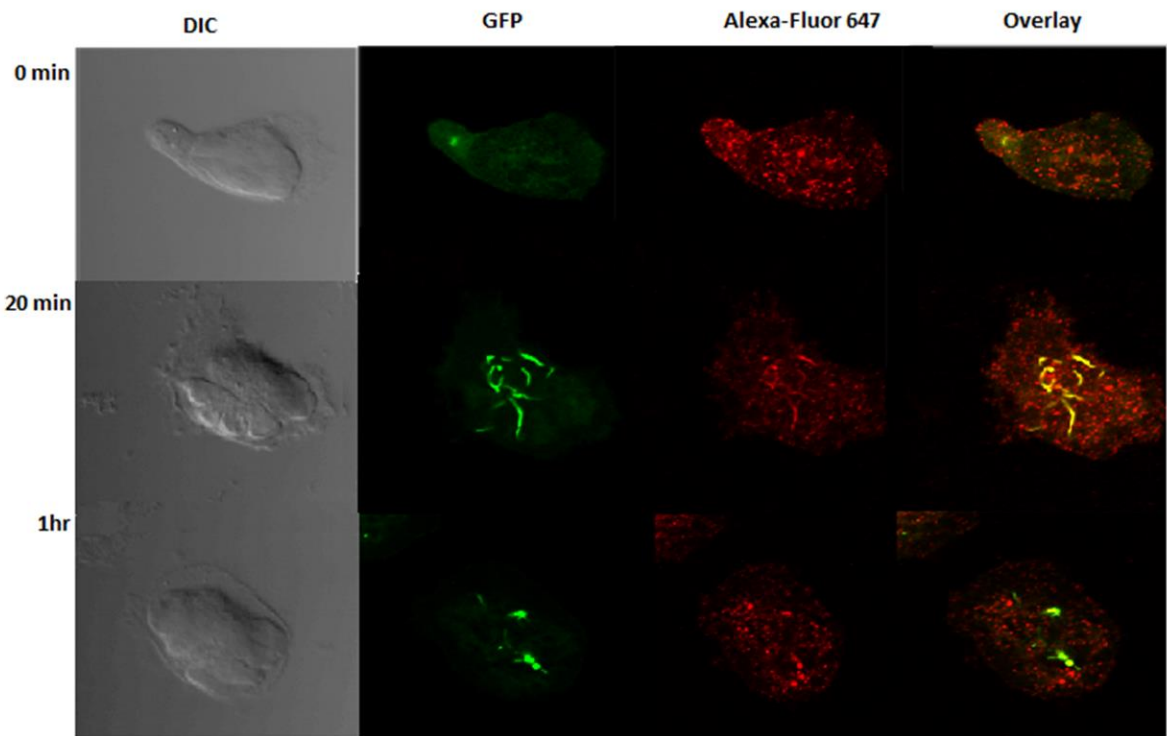
cells stably expressing HA-Bcl10-GFP and Flag-ZNF-4-7-TagRFPT were stimulated with plate bound anti-CD3 for 0 minutes to 1hr. Interestingly, Bcl10 appeared dim in the co-expressing cells which may be due to zinc finger 4-7 induced degradation (see Figure 25).   At 0 minutes post-stimulation, Bcl10 was diffuse in the cytosol and zinc fingers 4-7 displayed both diffuse and punctate localization. At 20 minutes post-stimulation Bcl10 did not form filamentous structures as it had in cell lines expressing only HA-Bcl10-GFP. This may also be due to zinc finger 4-7 induced degradation of Bcl10 or the zinc finger domains may modulate the kinetics of filament formation. However, by 1 hour post-stimulation Bcl10 filaments formed and recruited zinc fingers 4-7.

To exclude the possibility that the co-localization of A20 with Bcl10 in D10 T-cells is a cell-line dependent artifact we stimulated mouse primary CD8+ T-cells plate bound anti-CD3. We next stained with anti-A20 and anti-Bcl10 and utilized confocal microscopy for evaluation. Interestingly, at 20 minutes post-stimulation, both A20 and Bcl10 formed punctate structures and these structures colocalized with A20 punctate structures (Figure 26). These data demonstrate that the colocalization of A20 with Bcl10 in T-lymphocytes is not a cell line artifact.

Figure 25: A20 zinc fingers 4-7 colocalize with Bcl10 during T-cell activation. D10 T-cells co-expressing HA-Bcl10-GFP and Flag-A20-ZNF-4-7-TagRFP were stimulated for 0 minutes to 1 hour with plate bound anti-CD3. The cells were then evaluated by confocal microscopy.
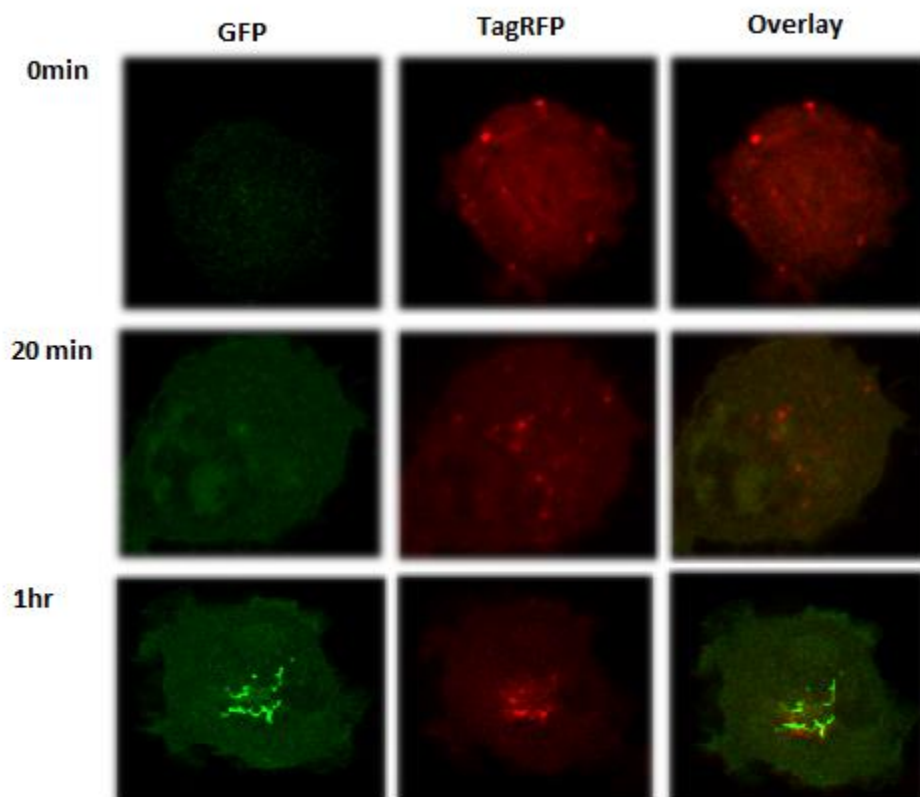
Figure 26: Endogenous A20 colocalizes with Endogenous Bcl10 in stimulated CD8+ Primary T-cells. Primary CD8 + T-cells were stimulated for 20 minutes with plate bound anti-CD3. The cells were then permeabilized and stained with rabbit anti-Bcl10 followed by an Alexa-fluor 488 (A488) secondary and mouse anti-A20 followed by an Alexa-fluor 647 (A647) secondary. Evaluation was performed by confocal microscopy.

	DIC	A488 (Bcl10)	A647(A20)	Overlay

Cell 1

Cell 2
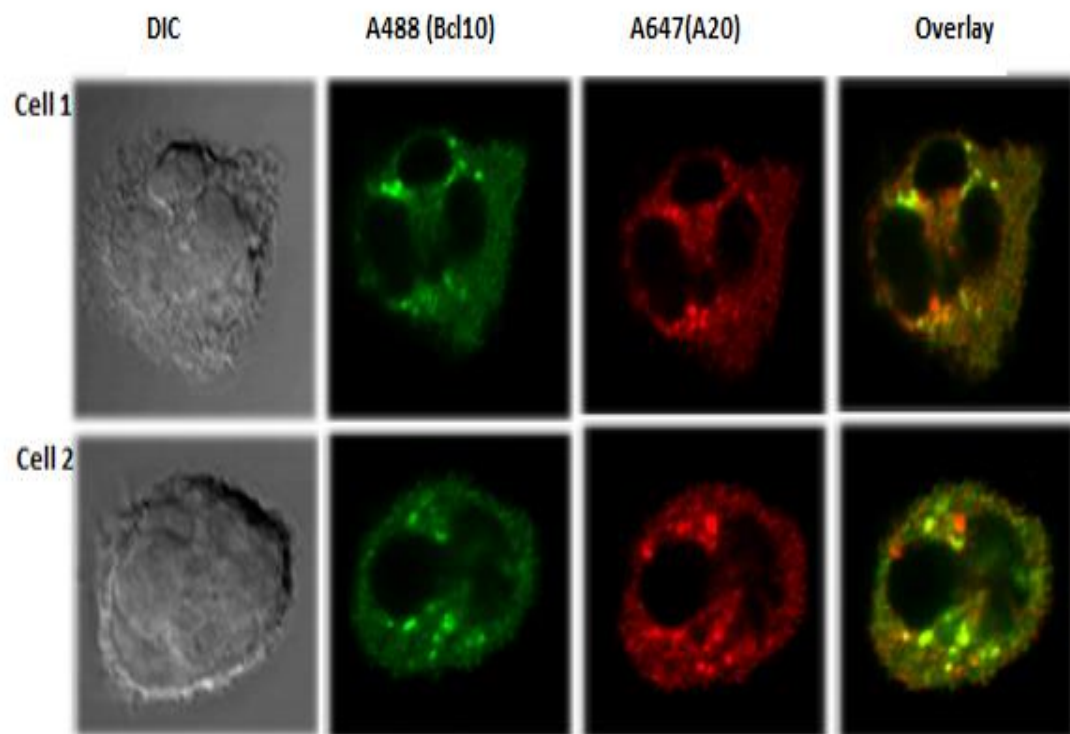
A20 is colocalizes with members of the autophagy cascade and is negatively regulated by BinCard

Recent work in the Schaefer laboratory has shown that Bcl10 can be degraded in T-lymphocytes by an autophagy based mechanism (89). Since A20 is recruited to Bcl10 filaments in T-cells, we performed several experiments to determine whether A20 associates with the mediators of autophagy. This work was initiated by transfecting HEK-293 cells with HA-A20-ycit and then staining transfectants with anti-light chain 3 (LC3). LC3 has been used for several years as a robust marker of autophagosomes. When the process of autophagy commences, LC3 is attached to phosphatidyl-ethanolamine and targeted to autophagic vesicles. As shown in Figure 27, A20 punctate structures frequently colocalize with LC3. Although not conclusive, this is evidence that A20 may regulate the process of Bcl10 autophagy.

p62 is an ubiquitin binding protein which interacts with proteins destined for degradation by the autophagy process (21). p62 auto-aggregates in the cytosol, and a subset of ubiquitinated proteins bind to these p62 aggregates. p62 also interacts with LC3, resulting in the transport of aggregates of p62 and associated ubiquitinated proteins into autophagosomes. In order to determine whether A20 is associated with the process of autophagy in T-cells, we stimulated D10 T-cells stably expressing

Figure 27: A20 Colocalizes with LC3 in the cytoplasm of HEK-293 cells. HEK-293 cells were transfected with 1500ng of pCDNA3-A20-ycit and stained with anti-LC3 as a primary antibody and an Alexa-fluor 647 substituted secondary antibody. Cell s were evaluated via confocal microscopy. The images below are representative 60X images zoomed in to reveal A20 co-localization with LC3. Ycit was detected with the GFP channel on the confocal microscope.

DIC GFP Alexa-Fluor 647 Overlay
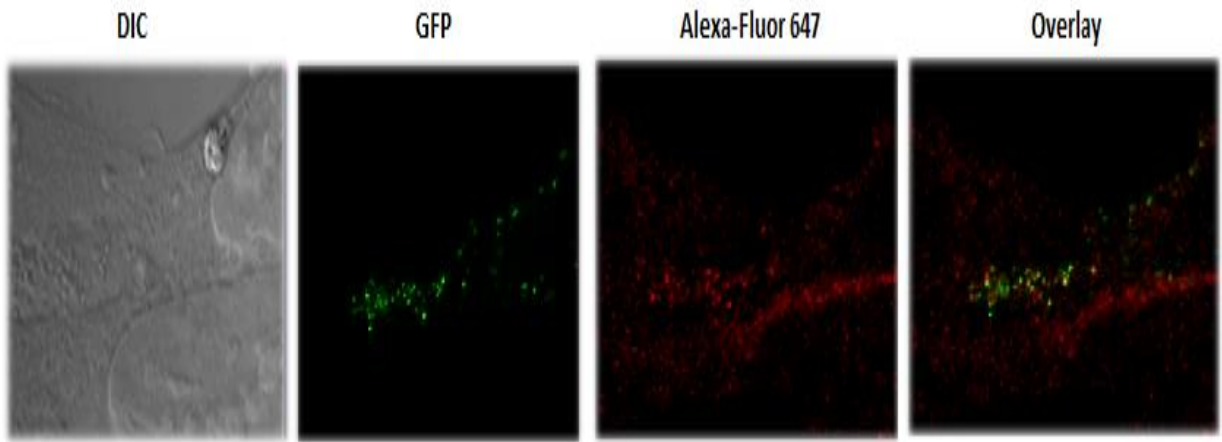
Flag-A20TagRFPT with plate bound anti-CD3 and then stained with anti-

p62 (see Figure 28). As can be seen in the resulting Figure, A20 punctate

structures clearly colocalize with p62 at 20 minutes post-stimulation.

However, this association is transient, and is no longer observed by 1 hour

post-stimulation (data not shown). These data indicate that A20 may be

involved in Bcl10 autophagy in T-lymphocytes and that Bcl10 association

with A20 is stimulation dependent and transient.

The Bcl10 interacting protein (BinCard) is a recently described

CARD containing protein (127). BinCard has been found to interact with

Bcl10 and unpublished studies by the Schafer lab have suggested that

BinCard may be involved in the negative regulation of Bcl10 signaling to

NF-κB. Since A20 also appears to be involved in the negative regulation of

Bcl10 and since A20 can be recruited to Bcl10 filaments in both lymphoid

and non-lymphoid cells, we performed a study to determine whether there is

evidence of functional interaction between BinCard and A20. HEK-293

cells were transfected with either a vector expressing HA-A20-YCit or co-

transfected with a vector expressing HA-A20-YCit and an equal quantity

Figure 28: A20 colocalizes with P62 in stimulated D10 T-cells. D10 T-cells stably expressing Flag-A20-TagRFPT were stimulated for 20 minutes with anti-CD3. The cells were permeabilized and stained with anti-P62 followed by an Alexa-fluor 647 secondary. Two representative cells are shown.

	DIC	TagRFPT	Alexa-Fluor 647	Overalay
Cell 1				
Cell 2				
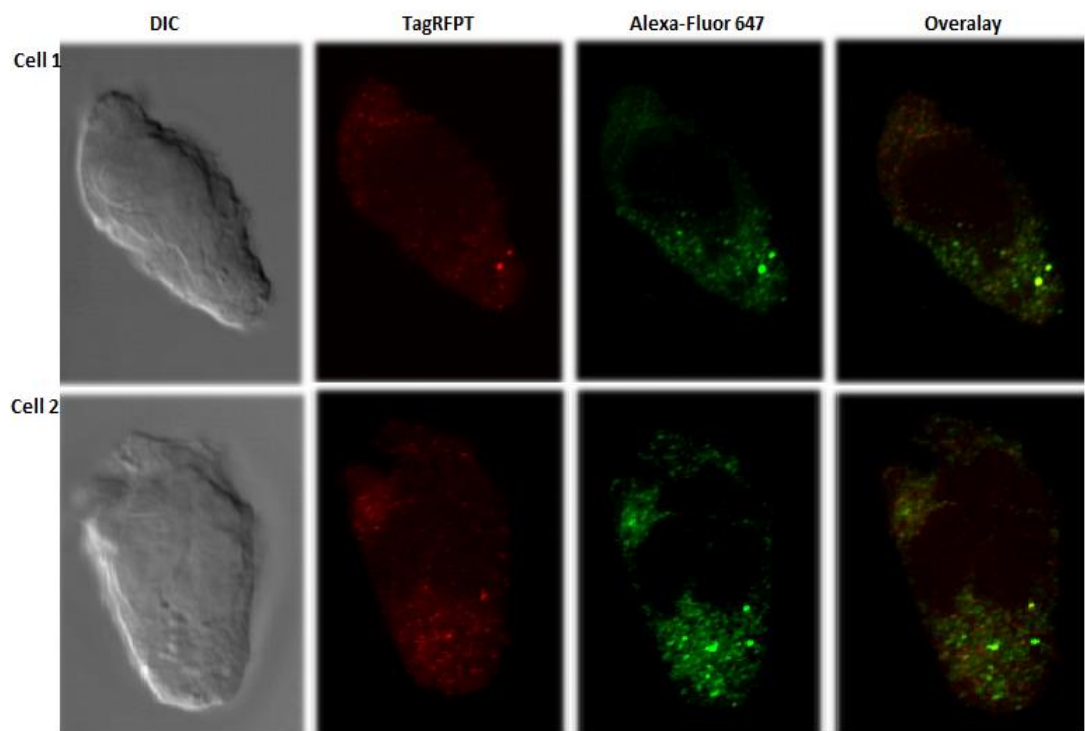
of a vector expressing Flag-BinCard. Interestingly, when A20 and BinCard are co-expressed, A20 punctate structures are no longer observed, and A20 becomes diffusely localized in the cytosol (see Figure 29). Thus, BinCard either regulates the formation and stability of A20 punctate structures or it regulates the levels of A20 in the cytosol. In an attempt to determine whether BinCard is capable of altering A20 protein levels, we transfected HEK-293 cells with a constant quantity of pcDNA3-HA-A20-YCit and increasing quantities of pcDNA3-Flag-BinCard. Interestingly, a linear decrease in the levels of A20 detectable by Western blot was found to be correlated with increasing levels of BinCard (Figure 30). These data suggest that BinCard either accelerates the degradation of A20 or blocks A20 transcription. Further experiments are required to determine the exact nature of the interaction of these two proteins.

Figure 29: Expression of exogenous BinCard leads to a loss of A20 compartmentalization and the degradation of A20 cytosolic punctate structures. HEK-293 cells were transfected with pcDNA3 expressing either HA-A20-ycit or co-transfected with equal quantities of HA-A20-ycit and HA-BinCard. The cells were then evaluated by confocal microscopy.

	Citrine	DIC	Overlay
HA-A20-ycit			
HA-A20-ycit + BinCard-nfp			
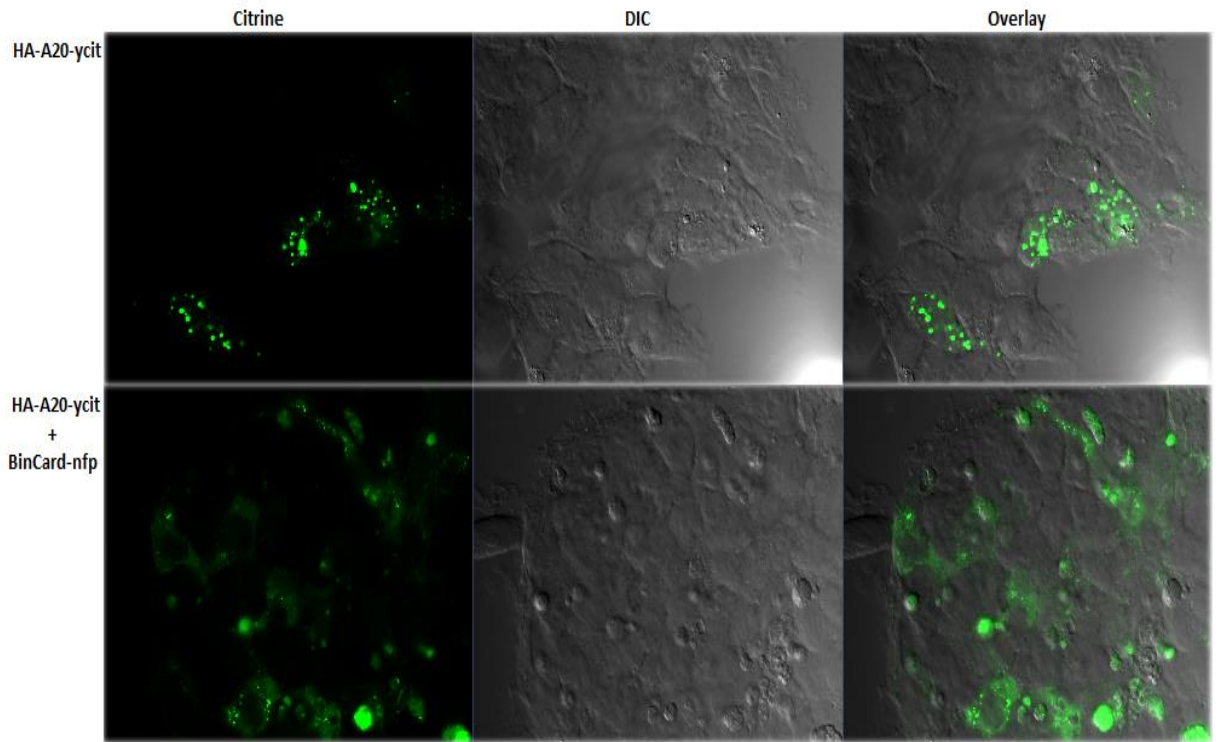
Figure 30: BinCard accelerates the degradation of A20 in HEK-293 cells. HEK-293 cells were transfected with 1500ng of pCDNA2-A20-NF-p and increasing quantities of pCDNA3-Flag-BinCard-NF-p. The cells were lysed and the resulting lysates were probed with Aviva anti-A20 and anti-Flag.
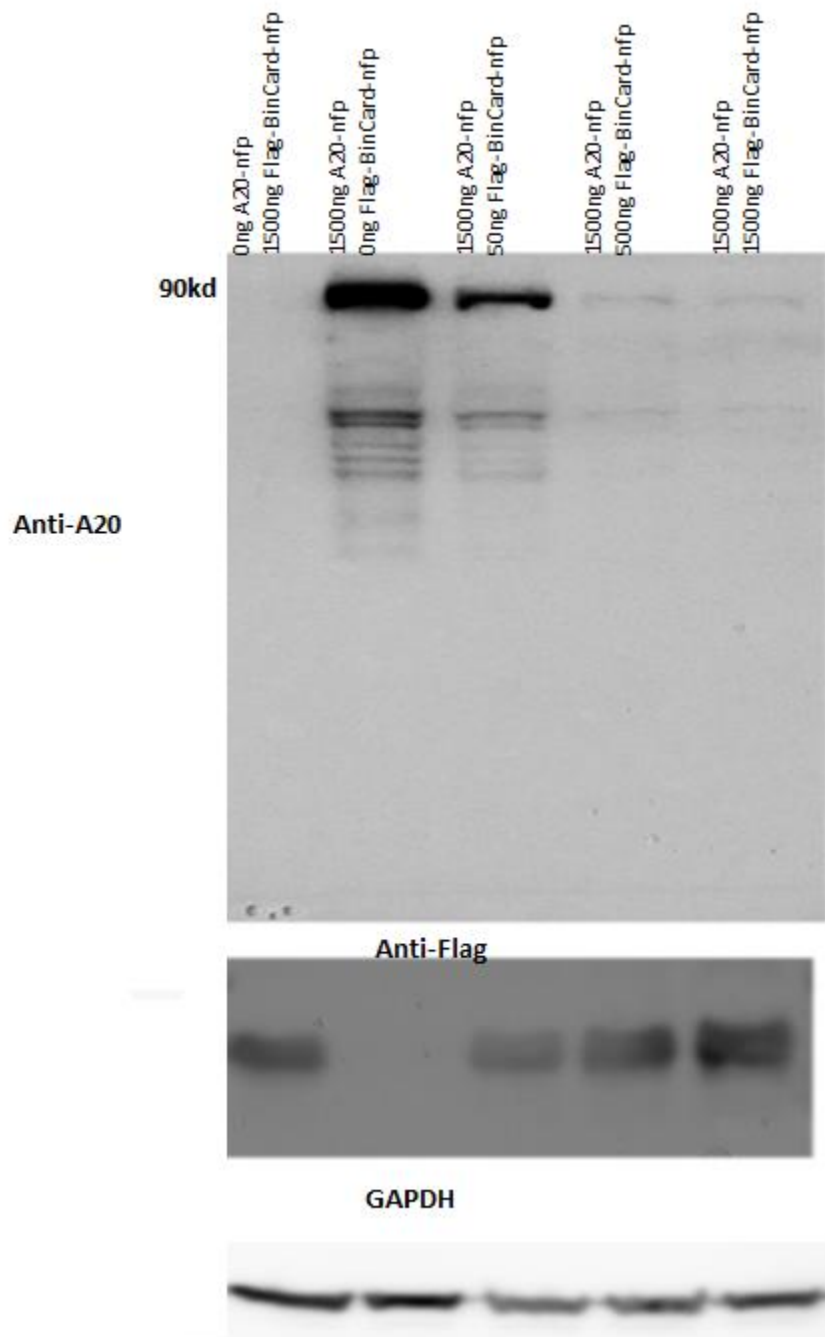
Chapter 4

Discussion

Preface

A20 is a unique ubiquitin-editing molecule (117, 118). A20 is involved in the negative regulation of the inflammatory cascade and is a central regulator of the both the innate and adaptive immune responses. It can behave as either a tumor suppressor or an oncogene, depending on the nature of the tissue in which it is expressed (118). A20 has been most extensively studied in non-lymphoid cells and in the context of inflammation. There are very few published reports emphasizing the intracellular localization of A20 or the interactions between A20 and the signal transduction pathways in lymphoid cells.

Here we have shown that the punctate cytosolic structures formed by A20 are very stable, and not in dynamic equilibrium with a non-localized cytosolic pool of A20. We have demonstrated that formation of these structures in non-lymphoid cells requires an intact A20 molecule, as truncated mutants do not form punctate structures and are freely diffusible in the cytosol. We have also shown that A20 is constitutively recruited to Bcl10 filaments in the cytoplasm of non-lymphoid cells. We have demonstrated that the association of A20 with Bcl10 in T-lymphocytes is stimulation dependent and that an A20 fragment accelerates the degradation

of Bcl10. Furthermore, we have shown that A20 associates with components of the autophagy pathway and that A20 itself may be regulated by the Bcl10 interacting protein, BinCard.

Experimental Results in the context of the Specific Aims of this Study

This study was undertaken to address three specific aims. The first specific aim was to define the assembly and dynamics of the A20 punctate structures formed in HEK-293 cells. Our initial hypothesis was as follows:

- *Localization of A20 into punctate structures requires an intact molecule. Truncated A20 will display a diffuse localization pattern.*

- *A20 punctate structures are non-membrane bound and in dynamic association with the cytoplasm.*

In order to address the first hypothesis, we compared the localization patterns of intact full length A20 with the localization patterns of an independent OTU domain, zinc fingers 1-7 and zinc fingers 4-7 in the cytoplasm of HEK-293 cells. We found that while the intact full length A20 molecule localized into discrete punctate structures as described in previous

reports, the OTU domain and the zinc finger domains tended diffuse throughout the cytoplasm. These results confirm our hypothesis. However, they also raise several questions concerning the formation of punctate structures by A20. For example, we do not yet know whether the transport of A20 from the site of synthesis to the punctate structure is an active process or a passive process. In other words, does the transport of A20 to these structures require the expenditure of ATP or does it occur by diffusion? We do not yet know if the formation of these structures is required for A20 function or if they simply form due to chemical nature of the A20 molecule. We also do not know whether these punctate structures form in particular disease states such as hematological malignancies in which A20 is mutated.

To test the second hypothesis, we performed a series of fluorescence recovery after photobleaching (FRAP) experiments. In these experiments, HEK-293 cells expressing either the intact full length A20 molecule or a truncation mutant coupled to the citrine variant of yellow fluorescent protein was photobleached with a high power 488nm laser. The cells were the monitored by confocal microscopy to determine the rate of fluorescence recovery. Interestingly, when the punctate structures formed by full length A20 were photobleached no recovery of the fluorescent signal occurred.

This indicates that full length A20 is not in a dynamic association with the cytoplasm. Typically, proteins that are not in dynamic association with the cytoplasm are sequestered into membrane bound vesicles (62). There have been reports that full length A20 is insoluble and tends to associate with lysosomes, however more studies would need to be conducted to determine whether A20 is actually localized within lysosomes and sequestered from the cytoplasm or if it merely associates with lysosomes (63). The A20 truncation mutants all demonstrated recovery after photobleaching. This indicates that they are freely diffusible in the cytoplasm and are not membrane bound. A recent publication indicated that a portion of total cellular A20 is cleaved by Malt1 in response to TCR stimulation (15). One of the murine cleavage products is a free zinc finger domain consisting of zinc fingers 4-7. The authors of this report speculate that A20 cleavage is a mechanism for down regulating the NF-κB inhibiting activity of A20 and that cleavage leads to A20 degradation. In our study, the zinc finger domains were freely diffusible within the cytoplasm, but did not appear to degrade rapidly. Since zinc fingers 4-7 have been shown to interact with ubiquitin, an attractive possibility is that the cleavage of A20 leads to the activation of freely diffusible cleavage products with enzymatic activity distinct from that of full length A20.

Our second specific aim was to determine whether A20 is involved in the regulation of Bcl10 stability in HEK-293 cells. Our hypotheses were as follows:

- *A20 is a negative regulator of Bcl10 in HEK-293 cells.*

- *A20 is itself under the regulation of Bcl10 interacting molecules.*

To test the first hypothesis, we first sought to determine whether A20 interacts with Bcl10 in the cytoplasm. To this end, we transfected HEK-293 cells with a plasmid expressing a Bcl10-GFP fusion protein. The overexpression of Bcl10-GFP in HEK-293 cells has been shown by previous investigators to result in the formation of filamentous structures in the cytoplasm. These structures have been shown to be highly correlated with NF-κB activation, and they tend to recruit various members of the NF-κB signaling cascade. Surprisingly, when we stained Bcl10-GFP transfected cells with an anti-A20 antibody, we found that A20 colocalized almost perfectly with the Bcl10 filaments suggesting that Bcl10 filaments are a site of Bcl10-A20 interaction. The ability of Bcl10 to recruit A20 was not related to the geometry of the Bcl10 filament or its placement within the

146

cytoplasm indicating that this is most likely an intrinsic feature of Bcl10. We next sought to determine whether Bcl10-GFP filament formation could be negatively regulated by A20 expression. HEK-293 cells were transfected with constant amount of Bcl10-GFP and an increasing quantity of A20. As the concentration of A20 increased within the cytoplasm, we observed a corresponding decrease in Bcl10-GFP filaments, indicating that A20 negatively regulates Bcl10 filament formation. To further clarify these results, we performed a series of Western blots in which the lysates from HEK-293 cells transfected with constant quantities of Bcl10-GFP and increasing quantities of A20 were compared. Interestingly, we did not see a significant decrease in levels of the Bcl10-GFP protein with increased concentrations of A20. Thus, the reduction in formation of Bcl10 filaments by full-length A20 does not appear to reflect proteolysis of Bcl10.

Since zinc fingers 4-7 are a product of A20 cleavage during T-cell activation and since this domain is believed to interact with ubiquitin we performed another series of western blot experiments in which a plasmid expressing HA-zinc finger 4-7-YCit was substituted for the full length A20-expressing plasmid (15). These experiments revealed that there is a linear decrease in the Bcl10-GFP signal on the blot corresponding to increased quantities of zinc fingers 4-7 transfected into the cell. In addition, we

observed a possible Bcl10 cleavage product in lysates from cells co-transfected with zinc fingers 4-7 and Bcl10-GFP. In order to determine whether or not this effect is specific to Bcl10, we probed several blots with anti-MALT1 and observed no decrease in the concentration of endogenous MALT1 with increased quantities of zinc fingers 4-7. We also performed a titration of a plasmid expressing zinc fingers 4-7 with constant quantities of a plasmid expressing GFP in HEK-293 cells. No decrease in the GFP signal was found by western blot.

The ubiquitination of Bcl10 at lysines 31 and 63 is necessary for TCR-mediated NF-κB activation (128). Since A20 is a negative regulator of NF-κB, we wondered whether ubiquitination at these two sites was necessary for zinc fingers 4-7 to negatively regulate Bcl10 stability. HEK-293 cells were transfected with a constant quantity of Bcl10 with lysine 31 and 63 replaced with arginine. We then transfected increasing quantities of zinc fingers 4-7. A linear decrease in Bcl10 protein levels was observed by western blotting as the amount of zinc fingers 4-7 increased. These data confirm that ubiquitination at lysine 31 and 63 are not required for zinc fingers 4-7 to regulate the stability of Bcl10.

The functional ability of zinc fingers 4-7 to down-regulate NF-κB expression was confirmed by NF-κB luciferase assay, and the ability of

Bcl10 to recruit the zinc finger domains of A20 was confirmed by confocal microscopy. Taken together, these data demonstrate that the zinc finger domains of A20 are stable in the cytosol, they can be recruited to Bcl10 filaments, and they act as negative regulators of Bcl10 stability. This confirms our hypothesis that A20 is a negative regulator of Bcl10 in HEK-293 cells.

The second hypothesis proposes that since Bcl10 is degraded by interacting with specific proteins during activation, then A20 should be degraded by these same molecules if it is in physical contact with Bcl10. Recent research by Suman Paul and others working in our laboratory has shown that Bcl10 can be degraded by the process of autophagy (89). We therefore performed several experiments to determine whether A20 associates with members of the autophagy pathway. We began by transfecting HEK-293 cells with A20-YCit and then staining with an anti-LC3 antibody. LC3 is a membrane-bound protein of autophagic vesicles. Interestingly, A20 punctate structures were found to colocalize with LC3-positive vesicles, indicating that A20 punctual may be associated with autophagic vesicles. We then took D10 T cells expressing an A20 fusion, stimulated them for 20 minutes and stained for anti-p62. p62 is a participant in certain autophagy pathways, and it also participates in TCR activation of

NF-κB in effector T cells (78, 79). A20 in stimulated T-cells colocalized with p62. Together, these results indicate that A20 may be associated with the autophagic process and may either have a similar degradation process as Bcl10 or be a participant in the degradation of Bcl10. Since p62 is a protein which binds ubiquitin and has been implicated in the oligomerization of signaling molecules, it may serve as a scaffolding molecule which brings A20 and Bcl10 into close association with one another (78,79). It is also possible that p62 serves to maintain a baseline level of A20 by shunting excess A20 to proteosome for degradation, or perhaps A20 delivers attached proteins to the proteosome for degradation, further studies will be required to determine the nature of this particular interaction.

BinCard is a recently described protein which has been shown by unpublished results from our laboratory to accelerate the degradation of Bcl10 (127). Again, since A20 colocalizes with Bcl10 we sought to determine whether BinCard may also be involved in the negative regulation of A20. This was initially approached by taking HEK-293 cells and cotransfecting them with a constant quantity of A20-ycit and increasing quantities of BinCard. These cells were analyzed by confocal microscopy which revealed that increasing quantities of BinCard led to a destabilization of the A20 punctate structures and a loss of A20-ycit signal. These results

indicate that BinCard may be either directly involved in the degradation of A20 or that it functions to antagonize punctate structure formation. We then performed a group of similar experiments in which we analyzed the stability of A20 by Western blot and found that increasing quantities of BinCard tends to decrease the levels of A20 protein, suggesting that BinCard does in fact accelerate the degradation of A20. These experiments confirm our second hypothesis that A20 is regulated by Bcl10 interacting proteins.

The third specific aim of this study was to evaluate the localization of A20 in T-lymphocytes. The experiments performed in support of this specific aim were undertaken with the following hypotheses in mind:

- *A20 forms punctate structures in the cytoplasm of T-cells.*

- *Localization of A20 in T-cells is stimulation dependent.*

The first and second hypotheses were tested together by generating a series of D10 T-cell lines stably expressing HA-Bcl10-GFP. These cell lines were stimulated with plate bound ant-CD3, stained for with anti-A20 and evaluated by confocal microscopy. In unstimulated cells, Bcl10 was found to be diffuse in the cytoplasm and A20 tended to be associated with punctate

structures. At 20 minutes post-stimulation, Bcl10 formed filamentous

structures which recruited A20. However, by 1 hour post stimulation, Bcl10

degenerated into punctate structures which still associated with A20. These

data show that Bcl10 is able to associate with A20 in the cytoplasm of a T-

lymphocyte and that this association occurs in a stimulation-dependent

manner. We performed a similar experiment in which we evaluated T-cells

stably co-expressing Bcl10-GFP and zinc fingers 4-7-tagRFPT. In this

experiment we were able to show that the zinc fingers also colocalize with

Bcl10 in a stimulation-dependent manner. However, as mentioned above,

the kinetics were different and Bcl10 tended to have a lower intensity in

cells co-expressing zinc fingers 4-7 than in cells expressing full-length A20.

This may indicate either that zinc fingers 4-7 are involved in regulating the

formation or stability of Bcl10 punctate structures or that they are merely

involved in regulating Bcl10 protein stability.

Experimental Results in the context of current literature

The data presented in this study both compliments and expands upon

the current literature regarding the role of A20 in both lymphoid and non-

lymphoid cell types. For example, a 2008 publication by Lianyun Li and co-

workers suggested that A20 may be associated with a lysosome-associated

cell compartment and that A20 may serve to shuttle substrate molecules to lysosomes for degradation (64). They began by utilizing confocal microscopy to demonstrate the localization of A20 to punctate structures in HeLa cells, they then performed biochemical fractionation experiments to demonstrate that A20 localizes to the membrane fraction, and performed immunofluorescence microscopy to demonstrate the co-localization of A20 with lysosomal components in HeLa cells. Our data complements the work of Li and co-workers by demonstrating colocalization of A20 with both LC3 in HEK-293 cells and p62 in t-lymphocytes. These data confirm that A20 tends to associate with participants in the autophagy-lysosome pathway. However, we also demonstrate that A20 is colocalized with Bcl10 filaments upon cell stimulation or Bcl10 overexpression. The fact that A20 colocalizes with Bcl10 filaments in HEK-293 cells and these Bcl10 filaments do not degrade directly upon association with A20, argues against a role for A20 in purely shuttling substrates such as Bcl10 to the lysosome. More research is required to fully explore this issue.

A recent report by Lu and co-workers summarized an elegant series of experiments in which the contributions relative contributions of zinc finger 4 are compared to those of the OTU domain in a physiological system (67). The biochemical and imaging data presented in this dissertation provide

support for their conclusions by examining the roles of the OTU and zinc

finger domains of A20 in an *in vitro* overexpression system. This group

began by generating a mouse model in which cysteine 609 and cysteine 613

of the A20 gene are replaced with arginine, generating a mouse expressing

A20 with a functionally defective zinc finger 4. They also generated a

mouse model in which cysteine 103 is replaced with arginine, resulting in a

mouse expressing A20 with a functionally defective OTU domain. In

addition, they bred mice harboring a defective zinc finger 4 domains with

mice harboring functionally defective OTU domains to generate compound

mutant mice expressing an approximately equal amount of cells with a

defective OTU domain and a defective zinc finger 4 domain. It was

immediately observed that these mice did not at first exhibit the runting and

cachexia which characterizes complete knockouts. However, by six months

of age both OTU defective mice and zinc finger 4 defective mice began to

exhibit splenomegaly and increased lymphocyte counts. In addition, they

were able to show that when both OTU defective mice and zinc finger 4

defective mice are challenged with dextran sodium sulfate they display

increased levels of intestinal inflammation indicating the both domains are

critical for restricting inflammation. These data indicate that both the zinc

finger 4 domain of A20 and the OTU domain are necessary for maintaining

homoeostasis (67). Our data has shown that the zinc fingers 4-7 are able to accelerate the degradation of Bcl10. Activation of the Bcl10-NF-κB pathway has been shown to initiate and maintain the inflammatory response in model systems. Thus, our data provides a possible mechanistic basis for the ability of the zinc finger domain to regulate the development of an inflammatory phenotype. This group also demonstrated that zinc finger 4 recruits A20 to ubiquitinated RIP1 (a member of the TNF- signaling cascade) and that in cells which have defective zinc finger 4 domains, A20 is not recruited to ubiquitinated RIP1 although it can associate with non-ubiquitinated RIP1. These data indicate a role for the zinc finger domain in A20 localization and association with members of a signal transduction cascade (67). Our data show that both full length A20 and independent zinc finger domains can be recruited to Bcl10 filaments in lymphoid as well as in non-lymphoid cells. These data compliment the data of the Lu group by demonstrating that the ability of the zinc finger domains to direct the localization of A20 with members of a signal transduction cascade is not limited to the TNF- pathway and may be a general feature of this molecule. One of the most interesting results reported by the Ma group was the observation that murine epidermal fibroblast (MEF) cells harboring a defective OTU domain or a defective zinc finger 4 domain are unable to

successfully be recruited to RIP1 (67). However, cells derived from

compound mutants are able to be successfully recruited to RIP1. These data

indicate that the expression of A20 with an intact OTU domain but a

defective zinc finger 4 domain and A20 with an intact zinc finger 4 domain

but a defective OTU domain in the same cytosol lead to complementation

and the restoration of the normal pattern of A20 localization and interaction

with RIP1. The authors went on to demonstrate that A20 tends to dimerize

and that the dimerization motif is located in the OTU domain and that zinc

finger 4 confers the ability to bind RIP1. Therefore, as long as a single copy

of an intact zinc finger 4 domain is present in the cytosol, this will be

recruited to RIP1 and allow the binding of further A20 molecules OTU

domain mediated dimerization (67).   It is tempting to hypothesize that the

A20 punctate structures which we observed in the current study are the

result of A20 dimerization and multimerization in the cytosol. However, in

contrast to the Ma group, we have observed that when OTU-GFP and zinc

fingers 1-7-GFP are co-expressed in HEK-293 cells complementation does

not occur. This may be due to the use of a cell line rather than primary cells

or reflect the inherent differences between HEKs and MEFs. It may also be

due to the fact that the Ma group utilized point mutations in their study

which retained the ability to dimerize, while we used truncation mutants

which did not retain that particular ability, and hence were unable to complement one another. However, it would be of interest to evaluate the ability of A20 mutants to complement each other in a variety of cell types to determine whether or not complementation is a general feature of A20 activity.

Interestingly, Xu and others have found that Bcl10 is able to up-regulate the expression of A20 in B-lymphocytes upon IgM receptor engagement (130). The activation of B-cells is analogous to the activation of T-lymphocytes. In brief, interaction of the B-cell receptor with antigenic peptide leads to an early signaling process which results in the phosphorylation of Carma1 and the formation of a complex consisting of Carma1, Bcl10 and Malt1. This complex is able to recruit the ubiquitin ligase TRAF6 which is able to interact with and activate the IKK complex resulting in the phosphorylation and degradation of IκBα allowing NF-κB to enter the nucleus. The ability of Bcl10 to interact with the A20 promoter during B-cell receptor activation suggests that A20 may be involved in a feedback loop with Bcl10 in which Bcl10 activates the expression of A20 which then down-regulates the expression of Bcl10 (130). Both our biochemical data demonstrating the degradation of Bcl10 mediated by zinc fingers 4-7 and our imaging data demonstrating the co-localization of A20

and A20 fragments with Bcl10 support this model and complement the data

of Xu and co-workers by providing a possible mechanistic explanation for

the interaction between A20 and Bcl10. In addition, our observation that

A20 can be degraded by the Bcl10 interacting protein, BinCard may provide

a mechanism for the down regulation of A20 upon the interaction with

Bcl10.

The exact mechanism by which A20 modulates NF-κB activation

differs from cell type to cell type and more than one mechanism may operate

in a given cell. In some reports, A20 has been found functions by

modulating the activity status of signaling intermediates. For example, in

non-lymphoid cells, A20 blocks NF-κB activation by modulating the

ubiquitin status of a signaling intermediate known as RIP1 by removing K63

linked ubiquitin chains followed by the addition of K48 linked ubiquitin

chains (124). The net effect of this activity is the disassembly of RIP1

containing complexes and the targeting of RIP1 to the proteosome for

degradation. A20 has also been shown to inhibit the ubiquitination and

activation of TRAF6 which is itself a ubiquitin ligase involved in cell

response to TNF-, IL-1 and lymphocyte activation. A group led by Edward

Harhaj, then at the University Miami (currently at Johns Hopkins) has

demonstrated that A20 blocks the activation of this molecule by inhibiting

the interaction between it and another class of ubiquitin ligase termed E2 ubiquitin ligases (101). In addition, A20 was found to ubiquitinate and degrade E2 ligases thereby preventing their interaction with substrate molecules. Brian Skaug and co-workers at the University of Texas Southwestern Medical Center, have shown that A20 has the ability to operate in a direct and non-catalytic fashion (104). Using HEK-293 cells as a model system, they performed a series of experiments which demonstrated that A20 is recruited to NEMO (the regulatory component of the IKK complex) and prevents its phosphorylation and activation by a kinase known as TAK1. This activity is dependent on the ubiquitin binding ability of the zinc finger domains and does not require an active OTU domain, suggesting a non-catalytic mechanism. In this dissertation, we have shown that zinc fingers 4-7 are able to accelerate the degradation of Bcl10, however we do not present data aimed at determining the mechanism. However, the fact that this activity occurs in the absence of the OTU domain there are two equally likely possibilities. One, is that zinc fingers 4-7 are able to independently bind to Bcl10 and modulate the ubiquitination status of this molecule via the attachment of K48 linked ubiquitin, which would target it for degradation by the proteosome. The other possibility is that these three zinc finger domains associate with Bcl10 and block the interaction of Bcl10

with other proteins, thereby preventing the normal process of post-translational modification leading to a loss of stability. Further research is required to discriminate between these two possibilities. In particular, it would be of interest to determine whether zinc fingers 4-7 are capable of modulating the ubiquitination status of Bcl10 and to determine whether zinc fingers 4-7 block the interaction of Bcl10 with other members of the CBM complex.

Conclusion

In this study we have confirmed that Bcl10 forms filamentous structures in the cytoplasm of non-lymphoid cells and stimulated lymphoid cells. We have shown that full length A20 is sequestered in punctate structures which do not communicate with the cytosol and we have demonstrated that truncated A20 mutants are freely diffusible in the cytosol. We have shown that A20 is recruited to Bcl10 filamentous structures in non-lymphoid cells and stimulated lymphoid cells. We have demonstrated that A20 zinc fingers 4-7 are freely diffusible in the cytosol and accelerate the degradation of Bcl10 in a dose dependent manner and that A20 is itself regulated by BinCard.

A proposed mechanistic interpretation of the data accumulated during this study can be formulated as follows: An external signal triggers cytosolic Bcl10 to aggregate into dimers and multimers forming the filamentous structures necessary for NF-κB activation. These filamentous structures recruit members of the NF-κB signaling cascade including MALT1 and A20. The proteolytic activity of MALT1 cleaves A20 releasing zinc fingers 4-7 which are then able to accelerate the degradation of Bcl10 thereby limiting the intensity and duration of NF-κB activation. The steady state levels of A20 are maintained by BinCard which accelerates the degradation of excess A20 allowing the cell to return to a resting state (Figure 31).

Future Directions

As stated above, the data presented in this study raise a number of important questions. In order to fully understand the nature of the A20 punctate structures and the association between A20 and Bcl10 it will be necessary to determine whether the A20 is actively or passively transported into the structures. It will also be necessary to determine whether A20 can still function if it is blocked from forming punctate structures while maintaining protein conformation. In addition, the minimum domains

necessary for the interaction between Bcl10 and A20 remain to be defined. While the work presented in this dissertation provide baseline data regarding the localization patterns of A20 with respect to Bcl10 in both lymphoid and non-lymphoid cells, lingering questions remain regarding the mechanistic aspects of A20 subcellular localization. The fact that A20 displays a stimulation dependent colocalization with Bcl10 suggests that several alternate processes may be occurring upon cell stimulation, resulting in A20-Bcl10 association. Ligation of cell surface receptors to their cognate ligands may trigger the diffusion of A20 in the 3-dimensional space of the cell cytoplasm followed by random association with Bcl10 oligomers, A20 may be membrane bound and reside in the same plane as Bcl10 (9, 40, 94, 120), in which case it may diffuse in a two-dimensional random walk followed by association with Bcl10, or A20 may diffuse in one-dimension along cytoskeletal filaments which are in direct communication with Bcl10. Differentiating among these possibilities may be accomplished by determining whether or not A20 is membrane bound using fluorescence microscopy and antibodies targeted toward common membrane components, and then determining whether the interaction of A20 with Bcl10 can occur in

Figure 31. Proposed model of A20 action based upon the data presented in this dissertation. An external signal leads to the oligomerization of Bcl10 via CARD-CARD interaction. Oligomerized Bcl10 recruits Malt1 which recruits A20. Malt 1 proteolytic activity cleaves A20 after arginine 439 releasing an active A20 fragment consisting of zinc fingers 4-7. This fragment accelerates the degradation of Bcl10 leading to complex degradation and the maintenance of homeostasis.

Proposed Model

BCL-10

External Signal induces
Bcl-10 oligomerization
allowing formation of
signaling complex

A20 is recruited to Bcl-10 oligomer and
activated by MALT-1 medicated cleavage
allowing A20 fragments to cleave Bcl-10

MALT1

BCL-10

MALT1

BCL-10   A20

Autophagy
Regulates
A20 steady
State levels

BinCard

Bincard regulates A20
steady state levels

BCL-10

BCL-10

BCL-10

BCL-10

BCL-10

BCL-10

MALT 1

A20 fragment cleavage
of Bcl-10 leads to
complex disassembly
and down regulation of
NF-kB

the presence of chemical agents designed to block the formation of actin filaments and cytoskeletal structures. In addition, the observation of A20 diffusion by real time fluorescence microscopy and techniques such as FRAP can be used to determine whether the diffusion of A20 is confined to a plane, travels a linear path, or extends in a 3-dimensional fashion throughout the cytoplasm.

It would also be of interest to determine the biochemical and physical nature of the A20 cytosolic punctate structures. For example, it is currently unclear whether these structures represent membrane bound A20, whether A20 is within the membrane or peripherally associated, whether they represent aggregations of A20 multimers, or whether they represent A20 forming insoluble complexes with other proteins. In addition, it is not known how cell stimulation results in the release of A20 from these structures. If A20 is membrane bound, then cell stimulation may result in the decay of the membrane freeing A20 to diffuse in the cytosol. Alternatively, cell stimulation may result in the formation of pores in the membrane which allow A20 egress. If A20 is peripherally associated with a membrane then it may be released by cleavage of the bound attaching A20 to the membrane or by a change in the local ionic strength of the cytosol. If the A20 punctate structures represent insoluble A20 multimers, then the

release of A20 may involve the dynamic association between A20 aggregates and the cytosol. Distinguishing among these possibilities will depend on first determining whether or not A20 is membrane bound. This can be accomplished with the aid of immunoelectron microscopy and biochemical methods such as subceullar fractionation to determine whether or not A20 is associated with a membrane and if it resides within the membrane or on the periphery.

Since A20 is involved in the regulation of both innate and adaptive immunity, it will be of interest to determine whether the ability of A20 to form punctate structures can be blocked by infectious agents. This can be determined for bacterial pathogens by either co-culturing the pathogen in question with cells expressing an A20 fusion protein or by inoculating such a culture with bacterial lysate. The role of viral proteins in modulating A20 activity can be determined by cloning individual structural and non-structural genes of a given viral pathogen into a mammalian vector and using this to transfect an A20 fusion-expressing cell line to determine whether there is any effect on punctate structure formation or protein stability.

The localization and activity of A20 may also be of diagnostic value. An examination of the localization properties of cancer associated A20

mutants may reveal specific patterns which can then be adapted to a confocal microscopy based assay for determining tumor etiology. Indeed recent studies have revealed that certain A20 mutations are associated with poor prognosis with respect to hematological malignancies (132). Thus A20 localization patterns may serve as a rapid means of staging the severity of a particular malignancy.

The nature of A20 enzymatic activity has yet to be fully explored. It will be of interest to determine if zinc fingers 4-7 degrade Bcl10 by catalytic activity or if they merely accelerate the degradation of Bcl10 by another protein or set of proteins. To this end, the essential amino acids necessary for zinc finger 4-7 mediated degradation of Bcl10 need to be mapped and any modulation of the ubiquitination status of Bcl10 in response to the presence of zinc fingers 4-7 needs to be determined.

Concluding Remarks

The research reported in this dissertation has revealed several interesting aspects of the ubiquitin-editing protein A20. We have shown that A20 tends to localize into stable punctate structures in the cells cytoplasm, that A20 can be recruited to Bcl10 filaments during NF-κB activation, that A20 zinc fingers 4-7 negatively regulate Bcl10 stability, and that the Bcl10

interacting protein BinCard negatively regulates the stability of A20.

However, this research has also raised several questions regarding the nature

of A20 and the interaction between A20 and Bcl10. The results presented

here provide a foundation upon which future research into the biochemical,

diagnostic or therapeutic implications of A20 can be based.

REFERENCES

1.   Ainbinder E, Amir-Zilberstein L, Yamaguchi Y, Handa H, Dikstein R. Elongation inhibition by DRB sensitivity-inducing factor is regulated by the A20 promoter via a novel negative element and NF-kappaB. Mol Cell Biol 2004;24:2444-54.

2.   Ainbinder E, Revach M, Wolstein O, Moshonov S, Diamant N, Dikstein R. Mechanism of rapid transcriptional induction of tumor necrosis factor alpha-responsive genes by NF-kappaB. Mol Cell Biol 2002;22:6354-62.

3.   Amir-Zilberstein L, Dikstein R. Interplay between E-box and NF-kappaB in regulation of the A20 gene by DRB sensitivity-inducing factor (DSIF).   J Biol Chem 2008;283:1317-23.

4.   Boone DL, Turer EE, Lee EG, Ahmad RC, Wheeler MT, Tsui C, et al. The ubiquitin-modifying enzyme A20 is required for termination of toll-like receptor responses. Nat Immunol 2004;5:1052-60.

5.   Bray D. Signaling complexes: biophysical constraints on intracellular communication. Annu Rev Biophys Struct 1998;27:59-75.

6.   Braun FC, Grabarczyk P, Mobs M, Braun FK, Eberle J, Beyer M, Sterry W, Busse F, Schroder J, Delin M, Przybylski GK, Schmidt CA. Tumor suppressor TNF-AIP3 (A20) is frequently deleted in Sezary syndrome. Leukemia 2011;25:1494-501.

7.   Bosanac I, Wertz IE, Pan B, Yu C, Kusam S, Lam C, Phu L, Phung Q, Maurer B, Arnott D, et al. Ubiquitin binding to A20 ZNF-4 is required for modulation of NF-kappaB signaling. Mol Cell 2010;40:548-57.

8.   Burnette, WN. "Western Blotting": electrophoretic transfer of proteins from sodium dodecyl sulfate polyacrylamide gels to unmodified nitrocellulose and radiographic detection with antibody an dradioiodinated protein A. Anal Biochem 1981;112:195-203.

9.   Cebecauer, M, Spitaler, M, Serge A, Magee AI. Signaling complexes and clusters: functional advantages and methodological hurdles. J Cell Sci 2010;123:309-320.

10.   Chanudet E, Huang Y, Ichimura K, Dong G, Hamoudi RA, Radford J, et al. A20 is targeted by promoter methylation, deletion and inactivating mutation in MALT lymphoma. Leukemia 2010;24:483-7.

11.   Chanudet E, Huang Y, Zeng N, Streubel B, Chott A, Raderer M, Du M-Q. TNF-AIP3 abnormalities in MALT lymphoma with autoimmunity. B J Haematol 2011;154:533-35.

12.   Chu Y, Vahl JC, Kumar D, Heger K, Bertossi A, Wojtowicz E, Soberon V, Schenten D, Mack B, Reutelshofer M, et al. B cells lacking the tumor suppressor TNF-AIP3/A20 display impaired differentiation and hyperactivation and cause inflammation and autoimmunity in aged mice. Blood 2011;117:2226-36.

13.   Codd JD, Salisbury JR Packham G, Nicholson LJ. A20 RNA expression is associated with undifferentiated nasopharyngeal carcinoma and poorly differentiated head and neck squamous cell carcinoma. J Pathol 1999;187: 549-55.

14.   Cooper JT, Stroka DM Brosjan C, Plmetshofer A, Bach FH, Ferran C. A20 blocks endothelial cell activation through a NF-kappaB dependent mechanism. J Biol Chem 1996;271:18068-73.

15.   Coornaert B, Baens M, Heyninck K, Bekaert T, Haegman M, Staal J, et al. T cell antigen receptor stimulation induces MALT1 paracaspase-mediated cleavage of the NF-kappaB inhibitor A20. Nat Immunol 2008;9:263-71.

16. De Valck D, Heyninck K, Van Criekinge W, Contreras R, Beyaert R, Fiers W. A20 an inhibitor of cell death, self-associates by its zinc finger domain. FEBS Lett 1996;384:61-4.

17. De Valck D, Jin DY, Heyninck K, Van de Craen M, Contreras R, Fiers W, et al. The zinc finger protein A20 interacts with a novel anti-apoptotic protein which is cleaved by specific caspases. Oncogene 1999;18:4182-90.

18. Dixit VM, Green S, Sarma V, Holzman LB Wold FW, O'Rourke K, et al. Tumor necrosis factor-alpha induction of novel gene products in human endothelial cells including a macrophage-specific chemotaxin. J Biol Chem 1990; 265: 2973-8.

19. Dixon AS, Constance JE, Tanaka T, Rabbitts TH, Lim CS. Changing the subcellular localization of the oncoprotein Bcr-Abl using randomly designed capture motifs. Pharm Res 2012;29:1098-109.

20. Dixon AS, Kakar M, Schneider KM, Constance JE, Paullin BC, Lim CS. Controlling subcellular localization to alter function: Sending oncogenic Bcr-Abl to the nucleus causes apoptosis. J Control Release 2009;140:245-9.

21. Duran A, Linares JF, Galvez AS, Wikenheiser K, Flores JM, Diaz-Meco MT, Moscat J. The signaling adaptor p62 is an important NF-κB mediator in tumorigenesis. Cancer Cell 2008;13: 343–354.

22. Duwel M, Welteke V, Oeckinghaus A, Baens M, Kloo B, Ferch U, et al. A20 negatively regulates T cell receptor signaling to NF-kappaB by cleaving Malt1 ubiquitin chains. J Immunol 2009;182:7718-28.

23. Evans PC, Ovas H, Hamon M, Kilshaw PJ, Hamm S, Bauer S, et al. Zinc-finger protein A20, a regulator of inflammation and cell survival has de-ubiquitinating activity. Biochem J 2004;378:727-34.

24. Evans PC, Smith TS, Lai MJ, Williams MG, burke DR, Heyninck K, et al. A novel type of deubiquitinating enzyme. J. Biol Chem 2003;278:23180-6.

25. Evans PC, Taylor ER, Coadwell J, Heyninck K, Beyaert R, Kilshaw PJ. Isolation and characterization of two novel A20-like proteins. Biochem J 2001;357:617-23.

26. Ferran C, Stroka DM, Badrichani AZ, Cooper JT, Bach FH. Adenovirus-mediated gene transfer of A20 renders endothelial cells resistant to activation: a means of evaluating the role of endothelial cell activation in xenograft refection. Transplant Proc 1997;29:879-80.

27. Fries KL, Miller WE, Raab-Traub N. Epstein-Barr virus latent membrane protein 1 blocks p53-mediated apoptosis through the induction of the A20 gene. J Virol 1996;70:8653-9.

28. Gon Y, Asai Y, Hashimoto S, Mizumura K, Jibiki I, Machino T, et al. A20 inhibits toll-like receptor 2- and 4-mediated interleukin-9 synthesis in airway epithelial cells. Am J Respir Cell Mol Biol 2004;31:330-6.

29. Garg AV, Ahmed M, Vallejo An, Ma A, Gaffen SL. The deubiquitinase A20 mediates feedback inhibition of interleukin-17 receptor signaling. Sci Signal 2013;6:ra44. doi: 10.1126/scisignal.2003699.

30. Graham FL Abrahams PJ, Mulder C, Heijneker HL, et al. Studies on in virtro transformation by DNA and DNA fragments of human adenovirus and SV40. Cold Spring Harbor symposium on quantitative biology. 1974;39:637-50.

31. Graham FL, Smiley J, Russel WC, Nairn R. Characteristics of a human cell line transformed by DNA from human adenovirus type 5. J Gen Virol 1977;36:59-72.

32. Graham FL, van der E. A new technique for the assay of infectivity of human adenovirus 5 DNA. Virology 1973;52:456-67.

33. Griesbeck O, Baird GS, Campbell RE, Zaharias DA, Tsien RY. Reducing the environmental sensitivity of yellow fluorescent protein. Mechanism and applications. J Biol Chem 2001;276:188-94.

34. Guiet C, Vito P. Caspase recruitment domain (card-dependent) cytoplasmic filaments mediate Bcl10-induced NF-kappaB activation. J Cell Bio 2000;148:1131-40.

35. He KL, Ting AT. A20 inhibits tumor necrosis factor (TNF) alpha-induced apoptosis by disrupting recruitment of TRADD and RIP to the TNF-receptor receptor 1 complex in Jurkat T cells. Mol Cell Biol 2002;22:6034-45.

36. Heyninck K, Beyaert R. The cytokine-inducible zinc finger protein A20 inhibits IL-1-induced NF-kappaB activation at the level of TRAF6. FEBS Lett 1999;442:147-50.

37. Heyninck K, Denecker G, De Valck D, Fiers W, Beyaert R. Inhibiton of tumor necrosis factor-induced necrotic cell death by the zinc finger protein A20. Anticancer Res 1999;19:2863-8.

38. Heyninck K, De Valck D, Vanden Berghe W, Van Criekinge W, Contereras R, Fiers W, et al. The zinc finger protein A20 inhibits TNF-induced NF-kappaB-dependent gene expression by interfering with an RIP- or TRAF2-mediated transactivation signal and directly binds to a novel NF-kappaB-inhibiting protein ABIN. J Cell Biol 1999;145:1471-82.

39. Honma K, Tsuzuki S, Nakagawa M, Tagawa H, Nakamura S, Morishima Y, et al. TNF-AIP3/A20 functions as a novel tumor suppressor gene in several subtypes of non-Hodgkin lymphomas. Blood 2009.

40. Houtman JC, Barda-Saad M, Samelson LE. Examining multiprotein signaling complexes from all angles. FEBS J 2005;21:5426-35.

41. Huang P, Geng XR, Yang G, Chen C, Liu Z, Yang PC. Ubiquitin E3 ligase A20 contributes to maintaining epithelial barrier function. Cell Physiol Biochem 2012;30:702-10.

42. Hung, M-C, Link W. Protein localization in disease and therapy. J Cell Sci 2011;124:3381-3392.

43. Hymowitz SG, Wertz IE. A20: from ubiquitin editing to tumor suppression. Nat Rev Cancer 2010; 10:332-41.

44. Jaattela M, Mouritzen H, Elling F, Bastholm L. A20 zinc finger protein inhibits TNF- and IL-1 signaling. J Immunol 1996;156:1166-73.

45. Jacobson K, Derzko Z, Wu ES, Hou Y, Poste G. Measurement of the lateral mobility of cell surface components in single, living cells by fluorescence after photobleaching. J Supramol Struct 1976;5:565-76.

46. Jin Z, Li Y, Pitti R, Lawrence D, Pham VC, Lill JR, Et al. Cullin3 – based poly-ubiquitination and P62-dependent aggregation of caspase-8 mediated extrinsic apoptosis signaling. Cell 2009;137:721-35.

47. Kato M, Sanada M, Kato I, Sato Y, Takita J, Takeuchi K, et al. Frequent inactivation of A20 in B-cell lymphomas. Nature 2009;459:712-6.

48. Kaye J, Porcelli S, Tite J, Jones B, Janeway C. Both a monoclonal antibody and antisera specific for determinants unique to individual cloned helper T cell lines can substitute for and antigen presenting cells in the activation of T-cells. J Exp Med 1983;158:836-56.

49. Kim SW, Ramasamy K, Bouamar H, Lin AP, Jiang DF, Aguiar RCT. MicroRNAs miR125a and miR-125b constitutively activate the NF-kappa B pathway by targeting the tumor necrosis factor alpha-induced protein 3 (TNF-AIP3, A20). Proc Natl Acad Sci 2012;109:7865-70.

50. Kindt TJ, Goldsby RA, Osborne BA, Kuby J. Kuby Immunology. New York: W.H. Freeman, 2007.

51. Klinkenberg M, Van Huffel S, Heyninck K, Beyaert R. Functional redundancy of the zinc fingers of A20 for inhibition of NF-kappaB activation and protein-protein interactions. FEBS Lett 2001;498:93-7.

52. Klug A, Rhodes D. Zinc fingers: a novel protein fold for nucleic acid recognition. Cold Spring Harb Symp Quant Biol 1987;52:473-482.

53. Kommander D, Barford D. Structure of the A20 OTU domain and mechanistic insights into deubiquitination. Biochem J 2008;409:77-85.

54. Krikos A, Laherty CD, Dixit VM. Transcriptional activation of the tumor necrosis factor alpha-inducible zinc finger protein A20, is mediated by kappa B elements. J Biol Chem 1992;267:17971-6.

55. Lademann U, Kallunki T, Jaattela M. A20 zinc finger protein inhibits TNF-induced apoptosis and stress response early in the signaling cascades and independently of binding to TRAF2 or 14-3-3 proteins. Cell Death Differ 2001;8:265-72.

56. Laherty CD, Hu HM, Opipari AW, Wang F, Dixit VM. The Epstein Barr LMP1 gene product induces A20 zinc finger protein expression by activating nuclear factor kappa B. J Biol Chem 1992;267:24157-60.

57. Laherty CD, Perkins ND, Dixit VM. Human T cell leukemia type I Tax and phorbol 12-myristate 13 acetate induce expression of the A20 zinc finger protein by distinct mechanisms involving nuclear factor kappa B. J Biol Chem 1993;268:5032-9.

58. Ledbetter JA, Gentry LE, June CH Rabinovich PS, Purchio AF. Stimulation of T cells through the CD3/T-cell receptor complex: role of cytoplasmic calcium, protein kinase C translocation, and phosphorylation of pp60c-src in the activation pathway. Mol Cell Biol 1987;7:860-8.

59. Lee EG, Boone DL, Chai S, Libby SL, Chien M, Lodolce JP, et al. Failure to regulate TNF-indiced NF-kappaB and cell death responses in A20-deficient mice. Science 2000;289:2350-4.

60. Lerebours F, Vacher S, Andrieu C, Espie M, Marty M, Lidereau R, et al. NF-kappa B genes have a major role in inflammatory breast cancer. BMC Cancer 2008;8:41.

61. Li MY, Zhu M, Zhu B, Wang ZQ. Cholera toxin suppresses expression of ubiquitin editing enzyme A20 and enhances transcytosis. Cell Physiol Biochem 2013;31:495-504.

62. Li Y, Begovich AB. Unraveling the genetics of complex diseases: susceptibility genes for rheumatoid arthritis and psoriasis. Semin Immunol 2009;21:318-27.

63. Li L, Hailey DW, Soetandyo N, Li W, Lippincott-Schwartz J, Shu HB et al. Localization of A20 to a lysosome-associated compartment and its role in NF-kappaB signaling. Biochem Biophys Acta 2008;1783:1140-9.

64. Lin SC, Chung JY, Lamothe B, Rajashankar K, Lu M, Lo YC, et al. Molecular basis for the unique deubiquitinating activity of the NF-kappaB inhibitor A20. J Mol Biol 2008;376:526-40.

65. Lin R, Yang L, nakhaei P, Sun Q, Sharif-Askari E, Julkunen I, et al. Negative regulation of the retinoic acid-inducible gene I-induced antiviral state by the ubiquitin-editing protein A20. J Biol Chem 2006;2095-103.

66. Longo CR, Arvelo MB, Patel VI, Daniel S, Mahiou J, Grey ST, et al. A20 protects from CD-40-CD40 ligand-mediated endothelial cell activation and apoptosis. Circulation 2003;108:1113-8.

67. Lu TT, Onizawa M, Hammer GE, Turer EE, Yin Q, Damko E, Agelids A, Shifrin N, Advincula R, Barrera J, Malynn BA, Wu H, Ma A. Dimerization and ubiquitin mediated recruitment of a20, a complex deubiquitinating enzyme. Immunity 2013;38:896-905.

68. Maelfait J, Roose K, Bogaert P, Sze M, Saelens X, Pasparakis M, Carpentier I, van Loo G, Beyaert R. A20 (TNF-aip3) deficiency in myeloid cells protects against influenza A virus infection. Plos Pathog 2012;8: e1002570. doi: 10.1371/journal.ppat.1002570.

69. Malynn BA, Ma A. A20 takes on tumors: tumor suppression by an ubiquitin-editing enzyme. J Exp Med 2009;206:977-80.

70. Malewicz M, Zeller N, Yilmaz ZB, Weih F. NF-kappaB controls the balance between FAS and tumor necrosis factor cell death pathways during T cell receptor-induced apoptosis via the expression of its target gene A20. J Biol Chem 2003;278:3285-33.

71. Marakova KS, Aravind L, Koonin EV. A novel superfamily of predicted cysteine proteases from eukaryotes, viruses and Chlamydia pneumonia. Trends Biochem Sci 2000;25:50-52.

72. Matta H, Gopalakrishnan R, Punj v, Yi H, Suo Y, Chaudhary PM. A20 is induced by Karposi scarcoma-associated herpesvirus encoded viral FLICE inhibitory protein (vFLIP) k13 an dblocks K13 induced nuclear factor-kappaB in a negative feedback manner. J Biol Chem 2011;286:1555-64.

73. Matthews JM, Kowalski K, Liew CK, Sharpe BK, Fox AH, Crossley M, MacKay JP. A class of zinc fingers involved in protein-protein interactions biophysical characterization of CCHC fingers from fog and U-shaped. Eur J biochem 2000;267:1030-8.

74. Mayer, BJ, Blinov ML, Loew LM. Molecular machines or pleiomorphic ensembles: signaling complexes revisited. J Biol 2009;8:81-81.8.

75. McCall KA, Huang C-C, Fierke CA. Function and mechanism of zinc metalloenzymes. J Nutrition 2000;5:14375-4465.

76. Miyashita T. Confocal microscopy for intracellular co-localization of proteins. Methods Mol Biol. 2004;261:399-410.

77. Moran TM, Isobe H, Fernandez-Sesma A, Schulman JL. Interleukin-4 causes delayed virus clearance in influenza virus infected mice. J Virol 1996;70:5230-35.

78. Moscat J, Diaz-Meco MT, Albert A, Campuzano S. Cell signaling and function organized by PB1 domain interactions. Mol Cell 2006;23: 631–640 .

79. Moscat J, Diaz-Meco MT, Wooten MW. Signal integration and diversification through the p62 scaffold protein. Trends Biochem Sci 2007;32: 95–100.

80. Newton K, Matsumoto ML, Wertz IE, Kirkpatrick DS, Lill JR, Tan J, et al. Ubiquitin chain editing revealed by polyubiquitin linkage-specific antibodies. Cell 2008;134:668-78.

81. Onose A, Hashimoto S, Hayashi S, Maruoka S, Kumasawa F, Mizumura K, et al. An inhibitory effect of A20 on NF-kappaB activation in airway epithelium upon influenza infection. Eur J Pharmacol 2006;541:198-204.

82. Opipari Jr AW, Boguski MS, Dixit VM. The A20 cDNA induced by tumor necrosis factor alpha encodes a novel type of zinc finger protein. J Biol Chem 1990;265:14705-8.

83. Opipari Jr AW, Hu HM, Yabkowitz R, Dixit VM. The A20 zinc finger protein protects cells from tumor necrosis factor cytotoxicity. J Biol Chem 1992;267:12424-7.

84. O'Reilly SM, Moynagh PN. Regulation of Toll-like receptor 4 signaling by the A20 zinc finger protein. Biochem Biophys Res Commun 2003;303:586-96.

85. Panchuk-Voloshina N, Haugland RP, Bishop-Stewart J, Bhalgat MK, et al. Alexa dyes, a series of new fluorescent dyes that yield exceptionally bright, photostable conjugates. J Histochem Cytochem 1999;47:1179-88.

86. Pavletich NP, Pabo CO. Zinc finger-dna recognition: crystal structure of a Zif268-DNA complex at 2.1 angstrom. Science 1991;252:809-16.

87.   Park JH, Bae JY, Park HH. Self-oligomerization of the CARD domain prevents complex formation in the CARMA1 signalsome. Int J Mol Med. 2013;5:12807.

88.   Park S, yang J-S, Shin Y-E, Park J, Key Jang SK, Kim S. Protein localization as a principal feature of the etiology and comorbidity of genetic disease. Mol Syst Biol 2011;7:494.

89.   Paul S, Kashyap AK, Jia W, He YW, Schaefer BC. Selective Autophagy of the Adaptor Protein Bcl10 Modulates T Cell Receptor Activation of NF-κB. Immunity 2012; 36:947-58.

90.   Ravasi, T, Huber, T, Zavlan M, Forrest A, et al. Systematic characterization of the zinc finger containing proteins in the mouse transcriptome. Genome Res 2003;13:1430-42.

91.   Riedel S. Biological warfare and bioterrorism: a historical review. Proc (Bayl Univ Med Cent) 2004;17:400-6.

92.   Rossman JS, Stoicheva NG, Langel FD, Patterson GH, Lippincott-Schwartz J, and Schaefer BC. POLKADOTS are foci of functional interactions between cytosolic intermediates in T cell receptor-induced activation of NF-κB. Mol. Biol. Cell 2006; 17:2166-76.

93.   Rosebeck S, Rehman AO, Lucas PC, McAllister-Lucas LM. From MALT lymphoma to the CBM signalsome: Three decades of discovery. Cell Cycle 2011;10:2485-96.

94.   Rudner DZ, Losick R. Protein Subcellular localization in bacteria. Cold Spring Harb Perspect Biol 2010.

95.   Saitoh t, Yamaoka S. A20, UCSD-Nature Molecule Pages 2013, doi:10.1038/mp.a000159.01.

96. Saitoh T, Yamamoto M, Miyagishi M, Taira K, Nakanishi M, Fujita T, et al. A20 is a negative regulator of IFN regulatory factor 3 signaling. J Immunol 2005;174:1507-12.

97. Saner, NC, Lin MZ, Mckeown MR, Steinbach PA, et al. Improving the photostability of bright monomeric orange and red fluorescent proteins.   Nat Methods 2008;5:545-51.

98. Schaefer BC, Mitchell TC, Kappler JW, Marrack P. A novel family of retroviral vectors for the rapid production of complex stable cell lines.   Anal Biochem 2001;297:86-93.

99. Schmitz R, Hansmann ML, Bohle V, Martin-Subero JI, Hartmann S, Mechtersheimer G, et al. TNF-AIP3 (A20) is a tumor suppressor gene in Hodgkin lymphoma and primary mediastinal B cell lymphoma. J Exp Med 2009;206:981-9.

100. Shembade N, Harhaj EW. Regulation of NF-kappaB signaling by the A20 deubiquitinase. Cell Mol Immunol 2012;9:123-30.

101. Shembade N, Harhaj NS, Parvatiyar K, Copeland NG, Jenkins NA, Matesic LE, et al. The E3 ligase Itch negatively regulates inflammatory signaling pathways controlling the function of the ubiquitin-editing enzyme A20.   Nat Immunol 2008;9:254-62.

102. Shembade N, Ma A, Harhaj EW. Inhibition of NF-kappaB signaling by A20 through disruption of ubiquitin enzyme complexes. Science 2010;327:1135-9.

103. Shembade N, Parvatiyar K, Harhaj NS, Harhaj EW. The ubiquitin editing enzyme A20 requires RNF-11 to down regulate NF-kappaB signaling. EMBO J 2009;28:513-22.

104. Skaug B, Chen J, Du F, He J, Ma A, Chen ZJ. Direct, noncatalytic mechanism of IKK inhibition by A20. Mol Cell 2011;18:559-71.

105. Smith-Garvin JE, Koretzky GA, Jordan MS. T cell Activation. Ann. Rev Immunol 2009;27:591-619.

106. Soule, HD, Vazquez J, Long A, Albert S, Brennan, M. A human cel line from a pleural effusion derived from breast carcinoma. J Natl Canc Institute 1973;51:1409-1416.

107. Song HY, Rothe M, Goeddel DV. The tumor necrosis factor-inducible zinc finger protein A20 interacts with TRAF1/TRAF2 and inhibits NF-kappaB activation. Proc Natl Acad Sci USA 1996;93:6721-5.

108. Song XT, Evel-Kabler K, Shen L, Rollins L, Huang XF, Chen SY. A20 is an antigen presentation attenuator, and its inhibition overcomes regulatory T-cell mediated suppression. Nat Med 2008;14:258-65.

109. Srivastav S, Kar S, Chande AG, Mukhopadhyaya R, Das PK. Leishmania donovani exploits host deubiquitinating enzyme A20, a negative regulator of TLR signaling to subvert host immune response. J Immunol 2012;189:924-34.

110. Stilo R, Varricchio E, Liguoro D, Leonardi A, Vito P. A20 is a negative regulator of BCL10- and CARMA 3-mediated activation of NF-kappaB. J Cell Sci 2008;121:1165-71.

111. Storz P, Doppler H, Ferran C, Grey ST, Toker A. Functional dichotomy of A20 in apoptotic and necrotic cell death. Biochem J 2005;387:47-55.

112. Stuart AL, Wilkening DA. Degradation of biological weapons agents in the environment: implications for terrorist response. 2005;39:2736-43.

113. Tewari M, Wolf FW, Seldin MF, Oshea KS, Dixit VM, Turka LA. Lymphoid expression and regulation of A20, an inhibitor of programmed cell death. J Immunol 1995; 154:1699-706.

114. Tokunaga F, Nishimasu H, Ishitani R, Goto E, et al. Specific recognition of linear polyubiquitin by A20 zinc finger 7 is involved in NF-kB regulation. EMBO J 2012;19:3856-70.

115. Turer EE, Tavares RM, Mortier E, Hitotsumatsu O, Advincula R, Lee B, et al. Homeostatic MyD88-dependent signals cause lethal inflammation in the absence of A20. J Exp Med 2008;205:451-64.

116. Vendrell JA, Ghayad S, Ben Larbi S, Dumontet C, Mechti N, Cohen PA. A20/TNF-AIP3, a new estrogen-regulated gene that confers tamoxifen resistance in breast cancer cells. Oncogene 2007; 26:4656-67.

117. Vereecke L, beyaert R, van Loo G. The ubiquitin-editing enzyme A20 (TNF-AIP3) is a central regulator of immunopathology. Trends Immunol 2009;30:383-91.

118. Verstrepen L, Verhelst K, van Loo G, Carpentier I, Ley SC, Beyaert R. Expression, biological activities and mechanisms of action of A20 (TNF-AIP3). Biochem Pharm 2010;2009-20.

119. Vincenz C, Dixit VM. 14-3-3 proteins associate with A20 in an isoform-specific manner and function both as chaperone and adapter molecules. J Biol Chem 1996;271:20029-34.

120. Vondriska TM, Pass JM, Ping P. Scaffold proteins and assembly of multiprotein signaling complexes. J Mol Cell Cardiol 2004;37:391-7.

121. Vucic DJ, and Dixit VM. Masking MALT1: the paracaspase's poetential for cancer therapy. J Exp Med 2009;206:2309-12.

122. Wang YY, Li L, han KJ, Zhai Z, Shu HB. A20 is a potent inhibitor of TLR3- and Sendai virus-induced activation of NF-KappaB and ISRE and the IFN-beta promoter. FEBS Lett 2004;576:86-90.

123. Wang X, Friesen J, Nishanth G, Thi XN, Matuschewski K, Schluter D. Hepatocyte-specific knockout of A20 augments defense against malaria liver stage infections. Int J Med Microbiol 2011;301:42-43.

124. Welchman RL, Gordon C, Mayer RJ. Ubiquitin and ubiquitin-like proteins as multifunctional signals. Nat Rev Mol Cell Biol 2005;6:599-609.

125. Wertz IK, O'Rourke KM, Zhou H, Eby M, Aravind L, Seshagiri, S, et al. Deubiquitination and ubiquitin ligase domains of A20 downregulate NF-kappaB signaling. Nature 2004;430:694-9.

126. Wheelis M. Biological warfare at the 1346 siege of Caffa. Emerg Infect Dis 2002;(8):971-5.

127. Woo HN, Hong GS, Jun JL, Cho DH, Choi HW et al. Inhibition of Bcl10-mediated activaton of NF-kappaB by BinCard, a Bcl10-interacting Card protein. FEBS Lett 2004;578:239-44.

128. Wu CJ, Ashwell JD. NEMO recognition of ubiquitinated Bcl10 is required for T-cell receptor mediated NF-kappaB activation. Proc Natl Acad Sci USA 2008;105:3023-28.

129. Wu WS, Xu ZX, Chang KS. The promyelocytic leukemia protein represses A20-mediated transcription. J Biol Chem 2002;277:31734-9.

130. Xu W, Xue L, sun Y, Henry A, Battle JM, Micault M, Morris SW. Bcl10 is an essential regulator for A20 gene expression. J Physiol Biochem. 2013.

131. Zhang SQ, Kovalenko A, Cantarella G, Wallach D. Recruitment of the IKK signalsome to the P55 TNF- receptor: RIP and A20 bind to NEMO (IKK gamma) upon receptor stimulation. Immunity 2000;12:301-11.

132. Zhang f, Yang L, Yangqiu Li. The role of A20 in the pathogenesis of lymphocytic malignancy. Cancer Cell Internl 2012;12:44-52.

133. Zetoune FS, Murthy AR, Shao Z, Hlaing T, Zeidler MG, Li Y, et al. A20 inhibits NF-kappa B activation downstream of multiple Map3 kinases and interacts with the I kappa B signalsome. Cytokine 2001;15:282-98.